Spring 4-13-2023

Chance Constrained Stochastic Optimal Control of Discrete Time Linear Stochastic Systems with Applications in Multi-satellite Operations

Shawn Priore

Shawn Priore

Candidate

Electrical Engineering

Department

This dissertation is approved, and it is acceptable in quality and form for publication:

Approved by the Dissertation Committee:

Meeko M. K. Oishi, Chairperson

Rafael Fierro

Claus Danielson

Christopher Petersen

Chance Constrained Stochastic Optimal Control of Discrete Time Linear Stochastic Systems with Applications in Multi-satellite Operations

by

Shawn Priore

A.A.B. International Business, Cuyahoga Community College, 2013

B.S. Economics, John Carroll University, 2016

M.B.A, John Carroll University, 2017

M.S. Statistics, University of Connecticut, 2020

DISSERTATION

Submitted in Partial Fulfillment of the

Requirements for the Degree of

Doctorate of Philosophy

Engineering

The University of New Mexico

Albuquerque, NM

May, 2023

Dedication

Ferda

Acknowledgments

I am grateful for everyone who has made this work possible. Foremost, I am grateful for my advisor, Meeko Oishi, for all of her patience and guidance throughout these past few years. Without her faith in my abilities, I would not be where I am today. I am also appreciative of my committee members, Chris Petersen, Claus Danielson, and Rafael Fierro. The collaborations, advice, and feedback has helped shape this work and given me several avenues for future research.

These past few years I have had the pleasure of working beside and with several astounding colleagues. I am glad to have met Abraham, Adam, Georgia, Jake, Karthik, Kendrick, Hayden, Rachel, and Vignesh. You have all made my time at UNM memorable and I wish you all the best.

I would like to thank those that help support me through this program. I thank my mom and stepdad for always believing in me and pushing me toward greatness. Thank you to Eric and Patrick for your camaraderie and encouragement throughout our doctorates. I thank Evelyn and John for their friendship and kindness. Last but not least, I would like to thank my fiancée, Jenny, for everything she does and for being there with me on this adventure.

This material is based upon work supported by the National Science Foundation under Grant Number CMMI-1254990, CMMI-2105631, and OIA-1757207, by the AFRL Cooperative Agreement FA9453-18-2-0022, Agile Manufacturing for High Value, Low Volume

Production, and the DoD SMART Scholarship-for-Service Program under The Under Secretary of Defense-Research and Engineering, National Defense Education Program (NDEP) / BA-1, Basic Research.

Chance Constrained Stochastic Optimal Control of Discrete Time Linear Stochastic Systems with Applications in Multi-satellite Operations

by

Shawn Priore

A.A.B. International Business, Cuyahoga Community College, 2013

B.S. Economics, John Carroll University, 2016

M.B.A, John Carroll University, 2017

M.S. Statistics, University of Connecticut, 2020

Ph.D Electrical Engineering, The University of New Mexico, 2023

Abstract

Stochastic disturbances arise in a variety of engineering applications. For tractability, Gaussian disturbances are often assumed. However, this may not always be valid, such as when a disturbance exhibits heavy-tailed or skewed phenomena. As autonomous systems become more ubiquitous, non-Gaussian disturbances will become more common due to the compounding effects of sensing, actuation, and external forces. Despite this, little has been done to develop formal methods that are both computationally efficient and allow for analytical assurances with non-Gaussian disturbances. Addressing convex polytopic set acquisition and non-convex collision avoidance chance constraints with quantile and moment-based reformulations, this dissertation proposes novel stochastic optimal control techniques that are computationally efficient and allow for analytic guarantees with arbitrary disturbances. These reformulations are amenable to optimization techniques while eliminating costly, and frequently intractable, high-dimensional integrals. These conservative reformulations guarantee chance constraint satisfaction and are numerically tractable. I demonstrate these methods with applications to multi-satellite operations.

Contents

List of Figures

List of Tables

Chapter 1

Introduction

1.1 Motivation

Enabling extended satellite lifetimes through advances in on-orbit refueling and servicing depots has been a focal point for many private and public organizations [7, 8, 9]. Such advances are requiring new technologies to enable efficient autonomous coordination between multiple satellites despite the harsh environment and limited resources such as fuel or computational abilities. These new technologies must accommodate path planning and optimization for mission critical vehicles under uncertain conditions that may arise from modeling inaccuracies, inaccurate or time delayed sensing, and faulty or inconsistent actuation mechanisms. These stochastic elements are frequently modeled using Gaussian disturbances for mathematical convenience. However, noise processes from conditions like these can take on non-Gaussian characteristics, such as heavy tailed, skewed, or multi-modal phenomena. In stochastic spacecraft systems, non-Gaussian phenomena can arise from drag [10], third body gravity effects [11], faulty thrusters or sensors, extreme weather or geological events such as hurricanes or earthquakes [12], or even magnetic disturbances caused by solar winds and solar flares [13]. Computation of controllers that meet required probabilistic safety thresholds for target acquisition and collision avoidance in these conditions require accurate assessments of disturbance characteristics.

To address arbitrary disturbances, many control theorists rely on stochastic optimal control principals to develop techniques for controller synthesis [14, 15, 16]. Within the stochastic optimal control framework, chance constraints have been widely used to account for target set and collision avoidance restrictions in a probabilistic manner [17, 18]. Ideally, control theorists seek to find a convex reformulation of chance constraints such that can be optimized with classical convex optimization guarantees [19, 20, 21].

In this dissertation, I propose three chance constrained stochastic optimal control methods that are computationally efficient and tractable for cooperative multi-vehicle coordination problems. Here, I focus on three challenges: 1) chance constraints for polytopic target sets and 2-norm based collision avoidance, 2) arbitrary and potentially unknown disturbances, and 3) computationally efficient methods. Individually, each of these challenges have solutions. While brute force method can be used to handle non-convex constraints or non-Gaussian distributions [5, 22], there is a dearth of computationally efficient methods that can handle both non-convexity and non-Gaussianity. This is particularly true for instances when non-Gaussian distributions are the cause of non-convexities, such as multi-modal distributions. Figure 1.1 demonstrates the stochastic motion planning scenario that is primarily considered throughout this work. In this scenario, three satellites must reach a refueling station, while avoiding colliding with each other, the refueling station, other spacecraft, and debris despite uncertainties corrupting the dynamics.

One of the major motivators for this work is that the existing work in this field primarily focuses on Gaussian disturbances and the few methods that can accommodate non-Gaussian disturbance typically cannot handle non-convex constraints and are not computationally efficient. There are several hurdles that each of these methods overcame to be able to handle non-convex collision avoidance, non-Gaussian disturbances, and do so in a computationally efficient manner. To address non-Gaussianity, the methods pre-

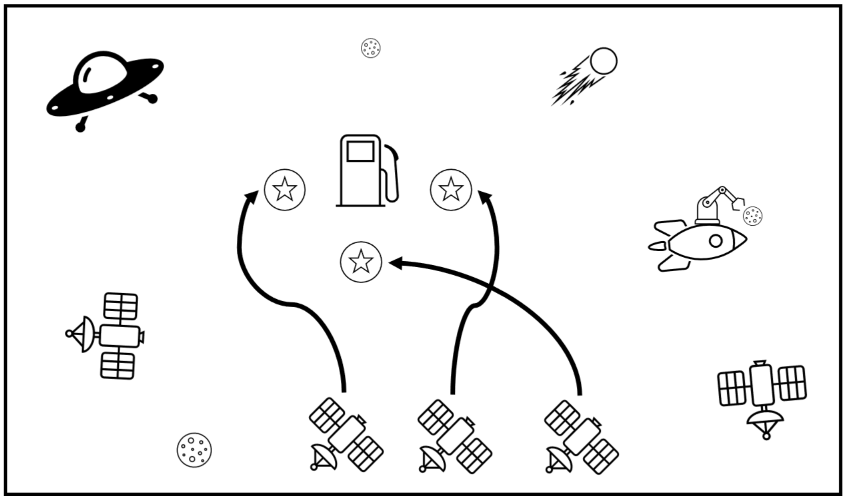

Figure 1.1: A scenario in which three satellites need to rendezvous with a refueling station while avoiding nearby spacecraft and space debris.

sented in this work are all based on general characteristics common to most disturbances, such as moments or quantile functions. Through this lens, each method manipulates elements of statistical theory to derive a closed form reformulation that can be applied to most disturbances. Special care was taken such that each closed form reformulation could be formatted as a difference of convex functions. While a difference of convex function is inherently non-convex, formatting the methods in this manner allows for guarantees of locally optimal solutions that do not inhibit the asymptotic or almost surely guarantees of chance constraint satisfaction. Further, difference of convex functions programs can be solved through an iterative convex approximation process. Despite being iterative, each iteration results in a convex subproblem that can be solved quickly, making the whole process relatively efficient.

The other primary motivator for developing several methods in this work is that not every distribution has closed form expressions for the various elements each method is based on. For example, Gaussian distributions do not have a closed form expression for the quantile and Cauchy distributions do not have moments. Hence, not every method can be applied to every distribution. Further, even if a distribution does have a closed form expression for a statistical characteristic of interest, it may not be known. As this work progresses, it is assumed that less detailed knowledge is known of the underlying disturbance processes than in the previous chapters. By the last method, no knowledge is assumed to be known about the underlying disturbance, implying it can handle any disturbance. However, the general utility of these methods comes at the cost of conservatism, which increases as the chapters progress.

1.2 Related Work

Several chance constrained stochastic optimal control methods already exist in the literature. The robust model predictive control (MPC) method utilizes bounded disturbance characteristics to develop upper and lower bounds the state must achieve to satisfy the constraints in all scenarios [23, 24, 25, 26, 27, 28]. For disturbances on infinite supports, the robust MPC method considers artificial bounds that represent a significant portion of the distributions support [28]. Robust methods can be particularly useful when high safety thresholds are required. However, by using upper and lower bounds that are predetermined, the robust MPC method often lacks optimally.

Several quantile and conditional value at risk (CVaR) based approaches have been posed to solve the chance constraints [29, 30, 31]. Both quantiles and CVaR are used as a measure of the tail probability of the state not being safe with respect to the underlying distribution. These methods rely on accurate knowledge of the underlying distribution and closed form expressions for the quantile and CVaR. Quantile and CVaR tend to result in less conservative controllers but the reliance on closed form expressions can be limiting. Methods have been posed to alleviate the need for closed form expressions. The work of [32, 33, 34] proposed the use of numerical inverse Fourier transforms to recover the quantile from the characteristic function.

Moment based approaches that rely on concentration inequalities, such as Markov's, Chebyshev's, and Cantelli's inequalities [35], have been developed for distributions that have analytic moments. For linear chance constraints reformulations have closed form based on the linear and quadratic properties of the expectation and variance function [1, 36, 37]. These methods benefit from linear systems and constraints allowing for closed form chance constraint reformulations that are tractable. However, for non-linear constraints, analytic computation of moments can be challenging, particularly for longer time horizon problems.

Sampling approaches are a common way to bypass the need for closed form expressions using sampled data. The two common sampling based approaches are the scenario approach [4, 38, 39, 5, 40, 41] and particle control approach [22, 6, 42, 43]. The scenario approach solves the stochastic optimal control problem with respect to each sample disturbance in the sample data. For a given problem, users specify a confidence bound for the likelihood of the solution satisfying chance constraints. As both the chance constraint satisfaction threshold and the confidence bound increase, so too do the number of samples required. Recent work has been posed to alleviate the computational burden of large sample size requirements thought a sample-and-discard approach [44] and an iterative solution finding process [45]. Like the scenario approach is the particle control approach. Commonly formatted as a mixed integer linear program, the particle control approach solves the chance constrained problem for a fraction of the samples corresponding to the chance constraint satisfaction threshold. Often this method more computationally burdensome than the scenario approach despite potentially using less disturbance samples. Unlike the scenario approach, the particle control approach does not provide a confidence bound and can only guarantee chance constraint satisfaction asymptotically. While both methods can accommodate chance constraints without knowledge of the underlying disturbance, they also suffer from the computational burden of large data sets.

1.3 Implications for Multi-Satellite Rendezvous

Multi-satellite rendezvous problems provide unique challenges in that the vehicles are often uniquely designed, safety critical, and (at time of writing) mostly unrepairable. These facts, combined the harsh nature of the environment in which they operate, provide a scenario in which even small inaccuracies in modeling or unexpected disturbances can lead to catastrophic failures that are cost prohibitive to rectify. However, as the statistician George Box stated, "All models are wrong, some are useful," so we should expect inaccuracies in our modeling techniques. Chance constrained stochastic optimal control methods are a practical solution to this problem as we can account for these inaccuracies probabilistically while maintaining considerations for finite resources, such as fuel.

The use of stochastic optimal control techniques is not new to the satellite community [46, 47]. Techniques to synthesize optimal rendezvous maneuvers have been modeled with robust methods [48], differential games [49], quantile approaches [3, 50], and moment based approaches [51]. However, many of the methods listed thus far have primarily focused on target set acquisition. However, with the near exponential increase in active satellites and debris over the past few years, collision avoidance has become an increasingly important consideration in satellite control. Sequential convex programming can be applied to saturation penalty functions based on 2-norm collision avoidance constraints but suffers from singularities and potential non-convergence during gradient decent [52, 53, 54, 55]. Techniques for calculating collision avoidance probabilities have been posed [56] but are difficult to embed in control algorithms and may be limited by the shape of the satellite. Methods for rendezvous and proximity operations between a controlled satellite and a stationary or potentially non-cooperative satellite have been proposed [57, 58, 59] but lack in their ability to accommodate multiple controlled vehicles.

In this work, multi-satellite rendezvous problems are the focus for application. For safety critical systems, such as satellites, methods that can provide assurances of constraint satisfaction apriori are required when developing new methodologies. As the methods presented in this work provide approximate or almost surely guarantees of chance constraint satisfaction, these methods may be of interest to the satellite community.

1.4 Contributions, Publications, and Organization

1.4.1 Contributions

The focus of this work is on the theory of chance constrained stochastic optimal control. The main contributions of this dissertation are summarized below.

1. Development of three controller synthesis methods in which stochastic optimal control problems with chance constraints for target sets and collision avoidance can be solved in the presence of arbitrary and potentially unknown disturbances.

2. Derivations of closed form reformulations of chance constraints for target sets and collision avoidance. These closed form reformulations result in a series on convex or difference of convex constraints that can easily be solved with an iterative convex approximation.

3. Derivation of probabilistic safety guarantees associated with each of the three developed methods. The developed probabilistic safety guarantees that are developed in this work are not dependent on the choice of disturbance.

1.4.2 Publications

All the work presented in this dissertation has been published or submitted for publication in peer-reviewed journals or conferences. The quantile based approach that is presented in Chapter 3 has been published or submitted for publication in:

- S. Priore, A. Vinod, V. Sivaramakrishnan, C. Petersen and M. Oishi, "Stochastic multi-satellite maneuvering with constraints in an elliptical orbit," 2021 American Control Conference (ACC), New Orleans, LA, USA, 2021, pp. 4261-4268, doi: 10.23919/ACC50511.2021.9483158.

- S. Priore, C. Petersen and M. Oishi, "Approximate Quantiles for Stochastic Optimal Control of LTI Systems with Arbitrary Disturbances," 2022 American Control Conference (ACC), Atlanta, GA, USA, 2022, pp. 1814-1821, doi: 10.23919/ACC53348.2022.9867580.

- S. Priore, C. Petersen and M. Oishi, "Approximate Stochastic Optimal Control for Linear Time Invariant Systems with Heavy-tailed Disturbances", submitted to *AIAA Journal of Guidance, Control, and Dynamics*

The analytic moment approach, which is presented in Chapter 4, has been submitted for publication in:

- S. Priore and M. Oishi, "Chance Constrained Stochastic Optimal Control for Arbitrarily Disturbed LTI Systems Via the One-Sided Vysochanskij–Petunin Inequality" submitted to *IEEE Transactions on Automatic Control*

The work on sample based moments, which is discussed in Chapter 5, has been submitted for publication in:

- S. Priore and M. Oishi, "Chance Constrained Stochastic Optimal Control Based on Sample Statistics With Almost Surely Probabilistic Guarantees" submitted to *IEEE Transactions on Automatic Control*

Although not discussed in this body of research, I have worked on several other theoretical contributions in the field of chance constrained stochastic optimal control. I have extended the work of Chapter 5 to a particular case involving Gaussian distributions with unknown mean and variance parameters in

- S. Priore and M. Oishi, ”Stochastic Optimal Control For Gaussian Disturbances with Unknown Mean and Variance Based on Sample Statistics” submitted to *2023 IEEE Conference on Decision and Control*

Further, I have considered chance constrained stochastic optimal control for cases when stochasticity is present in the state matrix or the control matrix. This work has been published or submitted for publication in

- S. Priore, A. Bidram and M. Oishi, ”Chance Constrained Stochastic Optimal Control for Linear Systems with Time Varying Random Plant Parameters” accepted, to appear in *2023 American Control Conference (ACC)*
- S. Priore and M. Oishi, ”Chance Constrained Stochastic Optimal Control for Linear Systems with a Time Varying Random Control Matrix” submitted to *2023 IEEE Conference on Control Technology and Applications*

1.4.3 Organization

The remainder of this dissertation will be organized as follows.

In Chapter 2, I provide an overview of the necessary mathematical concepts used in the remainder of this work. This includes a review of probability and optimization. I formulate the chance constrained stochastic optimization problem that this body of research focuses on solving. Finally, I provide a brief overview of the dynamics for relative motion of on-orbit satellites.

In Chapter 3, I present the quantile based approach to solving the chance constrained stochastic optimization problem. I detail how the chance constraints considered are amenable to a form in which the stochasticity is separable from the control input. In this form, I show the constraints can be written in terms of the input and the stochastic quantile. The quantile is then approximated with a Taylor series expansion under assumptions of existence and differentiability of the probability density function. This approach is demonstrated on three multi-satellite rendezvous scenarios.

In Chapter 4, I present the analytic moment based approach to solving the chance constrained stochastic optimization problem. I detail how the chance constraints considered can be satisfied with non-probabilistic constraints based on the mean and standard deviation of the event the chance constraint is bounding. For unimodal constraint, I show that the one-sided Vysochanskij-Petunin inequality [60] allows for guaranteed satisfaction of the chance constraints. This approach is demonstrated on two multi-satellite rendezvous scenarios.

In Chapter 5, I present the sample moment based approach to solving the chance constrained stochastic optimization problem. I detail how the chance constraints considered can be satisfied with non-probabilistic constraints based on the sample mean and sample standard deviation of the event the chance constraint is bounding. I derive two theorems that guarantee chance constraint satisfaction despite using sample statistics. This approach is demonstrated on two multi-satellite rendezvous scenarios.

Chapter 6 summarizes the contributions of this body of research and identifies avenues for future research.

Chapter 2

Preliminaries

2.1 Notation

The following notation standards will be used throughout the remainder of this work.

The set of natural numbers, including zero, is denoted as $\mathbb{N}$ and a subset of the natural numbers from a to b where $a < b$ is denoted as $\mathbb{N}_{[a,b]}$. The set of real numbers is $\mathbb{R}$. Scalars and vectors will be denoted with a lower-case letter, the latter having an arrow accent, i.e., $x \in \mathbb{R}$ or $\vec{x} \in \mathbb{R}^n$. Matrices will be denoted with a capital letter, i.e. $A \in \mathbb{R}^{n\times m}$. The denote an identity matrix as $I_n \in \mathbb{R}^{n\times n}$ and a matrix of all zeros as $0_n \in \mathbb{R}^{n\times n}$ or $0_{n\times m} \in \mathbb{R}^{n\times m}$. Concatenated vectors will be noted with accented uppercase letters, i.e. $\vec{X} = \begin{bmatrix} \vec{x}_1^\top & \vec{x}_2^\top \end{bmatrix}^\top \in \mathbb{R}^{2n}$ and concatenated matrices will use calligraphic uppercase letters, i.e. $\mathcal{A} = \begin{bmatrix} A_1 & A_2 \end{bmatrix} \in \mathbb{R}^{n\times 2m}$. For a matrix A, the operator $\text{vec}(A)$ vertically concatenates the columns of A into a column vector. For two matrices A and B, I denote the Kronecker product as $A \otimes B$. For matrix entries $A_1, \ldots, A_m$, I denote a block diagonal matrix constructed with these elements as $\text{blkdiag}(A_1, \ldots, A_m)$. I denote the 2-norm of a matrix or vector by $\|\cdot\|$.

The probability of an event A is demarcated as $\mathbb{P}(A)$. Random variables will be boldcase, $\boldsymbol{x}$, regardless of dimension. With respect to a random variable $\boldsymbol{x}$, I denote the probability density function (pdf) as $\phi_{\boldsymbol{x}}(\cdot)$, the cumulative distribution function (cdf) as $\Phi_{\boldsymbol{x}}(\cdot)$, and the quantile (or the inverse of the cdf) as $\Phi_{\boldsymbol{x}}^{-1}(\cdot)$. For a random variable $\boldsymbol{x}$, I denote the n^{th} moment as $\mathbb{E}(\boldsymbol{x}^n)$, variance as $\mathbb{V}(\boldsymbol{x})$, and standard deviation as $\mathbb{S}(\boldsymbol{x})$. For two random variables, $\boldsymbol{x}$ and $\boldsymbol{y}$, $\mathbb{C}(\boldsymbol{x}, \boldsymbol{y})$ denotes the covariance between the two variables. The i^{th} sample of the random variiable $\boldsymbol{x}$ will be denoted as $\boldsymbol{x}^{[j]}$ and sample estimates will have a hat accent $\hat{\cdot}$, such as $\hat{\mathbb{E}}(\boldsymbol{x})$ for the sample estimate of the first moment. The indicator function I_{cond} takes the value 1 if the condition, *cond*, is met and takes the value 0 otherwise.

2.2 Notions of Probability and Statistics

A random variable $\boldsymbol{x} : \mathcal{X} \to \mathcal{Y}$ is a Borel-measurable function from the probability space $(\mathcal{X}, \mathbb{B}(\mathcal{X}), \mathbb{P}_{\boldsymbol{x}})$ to a state space $(\mathcal{Y}, \mathbb{B}(\mathcal{Y}))$. Here, the probability space is defined by the set of outcomes $\mathcal{X}$, Borel σ-algebra $\mathbb{B}(\mathcal{X})$, and probability measure $\mathbb{P}_{\boldsymbol{x}}$. Similarly, the state space is defined by the set of outcomes $\mathcal{Y}$, and Borel σ-algebra $\mathbb{B}(\mathcal{Y})$. The probability that a random variable $\boldsymbol{x}$ takes a value in the measurable subset $\mathcal{S} \subseteq \mathcal{Y}$ is $\mathbb{P}_{\boldsymbol{x}}(\boldsymbol{x} \in \mathcal{S})$ [61]. For brevity, I drop the subscript on the probability function when the referenced random variable is referenced in the input of the function.

It is assumed throughout this work that all random variables are continuous. As such, the cdf $\Phi_{\boldsymbol{x}} : \mathcal{Y} \to [0, 1]$ is $\Phi_{\boldsymbol{x}}(x) = \mathbb{P}(\boldsymbol{x} \leq x) = \int_{-\infty}^{x} d\mathbb{P}_{\boldsymbol{x}}$. For a given cdf $\Phi_{\boldsymbol{x}}(x)$, the pdf is the function that satisfies the equality $\int_{-\infty}^{x} \phi_{\boldsymbol{x}}(t)\, dt = \Phi_{\boldsymbol{x}}(x)$ for all x. Note, the pdf of a function does not need to exist. The quantile $\Phi_{\boldsymbol{x}}^{-1} : [0, 1] \to \mathcal{Y}$ is the inverse of the cdf such that $\Phi_{\boldsymbol{x}}^{-1}(p) = \{x | \Phi_{\boldsymbol{x}}(x) = p\}$.

The n^{th} moment of a random variable is defined as $\mathbb{E}(\boldsymbol{x}^n) = \int_{-\infty}^{\infty} x^n \phi_{\boldsymbol{x}}(x)\, dx$ if the integral exists. The first moment is commonly referred to as the expectation or mean and is a measure of central tendency. The variance is a measure of dispersion and is defined as $\mathbb{V}(\boldsymbol{x}) = \mathbb{E}\big((\boldsymbol{x} - \mathbb{E}(\boldsymbol{x}))^2\big)$. The standard deviation $\mathbb{S}(\boldsymbol{x})$ is the square root of the variance and also measures dispersion.

For a sample of independent and identically distributed random variables, $\boldsymbol{x}^{[1]}, \ldots, \boldsymbol{x}^{[m]}$, the n^{th} sample moment is computed as $\hat{\mathbb{E}}(\boldsymbol{x}^n) = \sum_{i=1}^{m} (\boldsymbol{x}^{[i]})^n$. Similarly, for a function $f : \mathbb{R} \to \mathbb{R}$, the sample expectation of $f(\boldsymbol{x})$ is $\hat{\mathbb{E}}(f(\boldsymbol{x})) = \sum_{i=1}^{m} f(\boldsymbol{x}^{[i]})$. This formula can be used to compute the sample variance and standard deviation. It is not required that the moment to exist for the sample moments to exist.

2.3 Optimization

2.3.1 Convex Optimization

A convex optimization problem has the form

$$\min_{\vec{x}} f_0(\vec{x}) \tag{2.1a}$$

$$s.t.\ f_i(\vec{x}) \leq 0 \qquad \forall\ i \tag{2.1b}$$

$$A\vec{x} = \vec{b} \tag{2.1c}$$

where $\vec{x} \in \mathbb{R}^n$ is the decision variable, convex functions $f_i : \mathbb{R}^n \to \mathbb{R}$, and matrix $A \in \mathbb{R}^{m \times n}$ and vector $\vec{b} \in \mathbb{R}^m$. Convexity of the constraints and cost function guarantee that any local minima are also a global minima. Convex optimization problems are computationally efficient, and solutions can readily be found via the Lagrange duality principal [62].

2.3.2 Difference of Convex Optimization

Difference of convex programming is a type of optimization that can be used to solve non-convex optimization problems to a local minima. It is applicable to optimizations whose cost and constraints are difference of convex functions.

Definition 2.1 (Difference of Convex Function)**.** *A difference of convex function has the form*

$$f(\vec{x}) - g(\vec{x}) \tag{2.2}$$

in which $f, g : \mathbb{R}^n \to \mathbb{R}$ *are convex functions for* $\vec{x} \in \mathbb{R}^n$.

Generally, a difference of convex functions optimization has the form

$$\begin{aligned} &\min_{\vec{x}} \; f_0(\vec{x}) - g_0(\vec{x}) \\ &s.t. \; f_i(\vec{x}) - g_i(\vec{x}) \leq 0 \qquad \forall \; i \end{aligned} \tag{2.3}$$

where $\vec{x} \in \mathbb{R}^n$ is the decision variable, and $f_0, f_i(\cdot) : \mathbb{R}^n \to \mathbb{R}$ and $g_0, g_i(\cdot) : \mathbb{R}^n \to \mathbb{R}$ are convex. Here, the cost is a difference of convex function, and the constraints are difference of convex as per Definition 2.1. The difference of convex formulations in (2.3) covers a broad class of functions as any twice differentiable function can be expressed as a difference of convex function [63]. For example, x^3 can be written as $(x^3 + x^4 + x^2) - (x^4 + x^2)$ which is difference of convex as both functions are convex.

By taking a first order approximation of the $g_i(\cdot)$, I can solve the difference of convex function optimization problem iteratively as the convex optimization problem,

$$\begin{aligned} &\min_{\vec{x}} \; f_0(\vec{x}) - \big(g_0(\vec{x}^*) + \nabla g_0(\vec{x}^*)^\top (\vec{x} - \vec{x}^*)\big) \\ &s.t. \; f_i(\vec{x}) - \big(g_i(\vec{x}^*) + \nabla g_i(\vec{x}^*)^\top (\vec{x} - \vec{x}^*)\big) \leq 0 \qquad \forall \; i \end{aligned} \tag{2.4}$$

By updating the first order approximation at each iteration, the convex-concave procedure solves to a local optimum. The main benefit of solving this problem with the convex-concave procedure is the first order approximation makes the constraint convex while maintaining the convergence assurances [64]. Here, Algorithm 1 demonstrates the convex-concave procedure [64] used to solve (2.3).

Feasibility of (2.3) is dependent on the feasibility of the initial conditions $\vec{x}^*$. A common tactic is to add slack variables to accommodate potentially infeasible initial

Algorithm 1: Computing solutions to (2.3) with convex-concave procedure

Input: Feasible initial condition for $\vec{x}$, denoted $\vec{x}^*$, maximum number of iterations n_{max}.
Output: Solution to (2.3), $\vec{x}^*$
for $i = 1$ *to* n_{max} **do**
  Solve the convex problem (2.4)
  Set solution as new optimal solution, $\vec{x}^* = \vec{x}$
  if *Solutions converged* **then**
    break
  end
end

conditions [64, 65]. By penalizing the sum of slack variables, convergence and optimally guarantees are nearly equivalent to those of Algorithm 1.

2.4 Relative Motion Dynamics For On-Orbit Satellites

Consider a scenario, such as the one shown in Figure 1.1, where three satellites need to rendezvous with a refueling station while avoiding each other, other spacecraft, scientific instruments, and debris. I seek to synthesize the rendezvous maneuver, despite potentially non-Gaussian disturbances corrupting the satellite dynamics. We presume the evolution of vehicle i of v is governed by the discrete-time LTI system,

$$\vec{\boldsymbol{x}}_i(k+1) = A\vec{\boldsymbol{x}}_i(k) + B\vec{u}_i(k) + \vec{\boldsymbol{w}}_i(k) \tag{2.5}$$

with state $\vec{\boldsymbol{x}}_i(k) \in \mathcal{X} \subseteq \mathbb{R}^n$, input $\vec{u}_i(k) \in \mathcal{U} \subseteq \mathbb{R}^m$, $\vec{\boldsymbol{w}}_i(k) \in \mathbb{R}^n$ that follows an arbitrary but known disturbance, and initial condition $\vec{x}(0)$. I presume the initial conditions, $\vec{x}(0)$, are known, the bounded control authority, $\mathcal{U}$, is a convex polytope, and that the system evolves over a finite time horizon of $N \in \mathbb{N}$ steps. I presume each disturbance, $\vec{\boldsymbol{w}}_i(k)$ has probability space $(\Omega, \mathbb{B}(\Omega), \mathbb{P}_{\vec{\boldsymbol{w}}_i(k)})$ with outcomes Ω, Borel σ-algebra $\mathbb{B}(\Omega)$, and probability measure $\mathbb{P}_{\vec{\boldsymbol{w}}_i(k)}$ [61]. For the remainder of this work, the distribution of the stochastic elements will remain arbitrary.

We write the dynamics at time k as an affine sum of the initial condition and the concatenated control sequence and disturbance,

$$\vec{\boldsymbol{x}}_i(k) = A^k \vec{x}_i(0) + \mathcal{C}(k)\vec{U}_i + \mathcal{D}(k)\vec{\boldsymbol{W}}_i \tag{2.6}$$

with

$$\vec{U}_i = \left[\vec{u}_i(0)^\top \ \dots \ \vec{u}_i(N-1)^\top\right]^\top \quad \in \mathcal{U}^N \tag{2.7a}$$

$$\vec{\boldsymbol{W}}_i = \left[\vec{\boldsymbol{w}}_i(0)^\top \ \dots \ \vec{\boldsymbol{w}}_i(N-1)^\top\right]^\top \quad \in \mathbb{R}^{Nn} \tag{2.7b}$$

$$\mathcal{C}(k) = \left[A^{k-1}B \ \dots \ AB \ B \ 0_{n\times(N-k)m}\right] \in \mathbb{R}^{n\times Nm} \tag{2.7c}$$

$$\mathcal{D}(k) = \left[A^{k-1} \ \dots \ A \ I_n \ 0_{n\times(N-k)n}\right] \quad \in \mathbb{R}^{n\times Nn} \tag{2.7d}$$

Throughout the examples presented in this work, I will demonstrate the methods presented in the context of multi-satellite rendezvous and proximity operations for satellites orbiting Earth. Here, the motion of N_v satellites, dubbed the deputies, will be considered relative to the non-inertial, body fixed reference frame of a (potentially imaginary) satellite, dubbed the chief. The continuous time relative dynamics of each spacecraft, with respect to the chief are described by the Clohessy-Wiltshire-Hill (CWH) equations [66]

$$\ddot{x} - 3\omega^2 x - 2\omega\dot{y} = \frac{F_x}{m_c} \tag{2.8a}$$

$$\ddot{y} + 2\omega\dot{x} = \frac{F_y}{m_c} \tag{2.8b}$$

$$\ddot{z} + \omega^2 z = \frac{F_z}{m_c}. \tag{2.8c}$$

with input $\vec{u}_i = \left[\ F_x \quad F_y \quad F_z\ \right]^\top$, and orbital rate $\omega = \sqrt{\frac{\mu}{R_0^3}}$, gravitational parameter

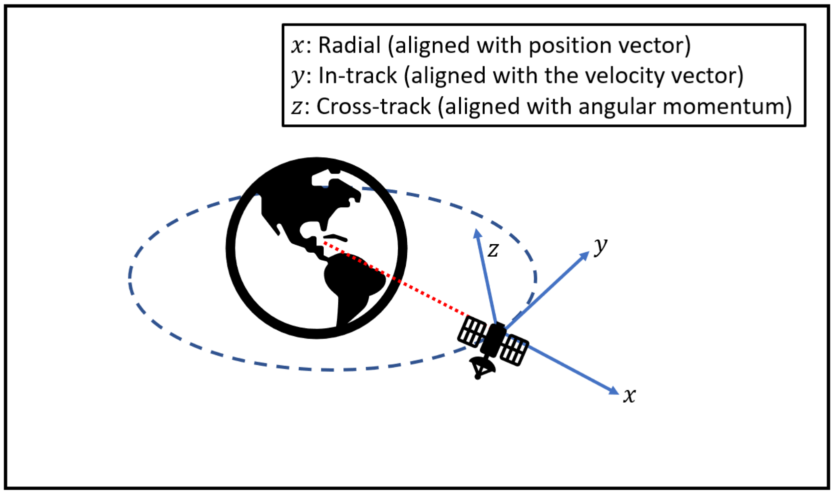

Figure 2.1: Graphic representation of non-inertial body fixed frame of reference used by the CWH equations.

$\mu = 3.986 \times 10^{14}$ m^3·s^{-2}, orbital radius of the chief R_0, and mass of the deputy m_c. Figure 2.1 is a graphic representation of the non-inertial body fixed frame of reference for the CWH equations.

I rewrite the second order equations of motion in (2.8) as the first order system,

$$\underbrace{\begin{bmatrix} \dot{x} \\ \dot{y} \\ \dot{z} \\ \ddot{x} \\ \ddot{y} \\ \ddot{z} \end{bmatrix}}_{\dot{\vec{x}}} = \underbrace{\begin{bmatrix} 0 & 0 & 0 & 1 & 0 & 0 \\ 0 & 0 & 0 & 0 & 1 & 0 \\ 0 & 0 & 0 & 0 & 0 & 1 \\ 3\omega^2 & 0 & 0 & 0 & 2\omega & 0 \\ 0 & 0 & 0 & -2\omega & 0 & 0 \\ 0 & 0 & -\omega^2 & 0 & 0 & 0 \end{bmatrix}}_{A_c} \underbrace{\begin{bmatrix} x \\ y \\ z \\ \dot{x} \\ \dot{y} \\ \dot{z} \end{bmatrix}}_{\vec{x}} + \underbrace{\begin{bmatrix} 0 & 0 & 0 \\ 0 & 0 & 0 \\ 0 & 0 & 0 \\ \frac{1}{m_c} & 0 & 0 \\ 0 & \frac{1}{m_c} & 0 \\ 0 & 0 & \frac{1}{m_c} \end{bmatrix}}_{B_c} \underbrace{\begin{bmatrix} F_x \\ F_y \\ F_z \end{bmatrix}}_{\vec{U}} \tag{2.9}$$

The autonomous first order system (2.9) has a closed form solution [67] for the state at time t for a given initial condition $\vec{x}(0)$, $\vec{x}(t) = e^{A_c t}\vec{x}(0)$ where

$$e^{A_c t} = \begin{bmatrix} 4-3\cos(\omega t) & 0 & 0 & \frac{1}{\omega}\sin(\omega t) & \frac{2}{\omega}(1-\cos(\omega t)) & 0 \\ 6(\sin(\omega t)-\omega t) & 1 & 0 & \frac{2}{\omega}(\cos(\omega t)-1) & \frac{4}{\omega}\sin(\omega t)-3t & 0 \\ 0 & 0 & \cos(\omega t) & 0 & 0 & \frac{1}{\omega}\sin(\omega t) \\ 3\omega\sin(\omega t) & 0 & 0 & \cos(\omega t) & 2\sin(\omega t) & 0 \\ 6\omega(\cos(\omega t)-1) & 0 & 0 & -2\sin(\omega t) & 4\cos(\omega t)-3 & 0 \\ 0 & 0 & -\omega\sin(\omega t) & 0 & 0 & \cos(\omega t) \end{bmatrix} \tag{2.10}$$

I discretize the first order system with sampling period $k = \Delta t$ seconds and impulsive control assumptions. Then, I arrive at the discrete time linear time invariant system

$$\vec{x}(k+1) = A\vec{x}(k) + B\vec{u}(k) \tag{2.11a}$$

$$A = e^{A_c \Delta t} \tag{2.11b}$$

$$B = e^{A_c \Delta t} B_c \tag{2.11c}$$

Through the remainder of this work, I assume an additive noise term is added to (2.11) such that the dynamics become

$$\vec{x}(k+1) = A\vec{x}(k) + B\vec{u}(k) + \vec{\boldsymbol{w}}(k) \tag{2.12}$$

Here, the disturbance is intended to capture uncertainties that can arise from faulty thrusters or sensors, third body gravitational effects, and other noise processes that can corrupt satellite dynamics.

Definition 2.2 (Reverse convex constraint)**.** *A reverse convex constraint is the complement of a convex constraint, that is,* $f(x) \geq c$ *for a convex function* $f : \mathbb{R} \to \mathbb{R}$ *and a scalar* $c \in \mathbb{R}$.

I presume each vehicle has a desired polytopic target sets that it must reach, known and static obstacles that it must avoid, as well as the need for collision avoidance between vehicles. Each of these constraints are considered probabilistically and must all hold with desired likelihoods. Formally,

$$\mathbb{P}\left(\bigcap_{i=1}^{N_v}\bigcap_{k=1}^{N} \vec{\boldsymbol{x}}_i(k) \in \mathcal{T}_i(k)\right) \geq 1-\alpha \tag{2.13a}$$

$$\mathbb{P}\left(\bigcap_{i=1}^{N_v}\bigcap_{k=1}^{N} \|S(\vec{\boldsymbol{x}}_i(k) - \vec{o}(k))\| \geq r\right) \geq 1-\beta \tag{2.13b}$$

$$\mathbb{P}\left(\bigcap_{i=1}^{N_v-1}\bigcap_{j=i+1}^{N_v}\bigcap_{k=1}^{N} \|S(\vec{\boldsymbol{x}}_i(k) - \vec{\boldsymbol{x}}_j(k))\| \geq r\right) \geq 1-\gamma \tag{2.13c}$$

I presume convex, compact, and polytopic sets $\mathcal{T}_i(k) \subseteq \mathbb{R}^n$, known matrix $S \in \mathbb{R}^{q\times n}$ designed to extract the translational elements of the state, positive scalar $r \in \mathbb{R}_+$, static object locations $\vec{o} \in \mathbb{R}^n$, and probabilistic violation thresholds α, β, γ. Note, the collision avoidance constraints are reverse convex as per Definition 2.2. For the remainder of this work, I will define the polytopic sets $\mathcal{T}_i(k)$ as the intersection of N_{ik} half-space constraints,

$$\mathcal{T}_i(k) \equiv \left\{ \vec{\boldsymbol{x}}_i(k) \middle| \bigcap_{a=1}^{N_{ik}} \vec{G}_{ika}\vec{\boldsymbol{x}}_i(k) \leq h_a \right\} \tag{2.14}$$

I presume a convex performance objective $J : \mathcal{X}^{Nv} \times \mathcal{U}^{Nv} \to \mathbb{R}$. I seek to solve the following optimization problem.

$$\underset{\vec{U}_1,\ldots,\vec{U}_{N_v}}{\text{minimize}} \quad J\left(\vec{\boldsymbol{X}}_1,\ldots,\vec{\boldsymbol{X}}_{N_v},\vec{U}_1,\ldots,\vec{U}_{N_v}\right) \tag{2.15a}$$

$$\text{subject to} \quad \vec{U}_i \in \mathcal{U}^N, \tag{2.15b}$$

$$\text{Stochastic linear dynamics (2.6) with } \vec{x}_i(0) \tag{2.15c}$$

$$\text{Probabilistic constraints (2.13)} \tag{2.15d}$$

where $\vec{\boldsymbol{X}}_i = \begin{bmatrix} \vec{\boldsymbol{x}}_i^\top(1) & \ldots & \vec{\boldsymbol{x}}_i^\top(N) \end{bmatrix}^\top$ is the concatenated state vector for vehicle i.

Throughout this work, I address the following problem,

Problem 1. *Solve the stochastic optimization problem* (2.15) *with open loop controllers* $\vec{U}_1, \ldots, \vec{U}_{N_v} \in \mathcal{U}^N$*, and probabilistic violation thresholds* α*,* β*, and* γ*.*

The main challenge in solving Problem 1 is assuring the joint chance constraints constraints (2.13). In general, the optimization problem (2.15) is non-convex because of the probabilistic constraints. For an arbitrary disturbance, there is no guarantee that the probability function has a closed form, let alone a convex one. Particularly, the reverse-convex collision avoidance constraints are inherently non-convex and for most disturbance assumptions lack a known distribution form. This is the case for many disturbances, such as Multivariate t, Weibull, or gamma disturbances.

Chapter 3

Quantile Based Approach

3.1 Introduction

As missions with multiple space vehicles become commonplace, new technologies are required for effective autonomous operation that enable coordination amongst multiple vehicles in a challenging environment, despite limited resources (such as fuel). Autonomy for spacecraft must accommodate the need to plan and optimize under uncertainty, which may arise due to modeling inaccuracies, nonlinearities in sensing and estimation processes, and actuation mechanisms. Many of these uncertainties may be stochastic, but may not necessarily follow Gaussian distributions. Constructing optimal controllers to ensure collision avoidance and performance constraints, despite such stochasticity, requires accurate assessment of risk.

Algorithms for stochastic optimization often face significant computational hurdles that can create undesirable trade-offs with accuracy [68], particularly in systems with limited computation. Particle approaches [4, 2] have employed sample reduction techniques for convex [44, 45] and non-convex [5] problems, but still are subject to tradeoffs between accuracy and computational burden. Approaches that rely upon moments [69, 70, 1] may create excessive conservativism, and typically require an iterative approach to controller synthesis and risk allocation, to circumvent non-convexity that arises in the process of separating joint chance constraints into individual chance constraints via Boole's inequality [71, 25, 72]. Recent work has employed Fourier transforms in combination with piecewise affine approximations [33, 29], to evaluate chance constraints without quadrature for LTI systems with disturbance processes that have log-concave pdf.

My approach to constrained stochastic optimization of LTI systems with potentially non-Gaussian disturbances is based on approximations of a quantile function, the inverse of the cdf. I consider multi-vehicle planning problems with two types of constraints: a) norm-based collision avoidance constraints, and b) polytopic feasibility constraints. These forms readily arise when vehicles must avoid each other, as well as static obstacles in the environment, while remaining in some desirable polytopic set and reaching a desired convex target set. I show that these constraints can be reduced to chance constraints that are affine in the control input and disturbance. The norm-based constraints yield reverse convex constraints and the feasibility constraints yield convex constraints. In both cases, assessment of a quantile function, the inverse of the cdf, is necessary to evaluate these constraints. However, quantile functions are notoriously difficult to compute and often do not have closed form.

My approach is to construct a Taylor series approximation of the quantile function that is amenable to arbitrary distributions. I generate an affine approximation of the quantile by evaluating the Taylor series approximation at regular intervals to yield a piecewise affine constraint that can be embedded within a standard difference of convex programming framework [64]. I employ an iterative approach as in [25], [3], to allocate risk and synthesize an optimal control. Although iterative, my approach can be considerably faster than a particle approach because it exploits convexity. *The main contribution of this chapter is the construction of a first-order quantile approximation that enables efficient evaluation of chance constraints.* My approach relies upon affine structure in the collision avoidance and target set chance constraints.

The chapter is organized as follows. Section 3.2 provides additional preliminaries required for Problem 1. Section 3.3 reformulates the chance constraints by approximating the quantile function. Section 3.4 demonstrates my approach on three multi-satellite rendezvous problems, and Section 3.5 provides concluding remarks.

3.2 Problem Formulation

In addition to the problem formulation in Chapter 2.4, I add several assumptions and observations that will be required for the work in this chapter. I first note that each constraint in (2.13) can be rewritten in one of the three following forms, which are convex in the control input and affine in a random variable (as shown in Section 3.3.1).

$$\mathbb{P}\left(\bigcap_{i=1}^{N_v}\bigcap_{k=1}^{N}\bigcap_{a=1}^{N_{ik}} f_a(\vec{x}_i(0),\vec{U}_i) + g_a\boldsymbol{y}_a \leq c_a\right) \geq 1-\alpha \tag{3.1a}$$

$$\mathbb{P}\left(\bigcap_{i=1}^{N_v}\bigcap_{k=1}^{N} f_{ik}(\vec{x}_i(0),\vec{U}_i) - g_{ik}\boldsymbol{y}_{ik} \geq c_{ik}\right) \geq 1-\beta \tag{3.1b}$$

$$\mathbb{P}\left(\bigcap_{i=1}^{N_v-1}\bigcap_{j=i+1}^{N_v}\bigcap_{k=1}^{N} f_{ijk}(\vec{x}_i(0)-\vec{x}_j(0),\vec{U}_i-\vec{U}_j) - g_{ijk}\boldsymbol{y}_{ijk} \geq c_{ijk}\right) \geq 1-\gamma \tag{3.1c}$$

As a reminder N_{ik}, as it appears in (3.1a), is the number of half-space constraints in the target set $\mathcal{T}_i(k)$. The function $f : \mathcal{X}\times\mathcal{U}^N \to \mathbb{R}$ is convex, $g \in \mathbb{R}_+$ is a positive scalar, $\boldsymbol{y}$ is a real and continuous random variable that is a function of the disturbance, and c is a constant.

For Problem 1 to be tractable for arbitrary disturbances, I make several key assumptions about the disturbance and its resulting impact on the constraints.

Assumption 3.1. *The pdf of the random variable* $\boldsymbol{y}$ *can be differentiated at least* N_d *times, and the quantile of* $\boldsymbol{y}$ *must be convex and non-negative in the region* $[1-\alpha, 1]$, $[1-\beta, 1]$, *or* $[1-\gamma, 1]$.

This assumption is not overly restrictive, as it can be met by most distributions. Differentiability is needed for the Taylor series approximation of the quantile; fewer derivatives means a coarser approximation. Convexity over this range is met when 1) the first derivative of the pdf is strictly negative on $\{y \mid \Phi_{\boldsymbol{y}}(y) \in [1-\alpha, 1]\}$, and 2) the pdf converges to zero as y increases on $\{y \mid \Phi_{\boldsymbol{y}}(y) \in [1-\alpha, 1]\}$. The intuition behind these criteria is that when both conditions are met, the cdf will be strictly concave on $\{y \mid \Phi_{\boldsymbol{y}}(y) \in [1-\alpha, 1]\}$, and hence, the quantile will be strictly convex. However, I note that not all distributions will have a convex quantile in $[1-\alpha, 1]$: Consider the beta distribution with shape parameters (α_0, β_0) both less than one, which results in a bi-modal distribution with modes at both ends of the support.

The reformulation (3.1a)-(3.1c) requires the quantile evaluations be non-negative to tighten the probabilistic constraints. For constraints like (2.13a), many models assume a symmetric distribution and $\mathbb{E}(\boldsymbol{y}) = 0$. This implies the quantile is non-negative in the convex region. Similarly, the use of distance metrics in (2.13b)-(2.13c) imply $\boldsymbol{y}$ will be strictly positive. In the event that this is not the case, a slight modification to (3.1a)-(3.1b) and Assumption 3.1 can be made to maintain tightening of the constraint.

Assumption 3.2. *The random variable $\boldsymbol{y}$ has a known quantile, $\Phi_{\boldsymbol{y}}^{-1}(p)$, for some $p \in (0, 1)$.*

This assumption is easily met by symmetric distributions; many have either a location parameter that represents the median or an easy way to find the median. For distributions on a semi-infinite support or that are skewed, satisfying this assumption may be more difficult. Approximations via brute force or other methods may be distribution dependent. In practice, it may be sufficient to choose $\Phi_{\boldsymbol{y}}^{-1}(1-\varepsilon)$ to be some value approaching the upper end of the support, setting ε to be arbitrarily small.

Problem 1.1. *Under Assumptions 3.1-3.2, solve Problem 1 with probabilistic violation thresholds α, β, and γ for open loop controllers $\vec{U}_1, \ldots, \vec{U}_{N_v} \in \mathcal{U}^N$.*

The main challenge in solving Problem 1.1 is assuring (2.15d). In this chapter, I use Assumptions 3.1-3.2 to introduce quantile based reformulations.

3.3 Methods

To solve Problem 1.1, I employ a standard risk allocation framework in conjunction with a quantile reformulation. I then approximate the quantile function over its convex region, via piecewise affine constraints. Lastly, I employ difference of convex programming to iteratively solve reverse convex constraints to a local optimum. These reformulations enable solution via a series of quadratic programs.

3.3.1 Reformulation of Constraints

Polytopic Target Set Constraint

Consider a polytopic target set constraint, captured by (2.13a) as

$$\mathbb{P}\left(\bigcap_{i=1}^{N_v}\bigcap_{k=1}^{N}\vec{\boldsymbol{x}}_i(k)\in\mathcal{T}_i(k)\right)\geq 1-\alpha, \tag{3.2}$$

From (2.14), I can write

$$\begin{aligned}
& & \vec{\boldsymbol{x}}_i(k)\in\mathcal{T}_i(k) & \qquad (3.3a)\\
\Leftrightarrow & & \bigcap_{a=1}^{N_{ik}}\vec{G}_{ika}\vec{\boldsymbol{x}}_i(k)\leq h_{ika} & \qquad (3.3b)\\
\Leftrightarrow & & \bigcap_{a=1}^{N_{ik}}\underbrace{\vec{G}_{ika}A^k\vec{x}_i(0)+\vec{G}_{ika}\mathcal{C}(k)\vec{U}_i}_{f_a(\vec{x}_i(0),\vec{U}_i)}+\underbrace{\vec{G}_{ika}\mathcal{D}(k)\vec{\boldsymbol{W}}_i}_{g_a\boldsymbol{y}_a}\leq\underbrace{h_{ika}}_{c_a} & \qquad (3.3c)
\end{aligned}$$

and

$$\mathbb{P}\left(\bigcap_{i=1}^{N_v}\bigcap_{k=1}^{N} \vec{\boldsymbol{x}}_i(k) \in \mathcal{T}_i(k)\right) \geq 1-\alpha \quad (3.4a)$$

$$\Leftrightarrow \quad \mathbb{P}\left(\bigcap_{i=1}^{N_v}\bigcap_{k=1}^{N}\bigcap_{a=1}^{N_{ik}} \underbrace{\vec{G}_{ika}A^k\vec{x}_i(0) + \vec{G}_{ika}\mathcal{C}(k)\vec{U}_i}_{f_a(\vec{x}_i(0),\vec{U}_i)} + \underbrace{\vec{G}_{ika}\mathcal{D}(k)\vec{\boldsymbol{W}}_i}_{g_a\boldsymbol{y}_a} \leq \underbrace{h_{ika}}_{c_a}\right) \geq 1-\alpha \quad (3.4b)$$

as in (3.1a), with random variable $\boldsymbol{y}_a$ that is a linear transformation of $\vec{\boldsymbol{W}}_i$.

Norm Based Constraint

For probabilistic collision avoidance between vehicles i and j with minimum L_2 distance $r \in \mathbb{R}_+$ and violation threshold $1-\gamma$, I consider

$$\mathbb{P}\left(\bigcap_{i=1}^{N_v-1}\bigcap_{j=i+1}^{N_v}\bigcap_{k=1}^{N} \|S(\vec{\boldsymbol{x}}_i(k) - \vec{\boldsymbol{x}}_j(k))\| \geq r\right) \geq 1-\beta \quad (3.5)$$

The derivation here follows similarly for the collision avoidance constraint with a (possibly static) object. Using the reverse triangle inequality, I obtain

$$\|S(\vec{\boldsymbol{x}}_i(k) - \vec{\boldsymbol{x}}_j(k)\| \quad (3.6a)$$

$$= \|SA^k(\vec{x}_i(0) - \vec{x}_j(0)) + S\mathcal{C}(k)(\vec{U}_i - \vec{U}_j) + S\mathcal{D}(k)(\vec{\boldsymbol{W}}_i - \vec{\boldsymbol{W}}_j)\| \quad (3.6b)$$

$$\geq \underbrace{\|SA^k(\vec{x}_i(0) - \vec{x}_j(0)) + S\mathcal{C}(k)(\vec{U}_i - \vec{U}_j)\|}_{f_{ijk}(\vec{x}_i(0)-\vec{x}_j(0),\vec{U}_i-\vec{U}_j)} - \underbrace{\|S\mathcal{D}(k)(\vec{\boldsymbol{W}}_i - \vec{\boldsymbol{W}}_j)\|}_{g_{ijk}\boldsymbol{y}_{ijk}} \quad (3.6c)$$

hence

$$\mathbb{P}\left(\bigcap_{i=1}^{N_v-1} \bigcap_{j=i+1}^{N_v} \bigcap_{k=1}^{N} \|\vec{\boldsymbol{x}}_i(k) - \vec{\boldsymbol{x}}_j(k)\| \geq r\right) \tag{3.7a}$$

$$\geq \mathbb{P}\left(\bigcap_{i=1}^{N_v-1} \bigcap_{j=i+1}^{N_v} \bigcap_{k=1}^{N} \underbrace{\|SA^k(\vec{x}_i(0)-\vec{x}_j(0))+S\mathcal{C}(k)(\vec{U}_i-\vec{U}_j)\|}_{f_{ijk}(\vec{x}_i(0)-\vec{x}_j(0),\vec{U}_i-\vec{U}_j)} - \underbrace{\|S\mathcal{D}(k)(\vec{\boldsymbol{W}}_i-\vec{\boldsymbol{W}}_j)\|}_{g_{ijk}\boldsymbol{y}_{ijk}} \geq \underbrace{r}_{c_{ijk}}\right) \tag{3.7b}$$

$$\geq 1-\gamma \tag{3.7c}$$

as in (3.1c). Note that this is a one-way implication.

3.3.2 Quantile Reformulation

First, consider the reformulation of (3.1a). I take the complement of (3.1a) such that the probability function consists of a union of events,

$$\mathbb{P}\left(\bigcup_{i=1}^{N_v} \bigcup_{k=1}^{N} \bigcup_{a=1}^{N_{ik}} \left[f_a(\vec{x}_i(0), \vec{U}_i) + g_a \boldsymbol{y}_a \leq c_a\right]^c\right) \leq \alpha \tag{3.8}$$

Next, I employ Boole's inequality to create an upper bound for the original probability.

Theorem 3.1. *Boole's Inequality [61, Theorem 1.2.11.b] If $\mathbb{P}_{\boldsymbol{x}}$ is a probability function, then $\mathbb{P}(\cup_{i=1}^{\infty} \boldsymbol{x} \in \mathcal{S}_i) \leq \sum_{i=1}^{\infty} \mathbb{P}(\boldsymbol{x} \in \mathcal{S}_i)$ for any sets $\mathcal{S}_1, \mathcal{S}_2, \ldots$.*

Hence,

$$\mathbb{P}\left(\bigcup_{i=1}^{N_v} \bigcup_{k=1}^{N} \bigcup_{a=1}^{N_{ik}} f_a(\vec{x}_i(0), \vec{U}_i) + g_a \boldsymbol{y}_a \geq c_a\right) \tag{3.9}$$

$$\leq \sum_{i=1}^{N_v} \sum_{k=1}^{N} \sum_{a=1}^{N_{ik}} \mathbb{P}\Big(f_a(\vec{x}_i(0), \vec{U}_i) + g_a \boldsymbol{y}_a \geq c_a\Big) \tag{3.10}$$

Using the approach in [25], I introduce risk variables ω_{ika} to allocate risk to each of the individual probabilities

$$\mathbb{P}\Big(f_a(\vec{x}_i(0),\vec{U}_i)+g_a\boldsymbol{y}_a\geq c_a\Big)\geq 1-\omega_{ika} \tag{3.11a}$$

$$\sum_{i=1}^{N_v}\sum_{k=1}^{N}\sum_{a=1}^{N_{ik}}\omega_{ika}\leq\alpha \tag{3.11b}$$

$$\omega_{ika}\geq 0 \tag{3.11c}$$

By inverting the argument of (3.11a), I obtain

$$\begin{aligned}
&\mathbb{P}\Big(\boldsymbol{y}_a\leq\tfrac{1}{g_a}\Big(c_a-f_a(\vec{x}_i(0),\vec{U}_i)\Big)\Big) &&\geq 1-\omega_{ika}\\
\Leftrightarrow\quad &\tfrac{1}{g_a}\Big(c_a-f_a(\vec{x}_i(0),\vec{U}_i)\Big) &&\geq\Phi^{-1}_{\boldsymbol{y}_a}(1-\omega_{ika})
\end{aligned} \tag{3.12}$$

Rearranging (3.12), I obtain

$$f_a(\vec{x}_i(0),\vec{U}_i)\leq c_a-g_a\Phi^{-1}_{\boldsymbol{y}_a}(1-\omega_{ika}) \tag{3.13}$$

The reformulation of (3.1b)-(3.1c) proceeds similarly, and results in reverse convex constraints.

By combining the reformulations of (3.1a)-(3.1c), I obtain

$$f_a(\vec{x}_i(0),\vec{U}_i)\ \leq c_a-g_a\Phi^{-1}_{\boldsymbol{y}_a}(1-\omega_{ika}) \tag{3.14a}$$

$$\sum_{i=1}^{N_v}\sum_{k=1}^{N}\sum_{a=1}^{N_{ik}}\omega_{ika}\leq\alpha \tag{3.14b}$$

$$\omega_{ika}\geq 0 \tag{3.14c}$$

$$f_{ijk}(\vec{x}_i(0)-\vec{x}_j(0),\vec{U}_i-\vec{U}_j)\geq c_{ijk}+g_{ijk}\Phi^{-1}_{\boldsymbol{y}_{ijk}}(1-\omega_{ijk}) \tag{3.14d}$$

$$\sum_{i=1}^{N_v-1}\sum_{j=i+1}^{N_v}\sum_{k=1}^{N}\omega_{ijk}\leq\gamma \tag{3.14e}$$

$$\omega_{ijk}\geq 0 \tag{3.14f}$$

Lemma 3.1. *For the controller* $\vec{U}_1, \ldots, \vec{U}_{N_v}$*, if there exists risk allocation variables* ω_{ika} *satisfying* (3.14b)-(3.14c) *for constraints in the form of* (3.14a) *and risk allocation variables* ω_{ijk} *satisfying* (3.14e)-(3.14f) *for constraints in the form of* (3.14d)*, then* $\vec{U}_1, \ldots, \vec{U}_{N_v}$ *satisfy* (2.15d).

Proof. Satisfaction of (3.14b)-(3.14c) and (3.14e)-(3.14f) implies (3.10) meets the probabilistic violation thresholds α, β, and γ. Boole's inequality and De Morgan's laws guarantee (2.15d) is satisfied. □

The constraint (3.14a) is convex in $\vec{U}$, however (3.14d) is reverse convex. Additionally, while Assumption 3.1 guarantees the convexity of (3.14a), the expressions $\Phi^{-1}_{\boldsymbol{y}_a}(1-\omega_{ika})$ and $\Phi^{-1}_{\boldsymbol{y}_{ijk}}(1-\omega_{ijk})$ are non-conic and cannot be readily handled by off-the-shelf solvers.

3.3.3 Quantile Approximation

The quantile for many continuous random variables does not have a closed form, and brute force numerical approximations may be costly to compute. Approximation methods are typically tailored to specific distributions [73], [74], [75], although some recent approaches have focused on generic methods to approximate quantile functions of arbitrary distributions.

I use an approach that relies on a Taylor series expansion of the quantile [76]. For a random variable X, and an initial evaluation point $\Phi_X^{-1}(p_0)$ for $p_0 \in (0,1)$, [76] proposes an iterative process that evaluates a finite Taylor series expansion at points that are an interval $h \in \mathbb{R}$ apart. With $N_d + 1$ Taylor series terms, a quantile approximation at $p_{c+1} = p_c + h$ is described by

$$\hat{\Phi}_X^{-1}(p_{c+1}) = \Phi_X^{-1}(p_c) + \sum_{d=1}^{N_d+1} (-1)^d \left.\frac{\partial^d \Phi_X^{-1}(p)}{(\partial\eta)^d}\right|_{p=p_c} \cdot \frac{\log(p_{c+1}/p_c)^d}{d!}$$

where $\eta = -\log(p)$ is a variable substitution used for numerical tractability. Typically, $N_d = 3$ or 4 derivatives are sufficient, and steps c are computed until a predetermined terminating percentile.

Derivatives of the quantile are obtained via the inverse function theorem [77],

$$\frac{\partial}{\partial \eta}\Phi_X^{-1}(p) = -\frac{e^{-\eta}}{\phi_X(p)} \tag{3.15}$$

where the i^{th} derivative of the quantile will elicit the the $i-1^{\text{th}}$ derivative of $\phi_X(\cdot)$. Analytical expressions for the first four derivatives are provided in [76].

The error in the approximation

$$\epsilon = \Phi_X^{-1}(\cdot) - \hat{\Phi}_X^{-1}(\cdot) \tag{3.16}$$

is characterized by the unused Taylor series terms, such that

$$\epsilon \in O\left([h/\min(p_{l-1}, p_0)]^{N_d}\right) \tag{3.17}$$

so that ϵ converges to 0 as $h \to 0$ and $N_d \to \infty$ [76].

I presume a piecewise affine approximation to connect evaluation points. However, to ensure a reasonable number of variables and constraints in the optimization, I selectively choose evaluation points, rather than connecting all points. Given an arbitrarily chosen error threshold, ξ, I seek a subset of l^* affine terms, such that

$$\hat{\Phi}_X^{-1}(p_c) \leq \max_{q \in \mathbb{N}_{[1,l^*]}} \left(\underline{m}_{ikaq}\,\omega_{ika} + \underline{c}_{ikaq}\right) \leq \hat{\Phi}_X^{-1}(p_c) + \xi \tag{3.18}$$

for slopes and intercepts $\underline{m}_{ikaq}$, $\underline{c}_{ikaq}$, respectively, for $\forall q \in \mathbb{N}_{[1,l^*]}$, as shown in Figure 3.1. Here, i and j refer to the vehicle and constraint indices, respectively. I propose Algorithm 2 to compute the reduced set $\{\underline{m}_{ikaq}, \underline{c}_{ikaq} \mid \forall q \in \mathbb{N}_{[1,l^*]}\}$. Note that ξ will affect the cardinality of the set $\{\underline{m}_{ikaq}, \underline{c}_{ikaq} \mid \forall q \in \mathbb{N}_{[1,l^*]}\}$, thus changing the number of constraints. However, the choice of ξ does not effect the analysis presented in this work.

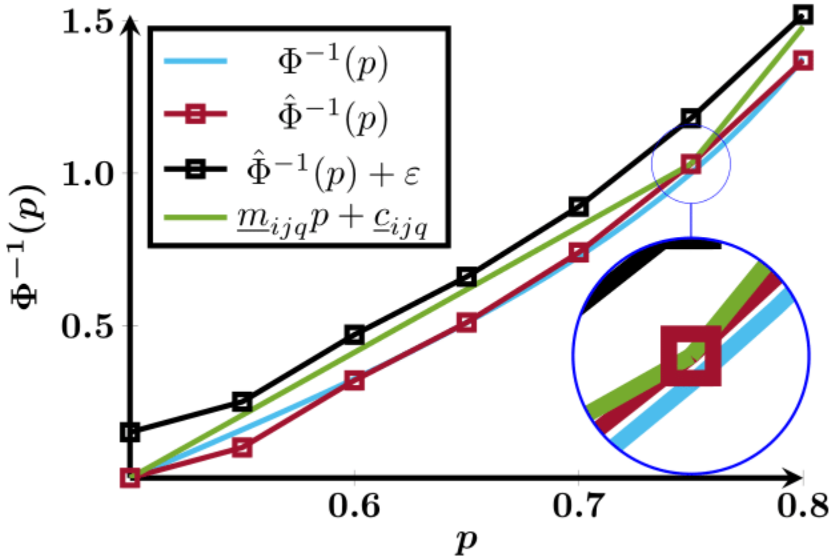

Figure 3.1: Quantile approximation method applied to a Cauchy distribution. The blue line represents the true quantile, the red points result from a Taylor series approximation (3.15), the black points show the error threshold ξ, and the green lines represent the affine approximation (3.18).

Further, although the error threshold, ξ, is formulated with respect to the approximation (not the true quantile), Assumption 3.1 guarantees that (3.18) becomes an affine overapproximation of the true quantile as $\epsilon \to 0$.

I reformulate (3.14a) with the piecewise affine approximation (3.18), as

$$f_a(\vec{x}_i(0), \vec{U}_i) \leq c_a - \frac{1}{g_a}\left(\underline{s}_{ika}\right) \tag{3.19a}$$

$$\underline{s}_{ika} \geq \underline{m}_{ikaq}\,\omega_{ika} + \underline{c}_{ikaq} \qquad \forall q \in \mathbb{N}_{[1,l^*]} \tag{3.19b}$$

$$\textstyle\sum_{i=1}^{N_v}\sum_{k=1}^{N}\sum_{a=1}^{N_{ik}} \omega_{ika} \leq \alpha \tag{3.19c}$$

$$\omega_{ika} \geq 0 \tag{3.19d}$$

with slack variables $\underline{s}_{ika}$. A similar reformulation can be posed for (3.14d). In the limit, as (3.18) becomes an affine overapproximation of $\Phi^{-1}(\cdot)$, (3.19) is a tightening of (3.14) and Assumption 3.1 ensures the convexity of (3.19).

Lemma 3.2. *For a controller $\vec{U}_1, \ldots, \vec{U}_{N_v}$, if there exists risk allocation variables ω_{ika}*

Algorithm 2: Computing $\{\underline{m}_{ijq}, \underline{c}_{ijq}\}$ from $\phi_{\boldsymbol{y}}$

Input: The pdf of $\boldsymbol{y}$, $\phi_{\boldsymbol{y}}$, and its derivatives $\phi_{\boldsymbol{y}}^{(1)}, \ldots, \phi_{\boldsymbol{y}}^{(n)}$, instantiating point p_0, termination point p_l, known quantile $\Phi_{\boldsymbol{y}}^{-1}(p_0)$, step size h, and maximum error threshold ξ.

Output: Affine terms of $\hat{\Phi}_{\boldsymbol{y}}^{-1}$, $\{\underline{m}_{ijq}, \underline{c}_{ijq}\}$

for $p_i = p_0 + h$ ***to*** p_l ***by*** h **do**
    $\mathcal{P}_i \leftarrow \hat{\Phi}^{-1}(p_i)$ # Via (3.15)
end
$i \leftarrow 0$
while $i < l$ **do**
    for $j = l$ ***to*** $i + 1$ ***by*** -1 **do**
        $\underline{m} \leftarrow \frac{\mathcal{P}_j - \mathcal{P}_i}{h(j-i)}$
        $\underline{c} \leftarrow \mathcal{P}_i - p_i \times \underline{m}$
        for $y = i + 1$ ***to*** $l - 1$ ***by*** 1 **do**
            $\epsilon_y = \mathcal{P}_y - (p_y \times \underline{m} + \underline{c})$
            if $\epsilon_y > \xi$ **then**
                then next j
            end
        end
        $\{\underline{m}_{ijq}, \underline{c}_{ijq}\} \leftarrow \underline{m}, \underline{c}$
        break
    end
    $i \leftarrow j$
end

and ω_{ijk}, and slack variables $\underline{s}$ satisfying (3.19)*, then $\vec{U}_1, \ldots, \vec{U}_{N_v}$ asymptotically satisfies* (2.15d) *as $h \to 0$ and $n \to \infty$.*

Proof. By (3.17), the approximation error $\epsilon \to 0$ as $h \to 0$ and $n \to \infty$. In this case, (3.19) conservatively enforces (3.14) by (3.18). By Lemma 3.1, (2.15d) is conservatively enforced. □

I note that a limitation of my approach is that I can only guarantee constraint satisfaction in the limit. In practice, a sufficiently differentiable distribution will likely behave well enough that four or more derivatives will result in an approximation with small errors given a small enough step size. Many common distributions will fall into this category, especially those of the exponential family of distributions. Where this methodology will likely fail is multi-modal distributions or distributions that have a non-smooth terminating derivative. I have found empirically that a step size, h, on the order of 10^{-6}, is sufficiently small that the approximation error, (3.16), is also on the order of 10^{-6}.

3.3.4 Difference of Convex Programming

Combining the results from Sections 3.3 and 3.3.3 I obtain a new optimization problem.

$$\underset{\substack{\vec{U}_1,\ldots,\vec{U}_{N_v} \\ \omega_{ika},\omega_{ijk} \\ \underline{s}_{ika},\ldots,\underline{s}_{ijk}}}{\text{minimize}} \quad J\left(\boldsymbol{X}_1, \ldots, \vec{\boldsymbol{X}}_{N_v}, \vec{U}_1, \ldots, \vec{U}_{N_v}\right) \tag{3.20a}$$

$$\text{subject to} \quad \vec{U}_1, \ldots, \vec{U}_{N_v} \in \mathcal{U}^N, \tag{3.20b}$$

$$\text{Dynamics (2.6) with initial states } \vec{x}_1(0), \ldots, \vec{x}_{N_v}(0) \tag{3.20c}$$

$$\text{Constraints (3.19)} \tag{3.20d}$$

Reformulation 3.1. *Under Assumptions 3.1-3.2, solve the stochastic optimization problem* (3.20) *with probabilistic violation thresholds α, β, and γ for open loop controllers*

$\vec{U}_1, \ldots, \vec{U}_{N_v} \in \mathcal{U}^N$, *and optimization parameters* λ_{ijk}.

Lemma 3.3. *Solutions to Reformulation 3.1 are conservative solutions to Problem 1.1 asymptotically.*

Proof. Lemma 3.2 guarantee the probabilistic constraints (2.13) are satisfied asymptotically as $h \to 0$ and $n \to \infty$. All other factors remain equivalent. □

While (3.20a)-(3.20c) are convex, (3.20) is difference of convex due to the constraint (3.14d) which is difference of convex when written as

$$g_{ijk}\Phi^{-1}_{\boldsymbol{y}_{ijk}}(1-\omega_{ijk}) - f_{ijk}(\vec{x}_i(0)-\vec{x}_j(0), \vec{U}_i - \vec{U}_j) \leq -c_{ijk} \tag{3.21}$$

We employ the convex-concave procedure [64] as outlined in Chapter 2.3.2 to solve (3.20). By taking a first order approximation of $f_{ijk}(\vec{x}_i(0) - \vec{x}_j(0), \vec{U}_i - \vec{U}_j)$, we can solve the difference of convex function optimization problem iteratively as a convex optimization problem. By updating the first order approximation at each iteration, the convex-concave procedure solves to a local optimum. Here, the first order approximation transforms the difference of convex function constraint (3.14d) into the convex constraint

$$\begin{aligned}
&-\underbrace{\left\| SA^k(\vec{x}_i(0)-\vec{x}_j(0)) + S\mathcal{C}(k)(\vec{U}_i^p - \vec{U}_j^p)\right\|^2}_{\text{Evaluation of } \|SA^k(\vec{x}_i(0)-\vec{x}_j(0))+S\mathcal{C}(k)(\vec{U}_i-\vec{U}_j)\|^2} \\
&-\underbrace{2\left(SA^k(\vec{x}_i(0)-\vec{x}_j(0)) + S\mathcal{C}(k)(\vec{U}_i^p - \vec{U}_j^p)\right)^\top S\mathcal{C}(k)\left((\vec{U}_i - \vec{U}_j) - (\vec{U}_i^p + \vec{U}_j^p)\right)}_{\text{Gradient of } \|SA^k(\vec{x}_i(0)-\vec{x}_j(0))+S\mathcal{C}(k)(\vec{U}_i-\vec{U}_j)\|^2} \\
&\leq \left(-r + \frac{1}{g_a}\left(\underline{s}_{ika}\right)\right)^2
\end{aligned} \tag{3.22}$$

where the superscript p indicated the value from the previous iteration's solution. The main benefit of solving this problem with the convex-concave procedure is the first order approximation makes the constraint convex while maintaining the probabilistic assurances. This problem can be readily solved via the methodologies outlined in Chapter

2.3.2.

3.4 Experimental Results

I demonstrate my algorithms in simulation on a multi-vehicle spacecraft navigation problem with three disturbances: Gaussian, Cauchy, and multivariate t. All computations were done on a 1.80GHz i7 processor with 16GB of RAM, using MATLAB, CVX [78] and Gurobi [79]. Polytopic construction and plotting was done with MPT3 [80]. All code is available at https://github.com/unm-hscl/shawnpriore-approximate-quantiles and https://github.com/unm-hscl/shawnpriore-t-dist-cwh.

Convergence criteria was defined as the difference of sequential outputs and the sum of slack variables both less than 10^{-8}; difference of convex programs were limited to 100 iterations.

3.4.1 Gaussian Disturbance

I consider Gaussian noise with zero mean and covariance $\Sigma = I_N \otimes \text{diag}(10^{-4} \cdot I_3, 5 \times 10^{-8} \cdot I_3)$. Once reformulated, the target set constraint has a Gaussian distribution and the collision avoidance has a Chi distribution with three degrees of freedom. As neither have an analytical expression for their quantile function, the use of standard tools or methods [29, 3] for Gaussian distributions is not viable.

Consider a scenario in which three satellites are stationed in low earth orbit. Each satellite is tasked with reaching a terminal target set, while avoiding other satellites. The equations of motion are described by (2.12) with sampling time $\Delta t = 30$s. I presume $\mathcal{U} = [-5, 5]^3$, and time horizon $N = 8$, corresponding to 4 minutes of operation.

The terminal sets $\mathcal{T}_i(N)$ are $5 \times 5 \times 5$m boxes centered around desired terminal locations in x, y, z coordinates, with speeds bounded in all three directions by $[-0.01, 0.01]$ m/s. For collision avoidance, I presume that all satellites must remain at least $r = 15$m away from each other, hence $S = \begin{bmatrix} I_3 & 0_3 \end{bmatrix}$ to extract the positions. Violation thresholds for terminal sets and inter-satellite collision avoidance are $\alpha = \gamma = 0.1$, respectively.

The performance objective is based on fuel consumption.

$$J(\vec{U}_1, \vec{U}_2, \vec{U}_3) = \sum_{i=1}^{3} \vec{U}_i^\top \vec{U}_i \tag{3.23}$$

The reformulation of the terminal constraint results in $\boldsymbol{y}_a$ that is a univariate Gaussian distribution with zero mean and variance $\vec{G}_{ika}\mathcal{D}_k\Sigma\mathcal{D}_k^\top\vec{G}_{ika}^\top$, such that

$$g_a\boldsymbol{y}_a = \left(\vec{G}_{ika}\mathcal{D}_k\Sigma\mathcal{D}_k^\top\vec{G}_{ika}^\top\right)^{1/2}\boldsymbol{z}_a$$

where $\boldsymbol{z}_a$ is a standard Gaussian random variable.

The reformulation of the collision avoidance constraint follows the derivation (3.7), and results in

$$g_{ijk}\boldsymbol{y}_{ijk} = \left\| \left(2S\mathcal{D}_k\Sigma\mathcal{D}_k^\top S^\top\right)^{\frac{1}{2}} \boldsymbol{\rho} \right\| \tag{3.24}$$

where $\boldsymbol{\rho}$ is a standard multivariate Gaussian. By the compatibility of matrix norms, I obtain

$$g_{ijk}\boldsymbol{y}_{ijk} = \left\| \left(2S\mathcal{D}_k\Sigma\mathcal{D}_k^\top S^\top\right)^{\frac{1}{2}} \right\| \cdot \|\boldsymbol{\rho}\| \tag{3.25}$$

where $\|\boldsymbol{\rho}\|$ follows a Chi distribution with three degrees of freedom.

When approximating the numerical quantile, I presume intervals $h = 5 \times 10^{-6}$, and maximum approximation error $\xi = 0.1$. For the Gaussian distribution, I set the instantiating point, p_0, to 0.5 with known quantile $\Phi^{-1}(p_0) = 0$. Computation of $\Phi^{-1}(p_0 = 0.9)$ was completed with MATLAB's implementation of the incomplete gamma function for the Chi quantile. Each quantile approximation used the first three derivatives of the pdf.

I compare the proposed method with the mixed integer particle approach using two polytopic overapproximations of the collision avoidance constraint, based on the L_∞ and L_1 norm. I generated 10 disturbance samples to generate an open-loop controller. Note that different disturbance samples were used when generating the controller for either variant.

The resulting trajectories, costs, and computation times differ dramatically, as shown in Figure 3.2 and Table 3.1. (Differences in the z-coordinates were minimal, so I only plot the x and y coordinates in Figure 3.2.) To assess constraint satisfaction, I generated 10^5 Monte-Carlo sample disturbances for each approach; the the L_2 distance between the mean positions at each time step are shown in Figure 3.3. Table 3.4.1 shows that while all three methods satisfied the collision avoidance constraint, neither particle control approach satisfied the terminal set constraint.

The proposed method performed two to three orders of magnitude faster than particle control. Given the significant increase in binary variables needed to perform particle control, this comes as no surprise. I attempted to increase the number of disturbance samples, however, I could not generate a solution in a under two hours. Conversely, the low number of disturbance samples is likely the cause for the poor performance with respect to the target set constraint. Given the random nature of the sampling process, ten samples is not enough to characterize the behaviour on a larger scale.

Figures 3.2 and 3.3 show that the differences in avoidance regions impacted the results. With the L_2 collision avoidance region overapproximated by both the L_∞ and L_1 regions, I expected the collision avoidance likelihood to be significantly higher than the proposed method. However, the sharp edges of the polytopes created control choices that led to more aggressive direction changes. This phenomena is apparent in the lack of smoothness in the particle control trajectories in Figure 3.2. Similarly, the larger avoidance regions effectively increased the avoidance distance to 18m for the L_∞ particle control run and 23m for the L_1 particle control run, as observed in Figure 3.3. The additional distance had a distinct impact on the overall cost of each of these controllers. To produce a closer comparison, I also used 14- and 26-faced polytopes, however neither resulted in a solution within a 24 hour time frame.

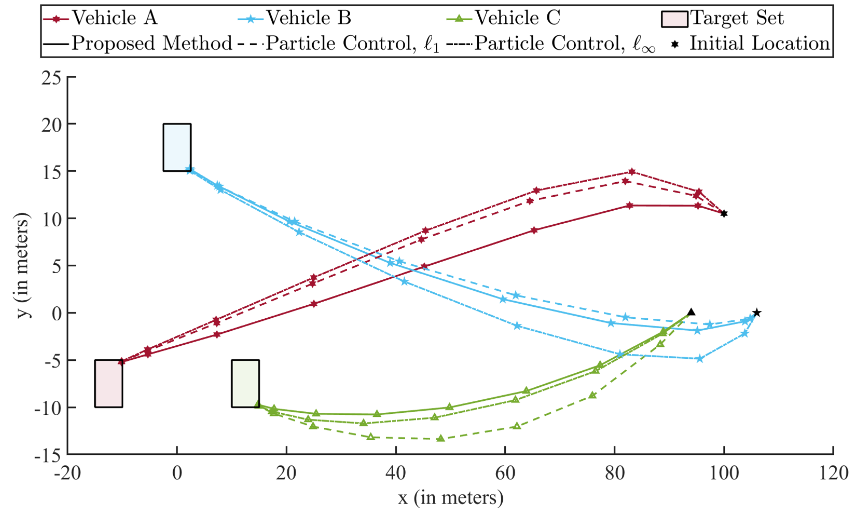

Figure 3.2: Comparison of trajectories in (x, y) coordinates from quantile method (solid) and particle control (dashed for L_1 norm; dotted for L_∞ norm).

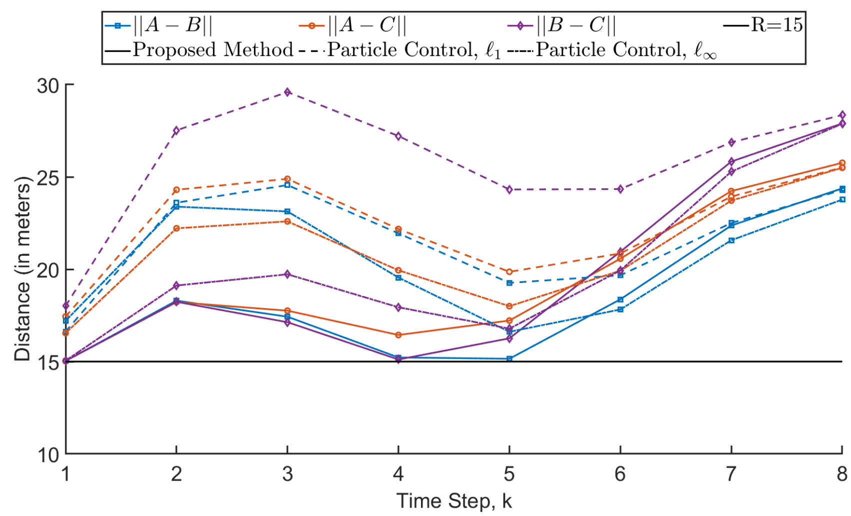

Figure 3.3: Comparison of L_2 inter-satellite distances between quantile method (solid) and particle control (dashed for L_1 norm; dotted for L_∞ norm).

Metric	Quantile method	Particle control	
		L_∞	L_1
Computation Time (sec)	6.82	245.65	4199.10
$J(\vec{U}_1, \vec{U}_2, \vec{U}_3)$	92.04	102.79	117.56

Table 3.1: Computation Time and Control Cost for CWH Dynamics with a Gaussian Disturbance. Comparison of Quantile Method and Particle Control.

Constraint	Quantile method	SAT	Particle control			
			L_∞	SAT	L_1	SAT
Terminal Sets	0.9127	✓	0.2183		0.0993	
Avoid Each Other	0.9630	✓	0.9997	✓	1.0000	✓

Table 3.2: Constraint Satisfaction ("SAT") for CWH dynamics with Gaussian Disturbance, with 10^5 Samples and Probabilistic Violation Threshold of $\alpha = \gamma = 0.1$. Comparison of Quantile Method and Particle Control.

3.4.2 Cauchy Disturbance

I consider the planar 4-d CWH dynamics with a Cauchy disturbance that is parameterized with location as zero and scale elements Γ,

$$\Gamma_j = \begin{cases} 10^{-4} & \text{if } j \in \{4n + \{1,2\} \mid n \in \mathbb{N}_{[0,N-1]}\} \\ 5 \times 10^{-8} & \text{if } j \in \{4n + \{3,4\} \mid n \in \mathbb{N}_{[0,N-1]}\} \end{cases} \tag{3.26}$$

corresponding to position and velocity elements, respectively.

Consider a scenario in which three satellites are stationed in low earth orbit. Each satellite is tasked with reaching a terminal target set, while avoiding other satellites. The equations of motion are described by (2.12) with sampling time $\Delta t = 30$s. I presume $\mathcal{U} = [-5, 5]^2$, and time horizon $N = 8$, corresponding to 4 minutes of operation.

The terminal sets $\mathcal{T}_i(N)$ are 5×5m boxes centered around desired terminal locations in x and y coordinates, with speeds bounded in all three directions by $[-0.01, 0.01]$m/s. For collision avoidance, I presume that all satellites must remain at least $r = 15$m away from each other, hence $S = \begin{bmatrix} I_2 & 0_2 \end{bmatrix}$ to extract the positions. Violation thresholds for terminal sets and inter-satellite collision avoidance are $\alpha = \gamma = 0.1$, respectively.

The performance objective is based on fuel consumption.

$$J(\vec{U}_1, \vec{U}_2, \vec{U}_3) = \sum_{i=1}^{3} \vec{U}_i^\top \vec{U}_i \tag{3.27}$$

For the terminal set constraint, because the set is axis-aligned, $g_a \boldsymbol{y}_a$ can be written as function of a single Cauchy random variable, Here,

$$g_a \boldsymbol{y}_a = \vec{G}_{ika}^{\top} \mathcal{D}(k) \Gamma \boldsymbol{z}_a \tag{3.28}$$

and $\boldsymbol{z}_a$ has a standard Cauchy distribution.

For the collision avoidance constraint, the main challenge arises from the coupling across random variables that arises from taking a norm. By falsely considering each dimension as independent, I can find

$$g_{ijk} \boldsymbol{y}_{ijk} = \max \left(S\mathcal{D}(k)\Gamma \right) \|\boldsymbol{\rho}\| \tag{3.29}$$

where $\boldsymbol{\rho}$ is a 2D vector consisting of independent and identically distributed standard Cauchy variables, and $\max(\cdot)$ returns the element of the argument vector with the maximum value. Note that the random variable of interest is $\|\boldsymbol{\rho}\|^2$, which I can show through convolution to have closed-form expressions for the pdf, cdf, and the quantile,

$$\phi_{\|\boldsymbol{\rho}\|^2}(x) = \frac{2}{\pi\sqrt{1+x}(2+x)} \tag{3.30a}$$

$$\Phi_{\|\boldsymbol{\rho}\|^2}(x) = \tfrac{4}{\pi} \arctan\left(\sqrt{1+x}\right) - 1 \tag{3.30b}$$

$$\Phi^{-1}_{\|\boldsymbol{\rho}\|^2}(p) = \tan^2\left(\tfrac{\pi}{4}(1+p)\right) - 1 \tag{3.30c}$$

When approximating the numerical quantile, I presume intervals $h = 5 \times 10^{-6}$, and maximum approximation error $\xi = 0.1$. For the Cauchy distribution, I set the instantiating point, p_0, to 0.5 with known quantile $\Phi^{-1}(p_0) = 0$. Analytical results were used to compute $\Phi^{-1}(p_0)$ for the sum of squared Cauchy random variables. Each quantile approximation used the first three derivatives of the pdf.

Figures 3.4 and 3.5, and Tables 3.4.2 and 3.4.2, show that the proposed method with the numerical quantile performed nearly identically to the proposed method with an

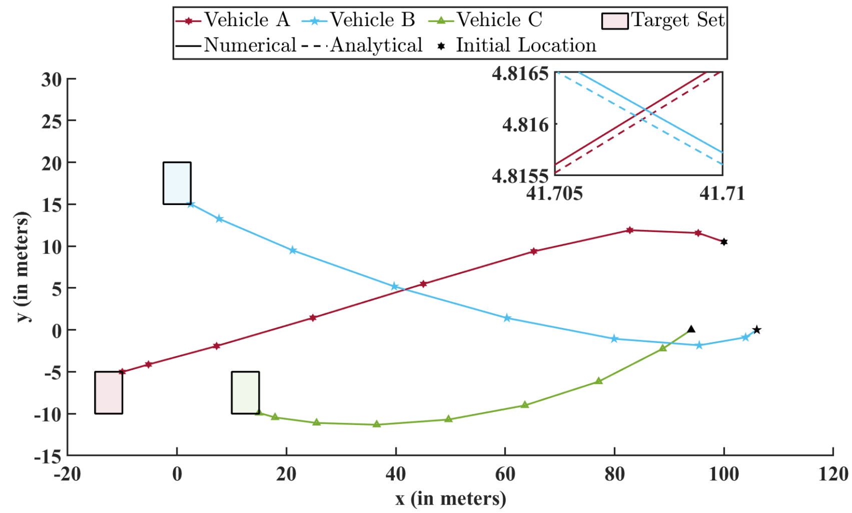

Figure 3.4: Comparison of trajectories in (x, y) coordinates for numerical quantile method (solid) and with an analytic quantile (dashed). The trajectories are nearly indistinguishable as seen in the magnified subplot.

Metric	Proposed method	
	Numerical	Analytical
Computation Time (sec)	153.86	157.98
$J(\vec{U}_1, \vec{U}_2, \vec{U}_3)$	93.11	93.11

Table 3.3: Computation Time and Control Cost for Proposed Method with Numerical and Analytic Quantiles for CWH Dynamics with Cauchy Disturbance.

analytical quantile. I observed differences on the order of 10^{-4}, as shown in the subplot of Figure 3.4. This is likely attributed to my choice of a very small interval h, which yielded a highly accurate quantile approximation.

Constraint	Proposed method			
	Numerical	SAT	Analytical	SAT
Terminal Sets	0.9086	✓	0.9085	✓
Avoid Each Other	0.9979	✓	0.9978	✓

Table 3.4: Constraint Satisfaction ("SAT") Between Numerical and Analytic Quantiles for CWH dynamics with Cauchy Disturbance, with 10^5 Samples and Probabilistic Violation Threshold of $\alpha = \gamma = 0.1$.

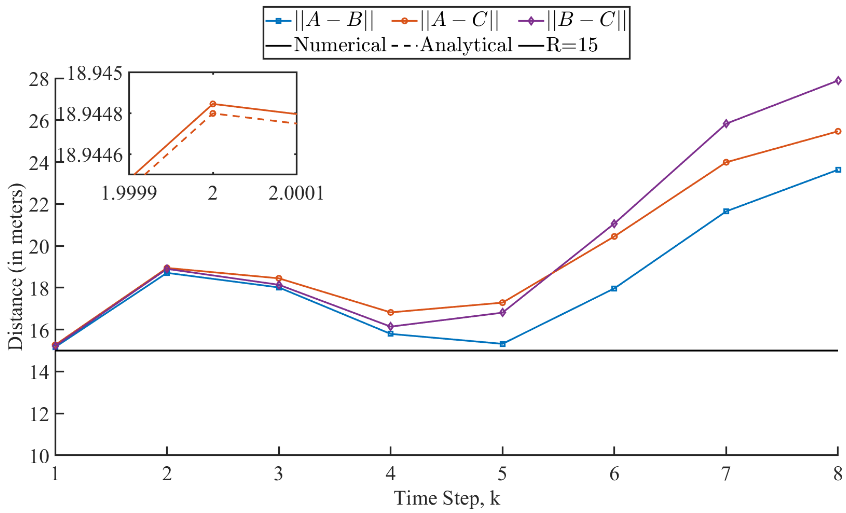

Figure 3.5: Comparison of inter-satellite distances between numerical quantile method (solid) and with an analytic quantile (dashed). The inter-satellite distances are nearly indistinguishable as seen in the magnified subplot.

3.4.3 Multivariate t Disturbance

Consider a scenario in which seven satellites are stationed in geosynchronous orbit. Each satellite is tasked with reaching a terminal target set representing a docking location with a static refueling station. Each satellite must avoid other satellites and the refueling station while navigating to their respective target sets. The relative dynamics of each spacecraft, with respect to the known location of the refueling station, are described by the CWH equations (2.12) with sampling time $\Delta t = 300$s. I presume $\mathcal{U} = [-3, 3]^3$, and time horizon $N = 8$, corresponding to 40 minutes of operation.

I consider a Multivariate t disturbance for this example. The multivariate t distribution is the vector generalization of the Student's t distribution [81]. The multivariate t distribution encompasses a family of distributions characterized by parameters describing location, correlation structure, and how heavy tailed a distribution is. It is defined as follows.

Definition 3.1 ([81]). *A n-dimensional multivariate random variable that elicits the pdf*

$$\phi_{\vec{\boldsymbol{x}}}\left(\vec{x}\right) = \frac{\Gamma\left((\nu+n)/2\right)\nu^{\nu/2}}{\Gamma(\nu/2)\pi^{n/2}\det(\Psi)^{\frac{1}{2}}}\left[\nu + (\vec{x}-\vec{\mu})^T\Psi^{-1}(\vec{x}-\vec{\mu})\right]^{-\frac{\nu+n}{2}} \tag{3.31}$$

is said to have a multivariate t distribution with location $\vec{\mu}\in\mathbb{R}^n$, positive definite scale matrix $\Psi\in\mathbb{R}^{n\times n}$, degrees of freedom $\nu\in\mathbb{N}^+$.

The degree of freedom parameter, ν, is a quantitative measure of how heavy the tails of the distribution are. Lower values of ν correspond to heavier tails. Note that $\nu = 1$ corresponds to the multivariate Cauchy distribution and the limiting distribution, as $\nu\to\infty$, is the multivariate Gaussian.

For this demonstration, I assume

$$\vec{\boldsymbol{W}}_i \sim t(0, \Psi, 20) \tag{3.32}$$

where $\Psi = I_8 \otimes \mathrm{diag}\left(10^{-4}I_3, 5\times 10^{-8}I_3\right)$. Here, the use of the multivariate t is used to model perturbation forces of interest but not captured in the CWH dynamics. This includes drag, solar radiation pressure, 3rd body acceleration from the Sun and Moon, and impacts with small but unknown debris. I choose $\nu = 20$ as the combined effect of these perturbation forces may be small but are likely outliers in comparison to a Gaussian distribution.

The terminal sets $\mathcal{T}_i(N)$ are $5\times 5\times 5$m boxes centered around desired terminal locations in x, y, z coordinates approximately 9m away from the origin, with velocity bounded in all three directions by $[-0.01, 0.01]$m/s. For collision avoidance, I presume that all satellites must remain at least $r = 8$m away from each other and the refueling station, hence $S = \begin{bmatrix} I_3 & 0_3\end{bmatrix}$ to extract the positions. I presume the collision avoidance constraints are valid only for the non-terminal time steps. Violation thresholds for terminal sets and collision avoidance are $\alpha = \beta = \gamma = 0.2$, respectively. I note that this problem has a combined 196 collision avoidance constraints to be embedded in the problem.

The performance objective is based on fuel consumption.

$$J(\vec{U}_1, \dots, \vec{U}_7) = \sum_{i=1}^{7} \vec{U}_i^\top \vec{U}_i \tag{3.33}$$

The reformulation of the terminal constraint results in $\boldsymbol{y}_a$ that is a univariate t distribution with zero mean and variance $\vec{G}_{ika}\mathcal{D}_k\Psi\mathcal{D}_k^\top\vec{G}_{ika}^\top$, such that

$$g_a\boldsymbol{y}_a = \left(\vec{G}_{ika}\mathcal{D}_k\Psi\mathcal{D}_k^\top\vec{G}_{ika}^\top\right)^{1/2}\boldsymbol{z}_a$$

where $\boldsymbol{z}_a$ is a Student's t random variable with $\nu = 20$ [82].

The reformulation of the collision avoidance constraints result in the use of the beta prime distribution.

Definition 3.2 ([83]). *A non-negative univariate variate random variable that elicits the pdf*

$$\phi_{\boldsymbol{x}}(x) = \frac{x^{-\theta-1}(1+x)^{-\theta-\delta}}{\beta(\theta,\delta)} \tag{3.34}$$

is said to have a beta prime distribution with shape parameters $\theta \in \mathbb{R}_+$ and $\delta \in \mathbb{R}_+$.

The shape parameters define the polynomial shape of the pdf and the quantile. Of note, when $\theta \leq 1$, the quantile is strictly convex as the pdf is monotonically decreasing. However, when $\theta > 1$, the quantile is only convex in the region $p \in \left[\Phi_{\boldsymbol{x}}\left(\frac{\theta-1}{\delta+1}\right), 1\right]$. Further, when $\theta = 1$ and/or $\delta = 1$, the cdf has an analytic form. However, in many cases analytic expressions of the cdf do not guarantee analytic expressions of the quantile.

The reformulation of the collision avoidance constraint follows the derivation (3.7), and results in

$$g_{ijk}\boldsymbol{y}_{ijk} = \sqrt{2\nu\lambda_{\max}\left(S\mathcal{D}(k)\Psi\mathcal{D}(k)^\top S^\top\right)}\underbrace{\sqrt{\frac{1}{\nu}\left(\|\vec{\boldsymbol{\tau}}_i\|^2 + \|\vec{\boldsymbol{\tau}}_j\|^2\right)}}_{\boldsymbol{y}_{ijk}} \tag{3.35}$$

where $\vec{\boldsymbol{\tau}} \sim t(\vec{0}, I_3, \nu)$. Here,

$$\boldsymbol{y}_{ijk}^2 \sim BPrime(\theta, \delta) \tag{3.36a}$$

$$\theta = \frac{2q\left(\frac{q}{2} + \left(\frac{\nu}{2}\right)^2 - \nu + \left(\frac{q\nu}{2}\right) - 2q + 1\right)}{(\nu - 2)(q + \nu - 2)} \tag{3.36b}$$

$$\delta = \frac{2\left(-q + \left(\frac{\nu}{2}\right)^2 - \left(\frac{\nu}{2}\right) + \left(\frac{q\nu}{2}\right)\right)}{q + \nu - 2} \tag{3.36c}$$

where $\nu = 20$ and $q = 3$ [84]. I recover the pdf of $\boldsymbol{y}_i$ as

$$\phi_{\boldsymbol{y}_{ijk}}(x) = 2x\phi_{\boldsymbol{y}_{ijk}^2}\left(x^2\right) \tag{3.37}$$

to be used in the quantile approximation. I note that the reformulation of (2.13b) follows similar. Since the object is not stochastic, the resulting distribution is $BPrime\left(\frac{q}{2}, \frac{\nu}{2}\right)$.

When approximating the numerical quantiles, I presume intervals $h = 5 \times 10^{-6}$, and maximum approximation error $\xi = 0.01$. For the Student's t distributions, I set the instantiating point, p_0, to 0.5 with known quantile $\Phi^{-1}(p_0) = 0$. For the beta prime distributions, I set the instantiating point to 0.5. Computation of $\Phi^{-1}(p_0)$ was completed using the median approximation [85]

$$\Phi^{-1}(0.5) = \sqrt{\frac{2^{-\frac{1}{\theta}}(\log(2) - \frac{1}{2} + \theta)}{2^{-\frac{1}{\delta}}(\log(2) - \frac{1}{2} + \delta)}} \tag{3.38}$$

Each quantile approximation used the first four derivatives of the pdf. This median approximation was compared against the mode of the distribution to verify that β and γ were in the convex region of the quantile.

The resulting trajectories are shown in Figure 3.6. To assess constraint satisfaction, I generated 10^4 Monte-Carlo sample disturbances for each approach. Table 3.4.3 shows that all constraints were satisfied to the required threshold. Note that all three constraints

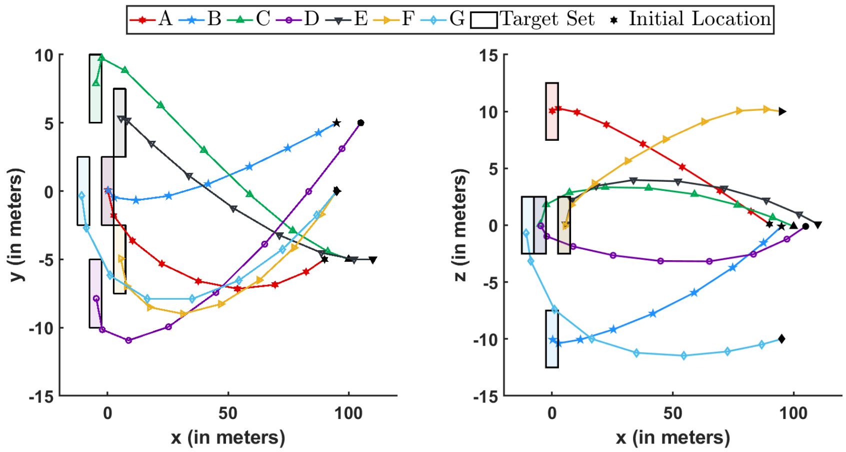

Figure 3.6: Trajectories of the seven satellites for CWH dynamics with Multivariate-t disturbance computed with Qauntile Method.

Constraint	Sample Satisfaction	SAT
Terminal Sets	0.8207	✓
Avoid The Refueling Station	0.9872	✓
Avoid Each Other	0.9869	✓

Table 3.5: Constraint Satisfaction for CWH Dynamics With Multivariate-t Disturbance Computed With Qauntile Method, and Probabilistic Violation Threshold of $\alpha = 0.2$. Satisfaction 'SAT' Was Computed as a Ratio of 10^4 Samples That Met the Constraint. Satisfaction Is marked With a ✓.

Metric	Value
Solution Computation Time	33.3759 sec
Total Computation Time	43.3393 sec
Iterations to Converge	34
Objective Cost for Derived Solution	0.015873

Table 3.6: Computation Statistics for CWH Dynamics With Multivariate-t Disturbance. Solutions Computed With Quantile Method.

are satisfied to a more conservative threshold implying that the reformulation is not a tight upper bound for the problem. I note that solutions using particle control could not be found within a weeks time for 25 disturbance samples; thus, I do not provide a comparison for this example.

Table 3.4.3 provides computational statistics on the difference of convex program. The proposed method computed the trajectories in under a minute. With nearly 200 collision avoidance constraints embedded in this problem, solution convergence of this speed warrants further consideration for this method.

3.5 Summary

In this chapter, I proposed a method for chance constrained stochastic optimal control of LTI systems that exploits a numerical approximation of the quantile function. I reformulated each chance constraint into one of two forms that allowed us to find a closed form quantile reformulation. I show that for random variables with a sufficiently differentiable pdf, I can approximate the quantile via a Taylor series approximation. I demonstrated my approach on three multi-vehicle satellite control problem with Gaussian, Cauchy, and multivariate t disturbances. The results show that the proposed method is not only computationally efficient but also adaptable to many scenarios.

Chapter 4

Analytic Moments Based Approach

4.1 Introduction

While quantile based approaches can be used to more directly evaluate chance constraints, there exists non-Gaussian processes which lack an analytic expressions for the pdf, cdf, and quantile of the state as it evolves over time. Thus making the method presented in Chapter 3 impossible. In contrast, methods that employ concentration inequalities provide almost surely assurances of chance constraint satisfaction through over-approximations based on analytic evaluations of moments. Chebyshev's inequality [35] and Cantelli's inequality [35] have been used to develop chance constraint reformulations that are an affine combination of a constraint's expectation and standard deviation [86, 87, 88, 1]. These inequalities only require knowledge of the expectation and the standard deviation, which can be easily calculated for linear constraints. However, reliance on these inequalities typically provides quite conservative bounds [1].

My approach also invokes concentration inequalities, and hence provides almost surely guarantees, but employs an inequality that is less conservative than those in [86, 87, 88, 1]. I use the one-sided Vysochanskij–Petunin inequality [60], a refinement of Cantelli's inequality that is tailored to unimodal distributions. Although it has less generality than

Cantelli's inequality, the one-sided Vysochanskij–Petunin inequality typically results in far less conservatism in the overapproximation. Indeed, its probabilistic bound is reduced by a factor of 5/9, as compared to the bound from Cantelli's inequality. Hence, I propose application of the one-sided Vysochanskij–Petunin inequality to chance constraint evaluation that arises in multi-vehicle planning problems: that is, in a) reaching a terminal target set and b) avoiding collision with obstacles in the environment as well as with other vehicles. The main drawback in my approach is the need for unimodality of each constraint, over the entire trajectory. Unimodality is assured for convex constraints in LTI systems for certain classes of disturbance processes (such as Gaussian, Laplacian, or uniform on a convex interval), however for other disturbance processes, unimodality must be validated empirically.

The main contribution of this chapter is a *closed-form* reformulation of chance constraints, for polytopic target sets and collision avoidance constraints, that is amenable to difference of convex programming solutions. My approach is relevant for LTI systems with arbitrary distributions with finite moments, and with chance constraints that are unimodal.

The chapter is organized as follows. Section 4.2 provides additional preliminaries required for Problem 1. Section 4.3 reformulates the chance constraints by approximating the quantile function. Section 4.4 demonstrates my approach on three multi-satellite rendezvous problems, and Section 4.5 provides concluding remarks.

4.2 Problem Formulation

In addition to the problem formulation in Chapter 2.4, I add several assumptions and observations that will be required for the work in this chapter. For this problem to be tractable for arbitrary disturbances, I make several key assumptions about the disturbance and its resulting impact on the constraints.

Assumption 4.1. *Disturbance vectors, $\vec{\boldsymbol{W}}_i$, are all pairwise independent. Hence, for any i and j, where $i \neq j$, the joint cdf, $\Phi_{\vec{\boldsymbol{W}}_i,\vec{\boldsymbol{W}}_j}(\vec{a},\vec{b})$ can be factored into the product of the marginal cdfs, $\Phi_{\vec{\boldsymbol{W}}_i}(\vec{a})$ and $\Phi_{\vec{\boldsymbol{W}}_j}(\vec{b})$. So, $\Phi_{\vec{\boldsymbol{W}}_i,\vec{\boldsymbol{W}}_j}(\vec{a},\vec{b}) = \Phi_{\vec{\boldsymbol{W}}_i}(\vec{a})\Phi_{\vec{\boldsymbol{W}}_j}(\vec{b})$.*

Assumption 4.2. *All components of the disturbance vector, $\vec{\boldsymbol{W}}_i = \begin{bmatrix}\boldsymbol{w}_{i1} & \boldsymbol{w}_{i2} & \dots & \boldsymbol{w}_{iNn}\end{bmatrix}$, are mutually independent. Hence, for any set of unique integers $\mathbb{S} \subseteq \mathbb{N}_{[1,Nn]}$, the subset $\{\boldsymbol{w}_{ij} | j \in \mathbb{S}\}$ has a joint cdf $\Phi_{\{\boldsymbol{w}_{ij}|j\in\mathbb{S}\}}(\cdot,\dots,\cdot)$ can be factored into the product of the marginal cdfs, $\Phi_{\boldsymbol{w}_{ij}}(\cdot)$ for $j \in \mathbb{S}$. So, $\Phi_{\{\boldsymbol{w}_{ij}|j\in\mathbb{S}\}}(\cdot,\dots,\cdot) = \prod_{j\in\mathbb{S}} \Phi_{\boldsymbol{w}_{ij}}(\cdot)$.*

Assumption 4.3. *Each component of the disturbance vector, $\vec{\boldsymbol{W}}_i = \begin{bmatrix}\boldsymbol{w}_{i1} & \boldsymbol{w}_{i2} & \dots & \boldsymbol{w}_{iNn}\end{bmatrix}$, has finite and well defined moments at least up to the fourth order, $\mathbb{E}\big(\boldsymbol{w}_{ij}^p\big) < \infty$ for $p \in \mathbb{N}_{[1,4]}$.*

Statistically, pairwise and mutual independence can be assumed in many cases without much consequence as most multivariate distributions can be constructed in this manner. However, the multivariate Cauchy and the multivariate t are the most prominent examples that cannot meet Assumption 4.2 as elements are not independent by construction. In many ways, Assumption 4.2 is the most restrictive of these assumptions as many physical phenomena may not disturb each state independently. Assumption 4.3 is easily met as most distributions have analytic expressions for moments.

Lastly, I consider the impact of $\vec{\boldsymbol{W}}_i$ on the chance constraints in (2.13).

Definition 4.1 (Unimodal Distribution [89])**.** *A unimodal distribution is a distribution whose cdf is convex in the region $(-\infty, a)$ and concave in the region (a, ∞) for some $a \in \mathbb{R}$.*

Definition 4.2 (Strong Unimodal Distribution [89])**.** *A strong unimodal distribution is one in which unimodality is preserved by convolution. That is, for two independent unimodal random variables, $\boldsymbol{y}$ and $\boldsymbol{z}$, the random variable $\boldsymbol{y} + \boldsymbol{z}$ is also unimodal.*

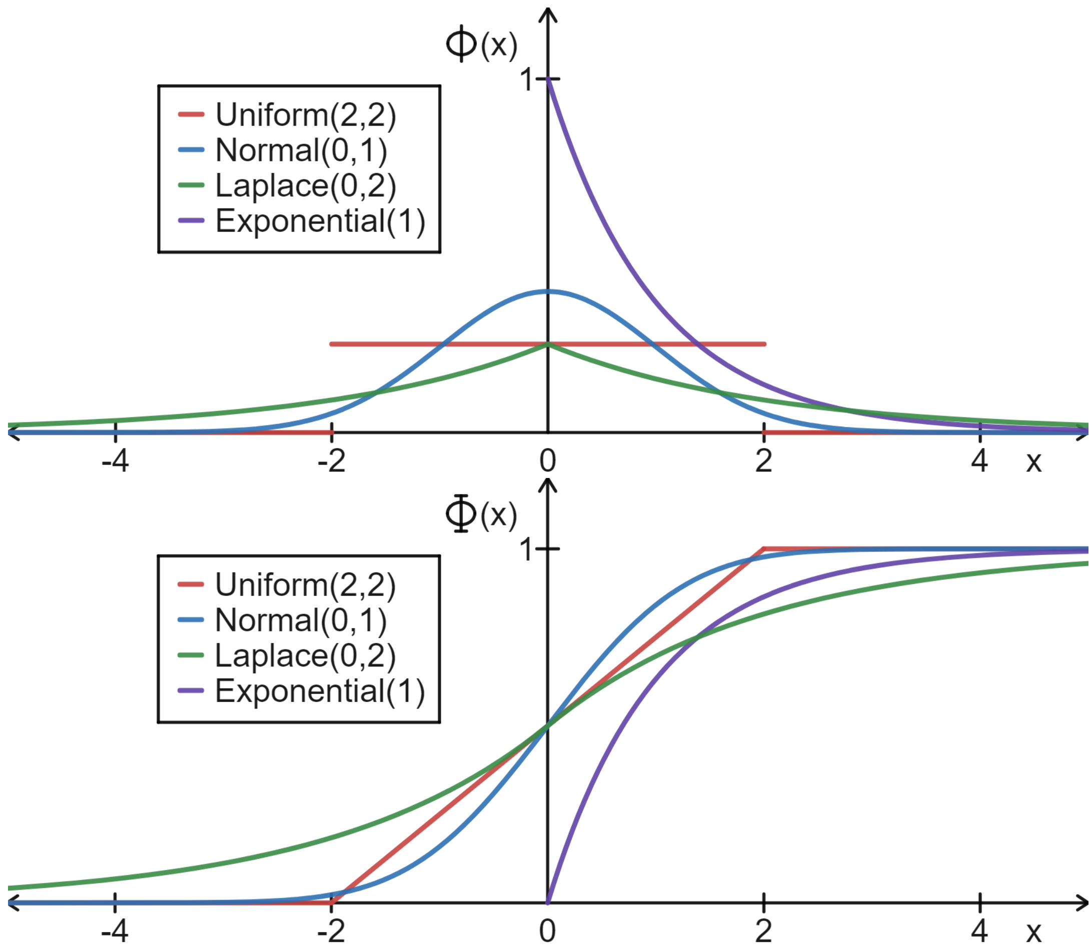

Figure 4.1: pdfs (top) and cdfs (bottom) of unimodal distributions as per Definition 4.1 with $a = 0$. Each of the distributions shown here have a log concave pdf, which in turn implies a log concave cdf. Log concavity of the pdf assures strong unimodality as per Definition 4.2.

Assumption 4.4. *The distribution that describes each probabilistic constraint in (2.13) is marginally unimodal.*

Assumption 4.4 is required such that I can develop bounds on the chance constraint probabilities. In rare cases, unimodality can be verified analytically by properties of strong unimodality. For example, Gaussian or exponential random variables are strong unimodal and any affine summation of these random variables will always be unimodal. One method to check for strong unimodality is to establish that the probability density function (pdf) is log concave as all distributions that are strong unimodal also have a log concave pdf per the Theorem of Ibragimov [90]. Figure 4.1 graphs the pdf and cdf of several common strong unimodal distributions with pdfs that are easy to show are log concave. As unimodality can be challenging to show analytically, the easiest method to validate unimodality is empirically. By numerically evaluating the empirical cumulative distribution function with a large enough sample size (I recommend at least on the order of 10^4 samples), one can validate unimodality in terms of Definition 4.1 via Algorithm 3. Algorithm 3 is constructing an affine approximation of empirical cumulative distribution function then testing whether there is a single inflection point by comparing the slopes of the affine segments.

Problem 1.2. *Under Assumptions 4.1-4.4, solve Problem 1 with probabilistic violation thresholds α, β, and γ for open loop controllers $\vec{U}_1, \dots, \vec{U}_{N_v} \in \mathcal{U}^N$.*

The main challenge in solving Problem 1.2 is assuring (2.15d). In this form, assuring (2.15d) requires the evaluation of high dimensional and frequently intractable integrals. Additionally, even if these integrals could be evaluated and closed forms could be found, the collision avoidance constraints (2.13b)-(2.13c) would still be reverse convex.

Algorithm 3: Numerical check for unimodality.

```
Input: Empirical cumulative distribution function points (x_i, F̂(x_i)) for samples
  x_i with i ∈ ℕ_[1,N_s], and maximum error threshold ξ.
Output: 1 if unimodal or 0 if not unimodal
i ← 0
S ← ∅
while i < N_s do
    for j = N_s to i + 1 by −1 do
        m ← (F̂(x_j) − F̂(x_i)) / (x_j − x_i)
        b ← F̂(x_j) − x_j × m
        for k = i + 1 to j − 1 by 1 do
            ε_k = F̂(x_k) − (p_y × m + b)
            if ε_k > ξ then
                next j
            end
        end
        S ← S ∪ {m}
        break
    end
    i ← j
end
w ← 0
N_c ← card(S)              # cardinality of set S
for i = 2 to N_c by 1 do
    # S_i is the i^th element of S
    if S_i ≥ S_{i−1} then
        if w = 1 then
            return 0
        end
    else
        w ← 1
    end
end
return 1
```

4.3 Methods

My approach to solve Problem 1.2 involves reformulating each chance constraint as an affine summation of the constraint's expectation and standard deviation, i.e., $\mathbb{E}(\|S(\vec{\boldsymbol{x}}_i(k)-\vec{\boldsymbol{x}}_j(k))\|)$ and $\mathbb{S}(\|S(\vec{\boldsymbol{x}}_i(k)-\vec{\boldsymbol{x}}_j(k))\|)$, respectively for the collision avoidance constraint. This form is amenable to the one-sided Vysochanskij–Petunin inequality [60], which allows for almost surely guarantees of chance constraint satisfaction.

Theorem 4.1 (One-sided Vysochanskij–Petunin Inequality [60]). *Let $\boldsymbol{x}$ be a real valued unimodal random variable with finite expectation $\mathbb{E}(\boldsymbol{x})$ and finite, non-zero standard deviation $\mathbb{S}(\boldsymbol{x})$. Then, for $\lambda > \sqrt{5/3}$,*

$$\mathbb{P}(\boldsymbol{x} - \mathbb{E}(\boldsymbol{x}) \geq \lambda\mathbb{S}(\boldsymbol{x})) \leq \frac{4}{9(\lambda^2+1)} \tag{4.1}$$

By applying (4.1) to the random variable $-\boldsymbol{x}$, I get the lower tail bound

$$\mathbb{P}(\boldsymbol{x} - \mathbb{E}(\boldsymbol{x}) \leq -\lambda\mathbb{S}(\boldsymbol{x})) \leq \frac{4}{9(\lambda^2+1)} \tag{4.2}$$

The one-sided Vysochanskij–Petunin inequality is applicable only to unimodal distributions. It is based on Gauss's inequality, which provides a bound for one sided tail probabilities of a unimodal random variable to be sufficiently far away from the expectation. Specifically, the bound encompasses values at least λ standard deviations away from the mean.

I first make use of (4.1) and (4.2) to bound the chance constraint probabilities based on an affine summation of the expectation and standard deviation.

4.3.1 Polytopic Target Set Constraint

First, consider the reformulation of (2.13a). Without loss of generality, I presume $N_v = 1$ and $N = 1$ for brevity. From (2.14), I can write

$$\mathbb{P}(\vec{\boldsymbol{x}}_i(k) \in \mathcal{T}_i(k)) = \mathbb{P}\left(\bigcap_{j=1}^{N_{ik}} \vec{G}_{ika}\vec{\boldsymbol{x}}_i(k) \leq h_{ika}\right) \tag{4.3}$$

where $\vec{G}_{ika} \in \mathbb{R}^n$ and $h_{ika} \in \mathbb{R}$. I take the complement and employ Boole's inequality to separate the combined chance constraints into a series of individual chance constraints,

$$\mathbb{P}(\boldsymbol{x}_i(k) \notin \mathcal{T}_i(k)) = \mathbb{P}\left(\bigcup_{j=1}^{N_{ik}} \vec{G}_{ika}\vec{\boldsymbol{x}}_i(k) \geq h_{ika}\right) \tag{4.4a}$$

$$\leq \sum_{j=1}^{N_{ik}} \mathbb{P}\Big(\vec{G}_{ika}\vec{\boldsymbol{x}}_i(k) \geq h_{ika}\Big) \tag{4.4b}$$

Using the approach in [25], I introduce variables ω_{ika} to allocate risk to each of the individual chance constraints,

$$\mathbb{P}\Big(\vec{G}_{ika}\vec{\boldsymbol{x}}_i(k) \geq h_{ika}\Big) \leq \omega_{ika} \tag{4.5a}$$

$$\sum_{j=1}^{N_{ik}} \omega_{ika} \leq \alpha \tag{4.5b}$$

$$\omega_{ika} \geq 0 \tag{4.5c}$$

To find a solution to (4.5), I need to find an appropriate value for ω_{ika}. To that end, I add an additional constraint

$$\mathbb{E}\Big(\vec{G}_{ika}\vec{\boldsymbol{x}}_i(k)\Big) + \lambda_{ika}\mathbb{S}\Big(\vec{G}_{ika}\vec{\boldsymbol{x}}_i(k)\Big) \leq h_{ika} \tag{4.6}$$

to (4.5). Enforcement of (4.6) allows us to write (4.5a) as

$$\begin{aligned}\mathbb{P}\Big(\vec{G}_{ika}\vec{\boldsymbol{x}}_i(k) \geq h_{ika}\Big) &\leq \mathbb{P}\Big(\vec{G}_{ika}\vec{\boldsymbol{x}}_i(k) \geq \mathbb{E}\Big(\vec{G}_{ika}\vec{\boldsymbol{x}}_i(k)\Big) + \lambda_{ika}\mathbb{S}\Big(\vec{G}_{ika}\vec{\boldsymbol{x}}_i(k)\Big)\Big) \\ &\leq \omega_{ika}\end{aligned} \tag{4.7}$$

Then, by Assumption 4.4 and Theorem 4.1, I can substitute ω_{ika} with $\frac{4}{9(\lambda_{ika}^2+1)}$ and change the risk allocation variable from ω_{ika} to λ_{ika}. Further, enforcement of (4.6) makes (4.5a), and by extension (4.7), an unnecessary intermediary step between (4.6) and (4.5c). Hence, I can remove (4.5a) from the system of equations to solve and write (4.5)-(4.7) as

$$\mathbb{E}\Big(\vec{G}_{ika}\vec{\boldsymbol{x}}_i(k)\Big) + \lambda_{ika}\mathbb{S}\Big(\vec{G}_{ika}\vec{\boldsymbol{x}}_i(k)\Big) \leq h_{ika} \tag{4.8a}$$

$$\sum_{j=1}^{N_{ik}} \frac{4}{9(\lambda_{ika}^2+1)} \leq \alpha \tag{4.8b}$$

$$\lambda_{ika} \geq \sqrt{\frac{5}{3}} \tag{4.8c}$$

which is enumerated over the indices, i, j, and k.

Lemma 4.1. *For the controllers $\vec{U}_1, \ldots, \vec{U}_{N_v}$, if there exists risk allocation variables λ_{ika} satisfying (4.8) for constraints (2.13a), then $\vec{U}_1, \ldots, \vec{U}_{N_v}$ satisfy (2.15d).*

Proof. Satisfaction of (4.8a) implies (4.7) holds. The Vysochanskij–Petunin inequality upper bounds (4.7). Boole's inequality and De Morgan's law guarantee that if (4.8b) holds then (2.15d) is satisfied. □

Lastly, I show that the constraint reformulation (4.8) will always be convex.

Lemma 4.2. *The constraint (4.8) is convex in $\vec{U}_i$ and in $(\lambda_{i1k}, \ldots, \lambda_{ipk})$*

Proof. I start by exploiting the properties of the expectation and variance operator to write (4.8a) as

$$\vec{G}_{ika}\left(A^k\vec{x}_i(0)+\mathcal{C}(k)\vec{U}_i+\mathcal{D}(k)\mathbb{E}\Big(\vec{\boldsymbol{W}}_i\Big)\right)+\lambda_{ika}\sqrt{\vec{G}_{ika}^\top\mathcal{D}^\top(k)\mathbb{V}\Big(\vec{\boldsymbol{W}}_i\Big)\,\mathcal{D}(k)\vec{G}_{ika}}\leq h_{ika} \tag{4.9}$$

which is affine, and hence convex, in $\vec{U}_i$ and λ_{ika}. Then

$$\frac{\partial^2}{\partial\lambda_{ika}^2}\frac{4}{9(\lambda_{ika}^2+1)}=-\frac{8\left(-3\lambda_{ika}^2+1\right)}{9\left(\lambda_{ika}^2+1\right)^3} \tag{4.10}$$

which is positive, and hence convex, when $\lambda_{ika}\geq 3^{-1/2}$. Hence, with the restriction (4.8c), (4.8b) is a convex constraint. Thus, the set over which $\lambda_{i1k},\dots,\lambda_{iqk}$ is optimized is convex. Further, in the problem formulation I defined the control authority to be a closed and convex set. Hence, I can conclude the chance constraint reformulation (4.8) is convex. □

4.3.2 2-Norm Based Collision Avoidance Constraints

Next, consider the reformulation of the constraints (2.13b)-(2.13c). Here, I will derive the reformulation for (2.13c), but the reformulation of (2.13b) is nearly identical. Without loss of generality, let

$$\vec{z}=SA^k(\vec{x}_i(0)-\vec{x}_j(0))+S\mathcal{C}(k)(\vec{U}_i-\vec{U}_j) \tag{4.11a}$$

$$\vec{\boldsymbol{z}}=S\mathcal{D}(k)(\vec{\boldsymbol{W}}_i-\vec{\boldsymbol{W}}_j) \tag{4.11b}$$

be the non-stochastic and stochastic element of $S(\vec{\boldsymbol{x}}_i(k)-\vec{\boldsymbol{x}}_j(k))$ from (2.13c), respectively. Then, I can write the norm as

$$\|S(\vec{\boldsymbol{x}}_i(k)-\vec{\boldsymbol{x}}_j(k))\|=\|\vec{z}+\vec{\boldsymbol{z}}\| \tag{4.12}$$

I start by observing

$$\mathbb{P}\left(\bigcap_{i=1}^{N_v-1}\bigcap_{j=i+1}^{N_v}\bigcap_{k=1}^{N}\|\vec{z}+\vec{\boldsymbol{z}}\|\geq r\right)=\mathbb{P}\left(\bigcap_{i=1}^{N_v-1}\bigcap_{j=i+1}^{N_v}\bigcap_{k=1}^{N}\|\vec{z}+\vec{\boldsymbol{z}}\|^2\geq r^2\right) \tag{4.13}$$

as the norm is non-negative. Thus, I can write the 2-norm constraint as

$$\mathbb{P}\left(\bigcap_{i=1}^{N_v-1}\bigcap_{j=i+1}^{N_v}\bigcap_{k=1}^{N}\|\vec{z}+\vec{\boldsymbol{z}}\|^2\geq r^2\right)\geq 1-\gamma \tag{4.14}$$

By taking the complement and applying Boole's inequality,

$$\mathbb{P}\left(\bigcup_{i=1}^{N_v-1}\bigcup_{j=i+1}^{N_v}\bigcup_{k=1}^{N}\|\vec{z}+\vec{\boldsymbol{z}}\|^2\leq r^2\right)\leq\sum_{i=1}^{N_v-1}\sum_{j=i+1}^{N_v}\sum_{k=1}^{N}\mathbb{P}\big(\|\vec{z}+\vec{\boldsymbol{z}}\|^2\leq r^2\big) \tag{4.15}$$

Using the approach in [25], I introduce risk variables ω_{ijk} to allocate risk to each of the individual probabilities

$$\mathbb{P}\big(\|\vec{z}+\vec{\boldsymbol{z}}\|^2\leq r^2\big)\leq\omega_{ijk} \tag{4.16a}$$

$$\sum_{i=1}^{N_v-1}\sum_{j=i+1}^{N_v}\sum_{k=1}^{N}\omega_{ijk}\leq\gamma \tag{4.16b}$$

$$\omega_{ijk}\geq 0 \tag{4.16c}$$

In a similar fashion to Section 4.3.1, I add an additional constraint based on the expectation and standard deviation of $\|\vec{z}+\vec{\boldsymbol{z}}\|^2$ to (4.16) such that the constraint becomes

$$\mathbb{P}\big(\|\vec{z}+\vec{\boldsymbol{z}}\|^2 \leq r^2\big) \leq \omega_{ijk} \tag{4.17a}$$

$$\mathbb{E}\big(\|\vec{z}+\vec{\boldsymbol{z}}\|^2\big) - \lambda_{ijk}\mathbb{S}\big(\|\vec{z}+\vec{\boldsymbol{z}}\|^2\big) \geq r^2 \tag{4.17b}$$

$$\sum_{i=1}^{N_v-1}\sum_{j=i+1}^{N_v}\sum_{k=1}^{N}\omega_{ijk} \leq \gamma \tag{4.17c}$$

$$\omega_{ijk} \geq 0 \tag{4.17d}$$

By enforcing (4.17b), I can write (4.17a) as

$$\begin{aligned}\mathbb{P}\big(\|\vec{z}+\vec{\boldsymbol{z}}\|^2 \leq r^2\big) &\leq \mathbb{P}\Big(\|\vec{z}+\vec{\boldsymbol{z}}\|^2 \leq \mathbb{E}\big(\|\vec{z}+\vec{\boldsymbol{z}}\|^2\big) - \lambda_{ijk}\mathbb{S}\big(\|\vec{z}+\vec{\boldsymbol{z}}\|^2\big)\Big)\\ &\leq \omega_{ijk}\end{aligned} \tag{4.18}$$

From Assumption 4.4 and Theorem 4.1, I know that (4.18) is upper bounded as per (4.2). Hence, I can use the substitution

$$\omega_{ijk} = \frac{4}{9(\lambda_{ijk}^2+1)} \tag{4.19}$$

and determine the value for λ_{ijk} in terms of ω_{ijk},

$$\lambda_{ijk} = \sqrt{\frac{4}{9\omega_{ijk}} - 1} \tag{4.20}$$

so long as $\lambda \geq \sqrt{5/3}$. This implies $\omega_{ijk} \leq 1/6$ is a necessary restriction on ω_{ijk}. As

$\gamma < 1/6$, any solution will require that $\omega_{ijk} < 1/6$. Then, I can write (4.17) as

$$\mathbb{P}\big(\|\vec{z} + \vec{\boldsymbol{z}}\|^2 \leq r^2\big) \leq \omega_{ijk} \tag{4.21a}$$

$$\mathbb{E}\big(\|\vec{z}+\vec{\boldsymbol{z}}\|^2\big) - \sqrt{\frac{4}{9\omega_{ijk}} - 1} \cdot \mathbb{S}\big(\|\vec{z}+\vec{\boldsymbol{z}}\|^2\big) \geq r^2 \tag{4.21b}$$

$$\sum_{i=1}^{N_v-1} \sum_{j=i+1}^{N_v} \sum_{k=1}^{N} \omega_{ijk} \leq \gamma \tag{4.21c}$$

$$\omega_{ijk} \in (0, 1/6) \tag{4.21d}$$

Since Theorem 4.1 guarantees that satisfaction of (4.21b) also satisfies (4.21a) for any value $\gamma \in (0, 1/6)$, (4.21a) is redundant and can be removed. The constraint is then

$$\mathbb{E}\big(\|\vec{z}+\vec{\boldsymbol{z}}\|^2\big) - \sqrt{\frac{4}{9\omega_{ijk}} - 1} \cdot \mathbb{S}\big(\|\vec{z}+\vec{\boldsymbol{z}}\|^2\big) \geq r^2 \tag{4.22a}$$

$$\sum_{i=1}^{N_v-1} \sum_{j=i+1}^{N_v} \sum_{k=1}^{N} \omega_{ijk} \leq \gamma \tag{4.22b}$$

$$\omega_{ijk} \in (0, 1/6) \tag{4.22c}$$

Note that (4.22a) is a biconvex constraint [91]. For known risk allocation values ω_{ijk}, the final constraint is,

$$\mathbb{E}\big(\|\vec{z} + \vec{\boldsymbol{z}}\|^2\big) - \sqrt{\frac{4}{9\tilde{\omega}_{ijk}} - 1} \cdot \mathbb{S}\big(\|\vec{z} + \vec{\boldsymbol{z}}\|^2\big) \geq r^2 \tag{4.23}$$

Lemma 4.3. *If the controller $\vec{U}_1, \ldots, \vec{U}_v$, satisfies (4.23) for constraints (2.13b)-(2.13c), then $\vec{U}_1, \ldots, \vec{U}_v$ satisfy (2.13).*

Proof. Satisfaction of (4.23) implies (4.18) is satisfied for $\lambda_{ijk} = \sqrt{\frac{4}{9\tilde{\omega}_{ijk}} - 1}$. Theorem 4.1 guarantees satisfaction of (2.13). □

Next, I find the expanded form of (4.23) and show that the constraint is always a difference of convex function constraint.

Definition 4.3 (Difference of Convex Functions Constraint). *A difference of convex functions constraint has the form*

$$f(\vec{x}) - g(\vec{x}) \leq 0 \tag{4.24}$$

in which $f, g : \mathbb{R}^n \to \mathbb{R}$ *are convex functions for* $\vec{x} \in \mathbb{R}^n$.

Lemma 4.4. *The constraint* (4.23) *is a difference of convex function constraint in* $\vec{U}_i$ *for the constraint* (2.13b) *in* $\vec{U}_i - \vec{U}_j$ *for the constraint* (2.13c).

Proof. I first find the expectation and variance of the norm. To find the expectation, I expand the norm,

$$\begin{aligned}
\mathbb{E}\big(\|\vec{z} + \vec{\boldsymbol{z}}\|^2\big) &= \mathbb{E}\Big(\vec{z}^\top \vec{z} + 2\vec{z}^\top \vec{\boldsymbol{z}} + \vec{\boldsymbol{z}}^\top \vec{\boldsymbol{z}}\Big) && (4.25a)\\
&= \vec{z}^\top \vec{z} + 2\vec{z}^\top \mathbb{E}(\vec{\boldsymbol{z}}) + \mathbb{E}\Big(\vec{\boldsymbol{z}}^\top \vec{\boldsymbol{z}}\Big) && (4.25b)\\
&= \left\| \begin{bmatrix} I_q & \mathbb{E}(\vec{\boldsymbol{z}}) \\ \mathbb{E}(\vec{\boldsymbol{z}})^\top & \mathbb{E}\Big(\vec{\boldsymbol{z}}^\top \vec{\boldsymbol{z}}\Big) \end{bmatrix}^{\frac{1}{2}} \begin{bmatrix} \vec{z} \\ 1 \end{bmatrix} \right\|^2 && (4.25c)
\end{aligned}$$

Remember q is the dimension of the matrix S designed to extract the position elements of the state. Here, $\mathbb{E}(\|\vec{z} + \vec{\boldsymbol{z}}\|^2)$ is the squared norm of a vector matrix product. Hence, the expectation is convex. I compute the variance in a similar manner to the expectation,

$$\begin{aligned}
\mathbb{V}\big(\|\vec{z} + \vec{\boldsymbol{z}}\|^2\big) &= \mathbb{V}\Big(\vec{z}^\top \vec{z} + 2\vec{z}^\top \vec{\boldsymbol{z}} + \vec{\boldsymbol{z}}^\top \vec{\boldsymbol{z}}\Big) && (4.26a)\\
&= \mathbb{V}\big(2\vec{z}^\top \vec{\boldsymbol{z}}\big) + 2\mathbb{C}\Big(2\vec{z}^\top \vec{\boldsymbol{z}}, \vec{\boldsymbol{z}}^\top \vec{\boldsymbol{z}}\Big) + \mathbb{V}\Big(\vec{\boldsymbol{z}}^\top \vec{\boldsymbol{z}}\Big) && (4.26b)\\
&= 4\vec{z}^\top \mathbb{V}(\vec{\boldsymbol{z}})\, \vec{z} + 4\vec{z}^\top \mathbb{C}\Big(\vec{\boldsymbol{z}}, \vec{\boldsymbol{z}}^\top \vec{\boldsymbol{z}}\Big) + \mathbb{V}\Big(\vec{\boldsymbol{z}}^\top \vec{\boldsymbol{z}}\Big) && (4.26c)
\end{aligned}$$

where

$$\mathbb{C}\Big(\vec{\boldsymbol{z}}, \vec{\boldsymbol{z}}^\top \vec{\boldsymbol{z}}\Big) = \mathbb{E}\Big(\vec{\boldsymbol{z}}\vec{\boldsymbol{z}}^\top \vec{\boldsymbol{z}}\Big) - \mathbb{E}(\vec{\boldsymbol{z}})\, \mathbb{E}\Big(\vec{\boldsymbol{z}}^\top \vec{\boldsymbol{z}}\Big) \tag{4.27}$$

Assumptions 4.1-4.3 guarantees a closed form for (4.26). Thus, I can write the standard deviation as the 2-norm

$$\mathbb{S}\left(\|\vec{z}+\vec{\boldsymbol{z}}\|^2\right) = \left\| \begin{bmatrix} 4\mathbb{V}(\vec{\boldsymbol{z}}) & 2\mathbb{C}\left(\vec{\boldsymbol{z}}, \vec{\boldsymbol{z}}^\top \vec{\boldsymbol{z}}\right) \\ 2\mathbb{C}\left(\vec{\boldsymbol{z}}, \vec{\boldsymbol{z}}^\top \vec{\boldsymbol{z}}\right)^\top & \mathbb{V}\left(\vec{\boldsymbol{z}}^\top \vec{\boldsymbol{z}}\right) \end{bmatrix}^{\frac{1}{2}} \begin{bmatrix} \vec{z} \\ 1 \end{bmatrix} \right\| \tag{4.28}$$

Since the standard deviation is the 2-norm of an affine function, the standard deviation is convex [62]. I can now write (4.23) as

$$\left\| \begin{bmatrix} I_q & \mathbb{E}(\vec{\boldsymbol{z}}) \\ \mathbb{E}(\vec{\boldsymbol{z}})^\top & \mathbb{E}\left(\vec{\boldsymbol{z}}^\top \vec{\boldsymbol{z}}\right) \end{bmatrix}^{\frac{1}{2}} \begin{bmatrix} \vec{z} \\ 1 \end{bmatrix} \right\|^2 - \sqrt{\frac{4}{9\tilde{\omega}_{ijk}} - 1} \left\| \begin{bmatrix} 4\mathbb{V}(\vec{\boldsymbol{z}}) & 2\mathbb{C}\left(\vec{\boldsymbol{z}}, \vec{\boldsymbol{z}}^\top \vec{\boldsymbol{z}}\right) \\ 2\mathbb{C}\left(\vec{\boldsymbol{z}}, \vec{\boldsymbol{z}}^\top \vec{\boldsymbol{z}}\right)^\top & \mathbb{V}\left(\vec{\boldsymbol{z}}^\top \vec{\boldsymbol{z}}\right) \end{bmatrix}^{\frac{1}{2}} \begin{bmatrix} \vec{z} \\ 1 \end{bmatrix} \right\| \geq r^2 \tag{4.29}$$

which can be written as the difference of convex constraint

$$\sqrt{\frac{4}{9\tilde{\omega}_{ijk}} - 1} \left\| \begin{bmatrix} 4\mathbb{V}(\vec{\boldsymbol{z}}) & 2\mathbb{C}\left(\vec{\boldsymbol{z}}, \vec{\boldsymbol{z}}^\top \vec{\boldsymbol{z}}\right) \\ 2\mathbb{C}\left(\vec{\boldsymbol{z}}, \vec{\boldsymbol{z}}^\top \vec{\boldsymbol{z}}\right)^\top & \mathbb{V}\left(\vec{\boldsymbol{z}}^\top \vec{\boldsymbol{z}}\right) \end{bmatrix}^{\frac{1}{2}} \begin{bmatrix} \vec{z} \\ 1 \end{bmatrix} \right\| - \left\| \begin{bmatrix} I_q & \mathbb{E}(\vec{\boldsymbol{z}}) \\ \mathbb{E}(\vec{\boldsymbol{z}})^\top & \mathbb{E}\left(\vec{\boldsymbol{z}}^\top \vec{\boldsymbol{z}}\right) \end{bmatrix}^{\frac{1}{2}} \begin{bmatrix} \vec{z} \\ 1 \end{bmatrix} \right\|^2 \leq -r^2 \tag{4.30}$$

□

4.3.3 Difference of Convex Programming

Combining the results from Sections 4.3.1 and 4.3.2, I obtain a new optimization problem.

$$
\begin{aligned}
\underset{\substack{\vec{U}_1,\dots,\vec{U}_{N_v}\\ \lambda_{ika}}}{\text{minimize}} \quad & J\left(\vec{\boldsymbol{X}}_1,\dots,\vec{\boldsymbol{X}}_{N_v},\vec{U}_1,\dots,\vec{U}_{N_v}\right) && \text{(4.31a)}\\
\text{subject to} \quad & \vec{U}_1,\dots,\vec{U}_{N_v}\in\mathcal{U}^N, && \text{(4.31b)}\\
& \text{Moments defined by dynamics (2.6)} && \text{(4.31c)}\\
& \text{with initial conditions } \vec{x}_1(0),\dots,\vec{x}_{N_v}(0) && \\
& \text{Constraints (4.8) and (4.30)} && \text{(4.31d)}
\end{aligned}
$$

Reformulation 4.1. *Under Assumptions 4.1-4.4, solve the stochastic optimization problem (4.31) with probabilistic violation thresholds α, β, and γ for open loop controllers $\vec{U}_1,\dots,\vec{U}_{N_v}\in\mathcal{U}^N$ and optimization parameters λ_{ika}.*

Lemma 4.5. *Solutions to Reformulation 4.1 are conservative solutions to Problem 1.2.*

Proof. Lemmas 4.1 and 4.3 guarantee the probabilistic constraints (2.13) are satisfied. The equations (4.1)-(4.2) are always conservative. Hence, the reformulated constraints will be conservative with respect to the chance constraint. The expectation and variance terms in Reformulation 4.1 encompass and replace the dynamics used in Problem 1.2. The cost function and input constraints remain unchanged. □

I note that (4.31) is a difference of convex functions optimization problem. While (4.31a)-(4.31c) are convex, (4.31d) is difference of convex due to the constraint (4.30). As in the previous chapter, I employ the convex-concave procedure [64] to solve (4.31). Here, the first order approximation transforms the difference of convex function constraint

(4.30) into the convex constraint

$$\sqrt{\frac{4}{9\tilde{\omega}_{ijk}}-1}\left\|\begin{bmatrix} 4\mathbb{V}(\vec{\boldsymbol{z}}) & 2\mathbb{C}\left(\vec{\boldsymbol{z}},\vec{\boldsymbol{z}}^\top\vec{\boldsymbol{z}}\right) \\ 2\mathbb{C}\left(\vec{\boldsymbol{z}},\vec{\boldsymbol{z}}^\top\vec{\boldsymbol{z}}\right)^\top & \mathbb{V}\left(\vec{\boldsymbol{z}}^\top\vec{\boldsymbol{z}}\right)\end{bmatrix}^{\frac{1}{2}}\begin{bmatrix}\vec{z}\\ 1\end{bmatrix}\right\| \\ -\underbrace{\left(\left\|\begin{bmatrix} I_q & \mathbb{E}(\vec{\boldsymbol{z}}) \\ \mathbb{E}(\vec{\boldsymbol{z}})^\top & \mathbb{E}\left(\vec{\boldsymbol{z}}^\top\vec{\boldsymbol{z}}\right)\end{bmatrix}^{\frac{1}{2}}\begin{bmatrix}\vec{z}^p\\ 1\end{bmatrix}\right\|^2 + 2\left(\vec{z}^p+\mathbb{E}(\vec{\boldsymbol{z}})\right)^\top S\mathcal{C}(k)\left((\vec{U}_i-\vec{U}_j)-(\vec{U}_i^p+\vec{U}_j^p)\right)\right)}_{\text{First order approximation of } \mathbb{E}(\|\vec{z}+\vec{\boldsymbol{z}}\|^2) \text{ based on previous iteration's solution.}} \\ \leq -r^2 \tag{4.32}$$

where the superscript p indicated the value from the previous iteration's solution. As I use a difference of convex functions optimization framework, Lemma 4.3 guarantees that any solution that is synthesized during this iterative process will be a feasible but locally optimal solution.

4.4 Results

I demonstrate my method on a multi-satellite rendezvous problem with two different disturbances that impact the relative satellite dynamics. All computations were done on a 1.80GHz i7 processor with 16GB of RAM, using MATLAB, CVX [78] and Gurobi [79]. Polytopic construction and plotting was done with MPT3 [80]. All code is available at https://github.com/unm-hscl/shawnpriore-moment-control.

Consider a scenario in which N_v satellites, called the deputies, are stationed in geostationary Earth orbit, and tasked to rendezvous with a refueling spacecraft, called the chief. The satellites are tasked with reaching a new configuration represented by polytopic target sets. The relative planar dynamics of each deputy, with respect to the position of the chief are described by the equations (2.12) with sampling time Δt= 60s. Note that

I only consider the planar dynamics of (2.12) for this demonstration. I assume that the disturbances adhere to Assumptions 4.1-4.2.

4.4.1 Exponential Disturbance

Exponential disturbances are the type of distribution that is a big motivator for my approach. They exist in real systems but very few methods can handle them. I presume, for the purpose of demonstration, that I have an exponential disturbance. This could occur because of inaccuracies in the impulsive thrust model, drag forces in low Earth orbit, or third body gravity.

The exponential distribution is defined as follows.

Definition 4.4 (Exponential Distribution)**.** *An exponential distribution is one which elicits the pdf*

$$\phi(x) = \lambda e^{-\lambda x} \tag{4.33}$$

with rate parameter $\lambda > 0$ *and* $x \geq 0$*.*

The exponential distribution presents several challenges for existing methods. I define the following two distributions to analyze these challenges.

Definition 4.5 (Hypoexponential Distribution)**.** *An hypoexponential distribution is one which elicits the pdf*

$$\phi(x) = -\vec{a} e^{x\Theta} \Theta \vec{1} \tag{4.34}$$

with probability row vector $\vec{a}$*, subgenerator matrix* Θ*, and* $x \geq 0$*.*

Definition 4.6 (Weibull Distribution)**.** *An Weibull distribution is one which elicits the pdf*

$$\phi(x) = \frac{k}{\lambda} \left(\frac{x}{\lambda}\right)^{k-1} e^{-(x/\lambda)^k} \tag{4.35}$$

with scale parameter $\lambda > 0$*, shape parameter* $k > 0$*, and* $x \geq 0$*.*

First, a linear sum of independent but not identically distributed exponential random variables, as the case for the polytopic target set constraint, results in a hypoexponential distribution. While a closed form expression of the cumulative distribution function exists, a closed form expression of the constraint would result in a reverse convex constraint. Further, as the cumulative distribution function is not invertible, quantile methods cannot be used.

Second, the squared difference of exponential random variables, as is the case with the collision avoidance constraint, results in the sum of Weibull random variables. The pdf, cdf, and characteristic function of a sum of Weibull random variables can only be expressed as an infinite summation [92, 93]. Thus, closed form evaluations of the chance constraint probabilities are practically impossible. At present, methods that create bounds based on moments are the only methods that allow for almost surely satisfaction of each chance constraint.

Experimental Setup

For this experiment, I presume there are three deputies such that $N_v = 3$. I presume the admissible control set is $\mathcal{U}_i = [-0.75, 0.75]^2 N \cdot \Delta\mathrm{t}^{-1}$ and time horizon $N = 8$, corresponding to 8 minutes of operation. The performance objective is based on fuel consumption,

$$J(\vec{U}_1, \ldots, \vec{U}_{N_v}) = \sum_{i=1}^{N_v} \vec{U}_i^\top \vec{U}_i \tag{4.36}$$

The terminal sets $\mathcal{T}_i(N)$ are 5×5m boxes centered around desired terminal locations in x, y coordinates with velocity bounded in both directions by $[-0.1, 0.1]$m/s. For collision avoidance, I presume that each deputy must remain at least $r = 12$m away from each other, hence $S = \begin{bmatrix} I_2 & 0_2 \end{bmatrix}$ to extract the positions. Violation thresholds for terminal sets and collision avoidance are $\alpha = \gamma = 0.075$. The chance constraints are defined as

$$\mathbb{P}\left(\bigcap_{i=1}^{3} \vec{\boldsymbol{x}}_i(N) \in \mathcal{T}_i(N)\right) \geq 1 - \alpha \tag{4.37}$$

$$\mathbb{P}\left(\bigcap_{k=1}^{8} \bigcap_{i,j=1}^{3} \|S\left(\vec{\boldsymbol{x}}_i(k) - \vec{\boldsymbol{x}}_j(k)\right)\| \geq r\right) \geq 1 - \gamma \tag{4.38}$$

Figure 1.1 provides a graphic representation of the demonstration presented.

As has been established [25, 91], biconvexity associated with having both risk allocation and control variables can be addressed in an iterative fashion, by alternately solving for the risk allocation variables, then for the control. However, for my demonstration, to isolate the impact of the one-sided Vysochanskij-Petunin inequality, I presume a fixed risk allocation. I uniformly allocate risk such that

$$\mathbb{P}(\|S\left(\vec{\boldsymbol{x}}_i(k) - \vec{\boldsymbol{x}}_j(k)\right)\| \geq r) \geq 1 - \hat{\gamma} \qquad \forall\, i, j, k \tag{4.39}$$

where $\hat{\gamma} = \frac{\gamma}{24 \text{ constraints}} = \frac{.15}{24} = 3.125 \times 10^{-3}$. These values remain constraint throughout the iterative solution finding process.

I define the solution convergence thresholds for the convex-concave procedure as both the difference of sequential performance objectives as less than 10^{-6} and the sum of slack variables as less than 10^{-8}. Difference of convex programs were limited to 100 iterations. The first order approximations of the reverse convex constraints were initially computed assuming no system input.

For a random variable $\boldsymbol{x} \sim Exp(\lambda)$, where λ is the rate parameter,

$$\mathbb{E}(\boldsymbol{x}^n) = \frac{n!}{\lambda^n} \qquad \forall\, n \in \mathbb{N} \tag{4.40}$$

Hence, Assumption 4.3 is valid. I keep with the notation used in Section 4.3.2. Since I assumed the disturbances are independent and identically distributed, from (4.40) I find

$$\begin{aligned} \mathbb{E}(\vec{\boldsymbol{z}}) &= 0_{q\times 1} \\ \mathbb{V}(\vec{\boldsymbol{z}}) &= 2S\mathcal{D}(k)\mathbb{V}\left(\vec{\boldsymbol{W}}_i\right)\mathcal{D}^\top(k)S^\top \end{aligned} \tag{4.41}$$

where

$$\mathbb{V}\left(\vec{\boldsymbol{W}}_i\right) = \operatorname{diag}\left(20^{-2}\cdot I_2, 10^{-8}\cdot I_2, \ldots, 20^{-2}\cdot I_2, 10^{-8}\cdot I_2\right) \tag{4.42}$$

Next, from (4.41)

$$\mathbb{E}\left(\vec{\boldsymbol{z}}^\top\vec{\boldsymbol{z}}\right) = \operatorname{tr}\left(\mathbb{V}(\vec{\boldsymbol{z}})\right) \tag{4.43}$$

Next, I find $\mathbb{V}\left(\vec{\boldsymbol{z}}^\top\vec{\boldsymbol{z}}\right)$. For brevity, I denote $\vec{\boldsymbol{W}}_i - \vec{\boldsymbol{W}}_j$ as $\vec{\boldsymbol{\mathcal{W}}}$. Then,

$$\mathbb{V}\left(\vec{\boldsymbol{z}}^\top\vec{\boldsymbol{z}}\right) = \mathbb{V}\left(\vec{\boldsymbol{\mathcal{W}}}^\top\mathcal{D}^\top(k)S^\top S\mathcal{D}(k)\vec{\boldsymbol{\mathcal{W}}}\right) \tag{4.44a}$$

$$= \mathbb{V}\left(\sum_{p=1}^{Nn}\sum_{q=1}^{Nn} a_{pq}\vec{\boldsymbol{\mathcal{W}}}_p\vec{\boldsymbol{\mathcal{W}}}_q\right) \tag{4.44b}$$

$$= \sum_{p=1}^{Nn}\sum_{q=1}^{Nn}\sum_{r=1}^{Nn}\sum_{s=1}^{Nn}\mathbb{C}(a_{pq}\boldsymbol{\mathcal{W}}_p\boldsymbol{\mathcal{W}}_q, a_{rs}\boldsymbol{\mathcal{W}}_r\boldsymbol{\mathcal{W}}_s) \tag{4.44c}$$

where a_{pq} is the $(p,q)^{\text{th}}$ element of $\mathcal{D}^\top(k)S^\top S\mathcal{D}(k)$. Then

$$\begin{aligned} &\sum_{p=1}^{Nn}\sum_{q=1}^{Nn}\sum_{r=1}^{Nn}\sum_{s=1}^{Nn}\mathbb{C}\left(a_{pq}\vec{\boldsymbol{\mathcal{W}}}_p\vec{\boldsymbol{\mathcal{W}}}_q, a_{rs}\vec{\boldsymbol{\mathcal{W}}}_r\vec{\boldsymbol{\mathcal{W}}}_s\right) \\ &= \sum_{p=1}^{Nn}\mathbb{V}\left(a_{pp}\vec{\boldsymbol{\mathcal{W}}}_p^2\right) + 4\sum_{1\le p<q\le Nn}\mathbb{V}\left(a_{pq}\vec{\boldsymbol{\mathcal{W}}}_p\vec{\boldsymbol{\mathcal{W}}}_q\right) \end{aligned} \tag{4.45}$$

Here, all remaining covariance terms is zero as each element is mutually independent by

Assumptions 4.1 and 4.2, and the first and third moments being zero. So,

$$\begin{aligned}
&\sum_{p=1}^{Nn} \mathbb{V}\left(a_{pp}\vec{\mathcal{W}}_p^2\right) + 4\sum_{1\le p<q\le Nn} \mathbb{V}\left(a_{pq}\vec{\mathcal{W}}_p\vec{\mathcal{W}}_q\right) \\
&= \sum_{p=1}^{Nn} a_{pp}^2 \left(\mathbb{E}\left(\vec{\mathcal{W}}_p^4\right) - \mathbb{E}\left(\vec{\mathcal{W}}_p^2\right)^2\right) + 4\sum_{1\le p<q\le Nn} a_{pq}^2 \mathbb{E}\left(\vec{\mathcal{W}}_p^2\right)\mathbb{E}\left(\vec{\mathcal{W}}_q^2\right) && \text{(4.46a)} \\
&= 3\sum_{p=1}^{Nn} a_{pp}^2 \mathbb{E}\left(\vec{\mathcal{W}}_p^2\right)^2 + 2\sum_{p=1}^{Nn}\sum_{q=1}^{Nn} a_{pq}^2 \mathbb{E}\left(\vec{\mathcal{W}}_p^2\right)\mathbb{E}\left(\vec{\mathcal{W}}_q^2\right) && \text{(4.46b)}
\end{aligned}$$

as in this example $\mathbb{E}\left(\vec{\mathcal{W}}_p^4\right) = 6\mathbb{E}\left(\vec{\mathcal{W}}_p^2\right)^2$. Then, let $\vec{a}$ be a vector consisting of the diagonal elements of $\mathcal{D}^\top(k)S^\top S\mathcal{D}(k)$. So,

$$\begin{aligned}
&\sum_{p=1}^{Nn} a_{pp}^2 \mathbb{E}\left(\vec{\mathcal{W}}_p^2\right)^2 + 2\sum_{p=1}^{Nn}\sum_{q=1}^{Nn} a_{pq}^2 \mathbb{E}\left(\vec{\mathcal{W}}_p^2\right)\mathbb{E}\left(\vec{\mathcal{W}}_q^2\right) && \text{(4.47a)} \\
&= 12\vec{a}^\top \mathbb{V}\left(\vec{\boldsymbol{W}}_i\right)^2 \vec{a} + 8\mathrm{tr}\left(\left(\mathcal{D}^\top(k)S^\top\mathbb{V}\left(\vec{\boldsymbol{W}}_i\right)S\mathcal{D}(k)\right)^2\right) && \text{(4.47b)}
\end{aligned}$$

Finally, I find $\mathbb{C}\left(\vec{z}, \vec{z}^\top\vec{z}\right)$.

$$\mathbb{C}\left(\vec{z}, \vec{z}^\top\vec{z}\right) = \mathbb{E}\left(\vec{z}\vec{z}^\top\vec{z}\right) - \mathbb{E}(\vec{z})\,\mathbb{E}\left(\vec{z}^\top\vec{z}\right) \tag{4.48}$$

The second term is zero by (4.41). For a random vector, the expectation is a vector of the expectations of each element. Then for the i^{th} element,

$$\mathbb{E}\left(\vec{z}_i\vec{z}^\top\vec{z}\right) = \mathbb{E}\left(\vec{z}_i^3\right) + \sum_{\substack{j=1\\ j\neq i}}^{Nn} \mathbb{E}(\vec{z}_i)\,\mathbb{E}\left(\vec{z}_j^2\right) \tag{4.49}$$

Since the first and third moments of $\vec{z}$ are zero, then the sum is zero. Thus, $\mathbb{C}\left(\vec{z}, \vec{z}^\top\vec{z}\right) = 0$.

For the target set constraint, I can determine that the chance constraint is unimodal as the exponential distribution is a strongly unimodal distribution, as per Definition 4.2.

Metric	Proposed Method	MPC with Cantelli's Inequality [1]
Solve Time	6.5230 s	10.7012 s
Iterations	9	13
Solution Cost	0.1156	0.1244

Table 4.1: Comparison of Solution and Computation Time for CWH Dynamics with Exponential Disturbance.

Hence, the affine constraint is unimodal. However, the Weibull random variables that result in the collision avoidance constraint are not strong unimodal. Here, unimodality of the constraint was validated numerically via Algorithm 3 for each vehicle pair and each time step after computing the solution. Validation was completed with randomly sampled 50,000 disturbances.

Comparison Methodology

I compare my method against the method in [1], the predecessor of the method proposed in this work based on Cantelli's inequality. This approach is effective for and has been demonstrated on systems which have target constraints and can be solved via convex optimization. I extend this method to accommodate 2-norm based collision constraints (as in Section 4.3.2) for the purpose of comparison with my own approach. I do not consider methods based on Chebyshev's inequality because they have shown to be less effective than [1] in a target constraint problem [87].

Theorem 4.2 (Cantelli's inequality [35]). *Let $\boldsymbol{x}$ be a real valued random variable with finite expectation $\mathbb{E}(\boldsymbol{x})$ and finite, non-zero standard deviation $\mathbb{S}(\boldsymbol{x})$. Then, for any $\lambda > 0$,*

$$\mathbb{P}(\boldsymbol{x} - \mathbb{E}(\boldsymbol{x}) \geq \lambda \mathbb{S}(\boldsymbol{x})) \leq \frac{1}{\lambda^2 + 1} \tag{4.50}$$

Experimental Results

The resulting trajectories are shown in Figure 4.2. I see that the two solutions result in similar trajectories. The most noticeable difference is that the trajectory of the proposed

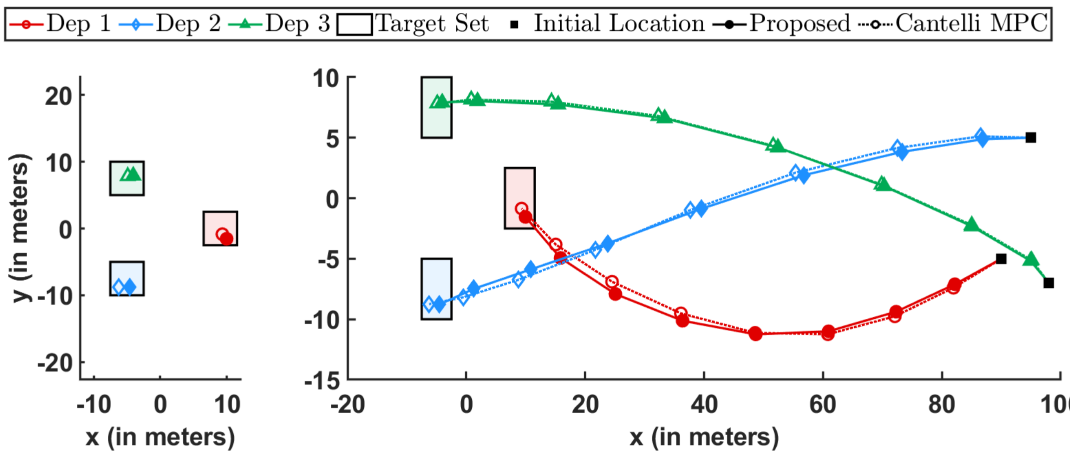

Figure 4.2: Comparison of mean trajectories between proposed method (solid line with filled in markers), and MPC with Cantelli's inequality [1] (dotted line with white markers) for planar CWH dynamics with exponential disturbance. The full trajectory is displayed on the right and the terminal state is on the left. I see the two methods had similar trajectories but notice the proposed method was closer to the boundary of the target sets.

Constraint	Proposed Method	MPC with Cantelli's Inequality [1]
Target Set (4.37)	0.9999	1.0000
Avoid Each Other (4.38)	1.0000	1.0000

Table 4.2: Constraint Satisfaction for CWH Dynamics with Exponential Disturbance, with 10^4 Samples and Probabilistic Violation Threshold of $\alpha = \gamma = 0.075$.

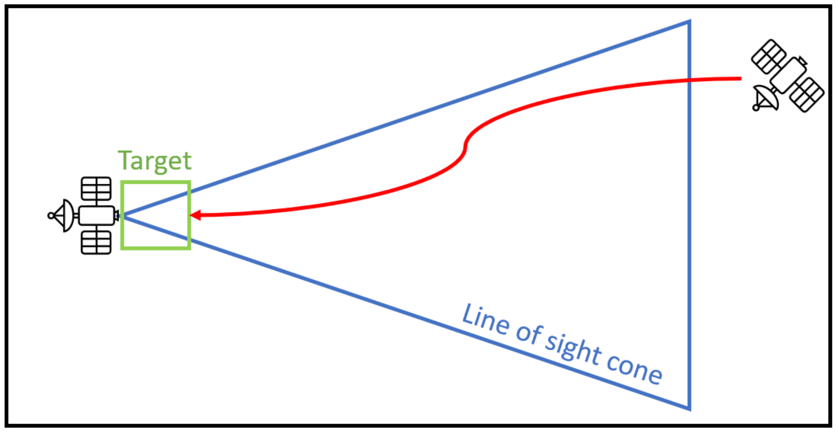

Figure 4.3: Scenario in which the deputy must reach a desired target set while staying within the chiefs line-of-sight cone.

method was consistently closer to the boundary of the target set. The solution cost, iterations needed to converge, and computation times are shown in Table 4.1. In all three categories, the proposed method performed better than the method of [1]. To assess constraint satisfaction, I generated 10^4 Monte Carlo sample disturbances for each approach. Table 4.2 shows that while both methods were conservative, the proposed method was less conservative.

As this example demonstrates, I can make probabilistic guarantees for disturbances that may arise in common circumstances. As discussed earlier, these distributional assumptions made in this example result in complicated distributions that lack analytical form. It is in distribution assumptions like these made in this example where this method will thrive.

4.4.2 Gaussian Disturbance

I include an example with a Gaussian disturbance to facilitate comparison with more conventional methods. In this example, I simplify the comparison example to only consider a convex joint chance constraint with a time-varying target set, as in Section 4.3.1. This scenario is demonstrated in Figure 4.3.

Experimental Setup

For this experiment, I presume there is a single deputy that must stay within a predefined line of sight cone and reach a terminal target set as shown in Figure 4.3. I presume the admissible control set is $\mathcal{U}_i = [-0.1, 0.1]^2 N \cdot \Delta \mathrm{t}^{-1}$ and time horizon $N = 5$, corresponding to 5 minutes of operation. The performance objective is based on fuel consumption,

$$J(\vec{U}_1) = \vec{U}_1^\top \vec{U}_1 \tag{4.51}$$

The line-of-sight cone is defined by the inequalities

$$\begin{aligned} -x + 2y &\leq 0 \\ -x - 2y &\leq 0 \\ x &\leq 10 \end{aligned} \tag{4.52}$$

The terminal sets $\mathcal{T}(N)$ is a 2×1m near the origin with velocity bounded in both directions by $[-0.1, 0.1]$m/s. The violation thresholds for joint target set constraint is $\alpha = 0.05$. The chance constraint is defined as

$$\mathbb{P}\left(\bigcap_{k=1}^{5} \vec{\boldsymbol{x}}_1(k) \in \mathcal{T}_1(k) \right) \geq 1 - \alpha \tag{4.53}$$

I presume the disturbance is Gaussian,

$$\vec{\boldsymbol{w}}_1(k) \sim N\left(\vec{0}, \mathrm{diag}\left(10^{-3}, 10^{-3}, 10^{-8}, 10^{-8}\right)\right) \tag{4.54}$$

Using the properties of the Gaussian disturbance, I know that all moments exist such that Assumption 4.3 is valid. Further, affine summations of Gaussian disturbances are still Gaussian. Hence, each target set constraint is unimodal, validating Assumption 4.4.

Comparison Methodologies

Here, I compare the proposed methodology against a broader field of chance constrained stochastic optimal control methods. Several methods exist to solve convex chance constraints in a Gaussian regime. Hence, I select comparison methodologies that have been used extensively to solve chance constrained problems with Gaussian disturbances but can also handle non-Gaussian disturbances. Specifically, I compare the proposed method with quantile approach in [2, 3], the scenario approach in [4, 5], and the particle control approach in [6].

The quantile approach results in a reformulation that is a convex in the input and the Gaussian quantile function. The quantile method allows for almost surely guarantees of chance constraint satisfaction as the disturbance is Gaussian. The particle control approach relies on sample disturbances and the chance constraint reformulation results in a mixed integer linear program. The particle control approach can only guarantee chance constraint satisfaction asymptotically as the number of samples goes to infinity. To minimize computational complexity, I select 200 sample disturbances to compute the optimal control trajectory with the particle control approach.

Like the particle control approach, the scenario approach relies on samples to compute an optimal controller. The reformulation of the scenario approach results in a linear program. The scenario approach can guarantee chance constraints up to a probabilistic confidence bound δ. By setting the confidence bound to a sufficiently small value, the probabilistic guarantees of the scenario approach closely resemble that of the proposed method. I compute the number of samples required for the scenario approach with the formula [38]

$$N_s \geq \frac{2}{\alpha}\left(\ln \frac{1}{\delta} + N_o\right) \tag{4.55}$$

where N_s is the number of samples required and N_o is the number of optimization variables. Here, $N_o = 10$, and I choose $\delta = 10^{-16}$ and $N_s = 937$.

Metric	Solve Time (sec)	Solution Cost ($10^{-4} N^2$)	Satisfaction of (4.53)
Proposed Method	0.1842	6.0075	1.0000
Quantile Method [2, 3]	1.0377	5.1885	0.9539
Scenario Approach [4, 5]	3.8575	5.3353	0.9937
Particle Control [6]	30.5232	5.1865	0.9449

Table 4.3: Comparison of Computation Time, Solution Cost, and Constraint Satisfaction for CWH Dynamics with Multivariate Gaussian Disturbance with violation threshold $\alpha = 0.05$. Chance constraint satisfaction was measured as a ratio of 10^4 samples satisfying the constraint.

I expect the proposed method to result in more conservative solutions compared with these approaches. This stems from the conservative nature of the one-sided Vysochanskij-Petunin inequality [60]. However, I also expect to see the proposed method compute solutions in less time than the comparison methods. I expect this as the proposed method doesn't rely on samples as the scenario and particle control method, and the simplicity of the proposed reformulation in comparison to the quantile approach.

Experimental Results

The resulting trajectories are not very different between the four methods as shown in Figure 4.4. The most notable difference is that the trajectory of the proposed method is further from the boundary of the target sets, implying conservatism of the trajectory, as expected. This is also shown in Table 4.3. Here, I see the proposed method has higher chance constraint satisfaction and larger solution cost. I note that in empirical testing of chance constraint satisfaction, only particle control was not able to meet the required probability violation threshold as expected.

Table 4.3 shows that the proposed method was able to compute the solution in significantly less time. Indeed, the proposed method was an order of magnitude faster than the quantile approach and the scenario approach, and two orders of magnitude faster than the particle control approach.

As shown in this example, the method sacrifices optimality for broad applicability. In

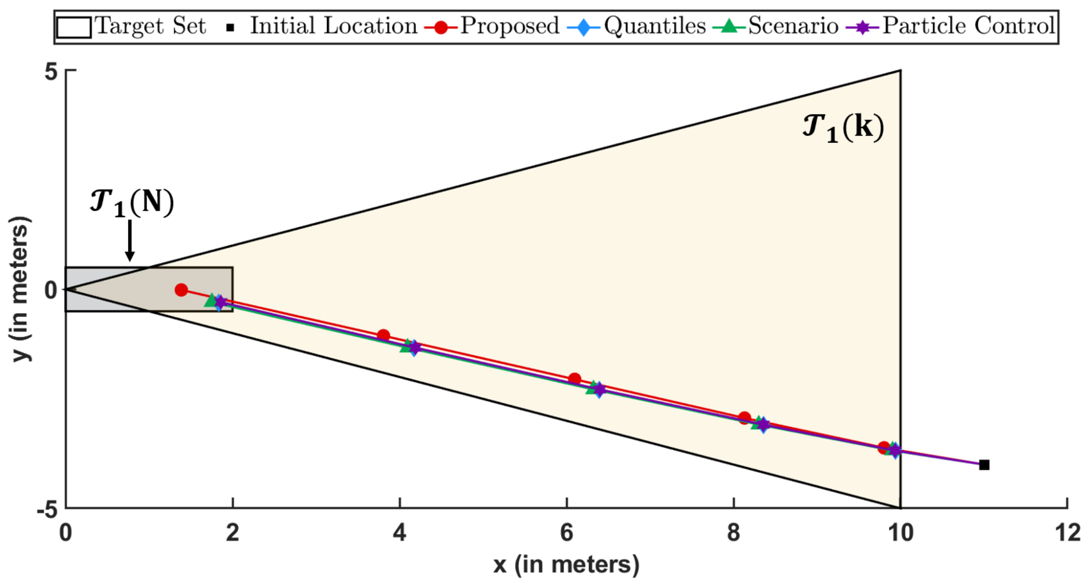

Figure 4.4: Comparison of mean trajectories between proposed method (red, circle), quantile-based approach [2, 3] (blue, diamond), the scenario approach [4, 5] (green, triangle), and the particle control approach [6] (purple, 6-pointed star) for CWH dynamics with multivariate Gaussian disturbance. Here, I observe the trajectories are very similar. Note that the quantile approach and the particle control approach had nearly identical trajectories. This makes it difficult to see the trajectory of the quantile approach in this figure.

this particular case, the sacrifice was a solution cost that was approximately 13% larger than the compared methods. However, the computational benefits, broad applicability of this method, and almost surely guarantees of chance constraint satisfaction present a strong case to use this method in instances where the improved speed is important.

4.5 Summary

I proposed a framework to solve chance-constrained stochastic optimal control problems for LTI systems subject to arbitrary disturbances under moment and unimodality assumptions. This work focuses on probabilistic requirements for polytopic target sets and 2-norm based collision avoidance constraints. My approach relies on the one-sided Vysochanskij–Petunin inequality to reformulate joint chance constraints into a series of inequalities that can be readily solved as a difference of convex functions optimization problem. I demonstrated my method on a multi-satellite rendezvous scenario under exponential and Gaussian disturbance assumptions and compare with an MPC approach using Cantelli's inequality (the predecessor of this work), a quantile-based approach, the scenario approach, and the particle control approach. I showed that this approach is amenable to disturbances that prove challenging or impossible to solve with other methods and demonstrated the proposed method has computational benefits in comparison to other commonly used methods.

Chapter 5

Sample Moments Based Approach

5.1 Introduction

In contrast to the previous two chapters, I now focus on a method based on samples of the disturbance vector. This chapter is motivated by scenarios in which there is no analytic knowledge of the underlying distribution, as can occur in space applications. For this chapter the disturbance is considered both unknown and arbitrary but sampled.

One of the primary challenges preventing sample based methods from providing assurances of probabilistic constraint satisfaction, is lack of knowledge of the underlying process. Without knowledge of the underlying distribution, analytic techniques cannot be evoked to evaluate the chance constraint probability. Particle control approaches utilize sample data to synthesize a controller that satisfies the constraint for a percentage of samples corresponding to the probabilistic safety threshold to avoid the need for analytic evaluations [6]. However, the particle control approach does not have a finite sample confidence bound and can only provide satisfaction assurances asymptotically [22]. In contrast, the scenario approach relies on synthesizing a control that satisfies the constraint for each disturbance sample in the sample set [4, 38]. For finite sample sizes, the scenario approach guarantees the synthesized controller satisfies the chance constraint and is optimal up to a probabilistic confidence bound [4]. While the scenario approach, and similarly the particle control approach, suffer from computational burden of large sample sizes, methods have been proposed to decrease the computational burden by discarding samples [44], as well as optimizing over a subset of the samples [45].

In contrast, data reduction methods have been posed to simplify sample-based approaches based on parameter estimation [94, 95, 96], a common tool from statistical literature. By computing moments or extremum of the sample set, probabilistic evaluations can be computed via robust control principals [28, 97] or taken as ground truth and incorporated into moment based approaches [98] such as the method presented in Chapter 4. While robust and ground truth assumptions can be sufficient asymptotically via the central limit theorem, computation with finite sample sizes can lead to maneuvers that are not safe when implemented.

My approach also relies on data reduction via moment estimation. However, through a theorem derived in this chapter, this approach allows for *almost surely* probabilistic guarantees of chance constraint satisfaction despite requiring no knowledge of the underlying disturbance process. Hence, I propose application of this approach to chance constraint evaluation that arises in multi-vehicle planning problems: that is, in a) reaching a terminal target set and b) avoiding collision with obstacles in the environment as well as with other vehicles. The main contribution of this chapter is a *closed-form* reformulation of chance constraints based on sample statistics, for polytopic target sets and collision avoidance constraints, that is amenable to difference of convex programming solutions. The main drawback in this approach is that solutions are conservative with respect to other sample based methods.

The chapter is organized as follows. Section 5.2 provides additional preliminaries required for Problem 1. Section 5.3 reformulates the chance constraints by approximating the quantile function. Section 5.4 demonstrates my approach on three multi-satellite rendezvous problems, and Section 5.5 provides concluding remarks.

5.2 Problem Formulation

In addition to the problem formulation in Chapter 2.4, I add several assumptions and observations that will be required for the work in this chapter. With arbitrary and unknown but sampled disturbances corrupting the satellite dynamics, I seek to synthesize a controller to construct an optimal rendezvous maneuver that satisfies chance constraints target set and collision avoidance.

Definition 5.1 (Almost Surely [61]). *Let* $(\Psi, \mathcal{B}(\Psi), \mathbb{P})$ *be a probability space with outcomes* Ψ*, Borel* σ*-algebra* $\mathcal{B}(\Psi)$*, and probability measure* $\mathbb{P}$*. An event* $\mathcal{A} \in \mathcal{B}(\Psi)$ *happens almost surely if* $\mathbb{P}(\mathcal{A}) = 1$ *or* $\mathbb{P}(\mathcal{A}^c) = 0$ *where* $\cdot^c$ *denotes the complement of the event.*

As the disturbance is unknown and arbitrary, I make several key assumptions about the quantity and quality of the sampled disturbance data that allow us to make (2.15) a tractable problem.

Assumption 5.1. *For each vehicle, the concatenated disturbance vector* $\vec{\boldsymbol{W}}_i$ *has been independently sampled* N_s *times. I denote the sampled values as* $\vec{\boldsymbol{W}}_i^{[j]}$ *for* $j \in \mathbb{N}_{[1,N_s]}$.

Assumption 5.2. *The sample size* N_s *must be sufficiently large such that the reformulations presented in this work are tractable.*

Assumption 5.3. *For each vehicle, the concatenated disturbance vector samples* $\vec{\boldsymbol{W}}_i^{[j]}$ *are almost surely not all equal.*

Assumptions 5.1-5.2 are required to compute sample mean and standard deviation. Assumption 5.2 guarantees that the sample based concentration inequality developed here can be applied for my reformulations. Assumption 5.3 guarantees the distribution is not degenerate or deterministic.

Problem 1.3. *Under Assumptions 5.1-5.3, solve Problem (1) with probabilistic violation thresholds* α*,* β*, and* γ *for open loop controllers* $\vec{U}_1, \dots, \vec{U}_{N_v} \in \mathcal{U}^N$.

The main challenge in solving Problem 1.3 is assuring (2.13). Without knowledge of the underlying distribution, analytic techniques cannot be used to derive reformulations that allow for guarantees. Further, current sample based methods can only guarantee chance constraint satisfaction approximately or asymptotically.

5.3 Methods

My approach to solve Problem 1.3 involves reformulating each chance constraint as an affine summation of the random variable's sample mean and sample standard deviation, i.e., $\hat{\mathbb{E}}(\|S(\vec{\boldsymbol{x}}_i(k)-\vec{\boldsymbol{x}}_j(k))\|)$ and $\hat{\mathbb{S}}(\|S(\vec{\boldsymbol{x}}_i(k)-\vec{\boldsymbol{x}}_j(k))\|)$, respectively for the collision avoidance constraint. The reformulation is a result of a concentration inequality based on sample statistics that is developed in this work. Said concentration inequality guarantees satisfaction of (2.13) almost surely.

5.3.1 Establishing Sample Bounds

Here, I state the pivotal theorem that allow us to solve Problem 1.3.

Theorem 5.1. *Let $\boldsymbol{x}$ follow some distribution f. Let $\boldsymbol{x}^{[1]}, \dots, \boldsymbol{x}^{[N_s]}$ be samples drawn independently from the distribution f, for some $N_s \geq 2$. Let*

$$\hat{\mathbb{E}}(\boldsymbol{x}) = \frac{1}{N_s}\sum_{i=1}^{N_s} \boldsymbol{x}^{[i]} \tag{5.1a}$$

$$\hat{\mathbb{S}}(\boldsymbol{x}) = \sqrt{\frac{1}{N_s}\sum_{i=1}^{N_s} (\boldsymbol{x}^{[i]} - \hat{\mathbb{E}}(\boldsymbol{x}))^2} \tag{5.1b}$$

be the sample mean and sample standard deviation, respectively, with $\hat{\mathbb{S}}(\boldsymbol{x}) > 0$ almost surely. Then for any $\lambda > 0$

$$\mathbb{P}\Big(\boldsymbol{x} - \hat{\mathbb{E}}(\boldsymbol{x}) \geq \lambda \hat{\mathbb{S}}(\boldsymbol{x})\Big) \leq \frac{(\sqrt{N_s+1}+\lambda)^2}{\lambda^2 N_s + (\sqrt{N_s+1}+\lambda)^2} \tag{5.2}$$

For brevity, I define $N_s^* = N_S + 1$ and

$$f(\lambda) = \frac{(\sqrt{N_s^*} + \lambda)^2}{\lambda^2 N_s + (\sqrt{N_s^*} + \lambda)^2} \tag{5.3}$$

To prove Theorem 5.1, I first need to state and prove the following Lemma.

Lemma 5.1. *Let $\boldsymbol{x}^{[1]}, \ldots, \boldsymbol{x}^{[N_s]}$ be identically distributed samples drawn independently where $N_s \geq 2$. Let*

$$\hat{\mathbb{E}}(\boldsymbol{x}) = \frac{1}{N_s} \sum_{i=1}^{N_s} \boldsymbol{x}^{[i]} \tag{5.4a}$$

$$\hat{\mathbb{S}}(\boldsymbol{x}) = \sqrt{\frac{1}{N_s} \sum_{i=1}^{N_s} (\boldsymbol{x}^{[i]} - \hat{\mathbb{E}}(\boldsymbol{x}))^2} \tag{5.4b}$$

be the sample mean and sample standard deviation, respectively, with $\hat{\mathbb{S}}(\boldsymbol{x}) > 0$ almost surely. Then for $\lambda > 0$

$$\mathbb{P}\Big(\boldsymbol{x}^{[i]} - \hat{\mathbb{E}}(\boldsymbol{x}) \geq \lambda \hat{\mathbb{S}}(\boldsymbol{x})\Big) \leq \frac{1}{\lambda^2 + 1} \tag{5.5}$$

for $i \in \mathbb{N}_{[1,N_s]}$.

Proof. Observe

$$\mathbb{P}\Big(\boldsymbol{x}^{[i]} - \hat{\mathbb{E}}(\boldsymbol{x}) \geq \lambda \hat{\mathbb{S}}(\boldsymbol{x})\Big) \tag{5.6a}$$

$$= \mathbb{P}\left(\frac{\boldsymbol{x}^{[i]} - \hat{\mathbb{E}}(\boldsymbol{x})}{\hat{\mathbb{S}}(\boldsymbol{x})} \geq \lambda\right) \tag{5.6b}$$

$$= \mathbb{P}\left(\frac{\boldsymbol{x}^{[i]} - \hat{\mathbb{E}}(\boldsymbol{x})}{\hat{\mathbb{S}}(\boldsymbol{x})} - \mathbb{E}\left(\frac{\boldsymbol{x}^{[i]} - \hat{\mathbb{E}}(\boldsymbol{x})}{\hat{\mathbb{S}}(\boldsymbol{x})}\right) \geq \lambda \mathbb{S}\left(\frac{\boldsymbol{x}^{[i]} - \hat{\mathbb{E}}(\boldsymbol{x})}{\hat{\mathbb{S}}(\boldsymbol{x})}\right)\right) \tag{5.6c}$$

as

$$\mathbb{E}\left(\frac{\boldsymbol{x}^{[i]}-\hat{\mathbb{E}}(\boldsymbol{x})}{\hat{\mathbb{S}}(\boldsymbol{x})}\right)=0 \tag{5.7a}$$

$$\mathbb{S}\left(\frac{\boldsymbol{x}^{[i]}-\hat{\mathbb{E}}(\boldsymbol{x})}{\hat{\mathbb{S}}(\boldsymbol{x})}\right)=1 \tag{5.7b}$$

Then by Cantelli's inequality

$$\mathbb{P}\left(\frac{\boldsymbol{x}^{[i]}-\hat{\mathbb{E}}(\boldsymbol{x})}{\hat{\mathbb{S}}(\boldsymbol{x})}-\mathbb{E}\left(\frac{\boldsymbol{x}^{[i]}-\hat{\mathbb{E}}(\boldsymbol{x})}{\hat{\mathbb{S}}(\boldsymbol{x})}\right)\geq\lambda\mathbb{S}\left(\frac{\boldsymbol{x}^{[i]}-\hat{\mathbb{E}}(\boldsymbol{x})}{\hat{\mathbb{S}}(\boldsymbol{x})}\right)\right)\leq\frac{1}{\lambda^2+1} \tag{5.8}$$

for any $\lambda > 0$. □

With Lemma 5.1 established, I can prove Theorem 5.1.

Proof of Theorem 5.1. Let $\hat{\mathbb{E}}(\boldsymbol{x})^*$ and $\hat{\mathbb{S}}(\boldsymbol{x})^*$ be the sample mean and sample standard deviation calculates with $N_s^* = N_s + 1$ samples. Note that

$$\boldsymbol{x}^{[N_s^*]}-\hat{\mathbb{E}}(\boldsymbol{x})^* = \frac{N_s}{N_s^*}(\boldsymbol{x}^{[N_s^*]}-\hat{\mathbb{E}}(\boldsymbol{x})) \tag{5.9a}$$

$$N_s^{*2}\hat{\mathbb{V}}(\boldsymbol{x})^* = N_sN_s^*\hat{\mathbb{V}}(\boldsymbol{x})+N_s(\boldsymbol{x}^{[N_s^*]}-\hat{\mathbb{E}}(\boldsymbol{x}))^2 \tag{5.9b}$$

Then for $\lambda > 0$

$$\mathbb{P}\left(\boldsymbol{x}^{[N_s^*]}-\hat{\mathbb{E}}(\boldsymbol{x})\geq\lambda\hat{\mathbb{S}}(\boldsymbol{x})\right) \tag{5.10a}$$

$$=\mathbb{P}\left(\sqrt{N_sN_s^*}(\boldsymbol{x}^{[N_s^*]}-\hat{\mathbb{E}}(\boldsymbol{x}))\geq\lambda\sqrt{N_sN_s^*}\hat{\mathbb{S}}(\boldsymbol{x})\right) \tag{5.10b}$$

$$=\mathbb{P}\left((\sqrt{N_sN_s^*}+\lambda\sqrt{N_s})(\boldsymbol{x}^{[N_s^*]}-\hat{\mathbb{E}}(\boldsymbol{x}))\geq\lambda\sqrt{N_sN_s^*}\hat{\mathbb{S}}(\boldsymbol{x})+\lambda\sqrt{N_s}(\boldsymbol{x}^{[N_s^*]}-\hat{\mathbb{E}}(\boldsymbol{x}))\right) \tag{5.10c}$$

$$\leq\mathbb{P}\left((\sqrt{N_sN_s^*}+\lambda\sqrt{N_s})(\boldsymbol{x}^{[N_s^*]}-\hat{\mathbb{E}}(\boldsymbol{x}))\geq\lambda\sqrt{N_sN_s^*\hat{\mathbb{V}}(\boldsymbol{x})+N_s(\boldsymbol{x}^{[N_s^*]}-\hat{\mathbb{E}}(\boldsymbol{x}))^2}\right) \tag{5.10d}$$

where (5.10d) results from the triangle inequality. Then,

$$
\begin{aligned}
&\mathbb{P}\left((\sqrt{N_sN_s^*}+\lambda\sqrt{N_s})(\boldsymbol{x}^{[N_s^*]}-\hat{\mathbb{E}}(\boldsymbol{x}))\geq\lambda\sqrt{N_sN_s^*\hat{\mathbb{V}}(\boldsymbol{x})+N_s(\boldsymbol{x}^{[N_s^*]}-\hat{\mathbb{E}}(\boldsymbol{x}))^2}\right)\\
&=\mathbb{P}\left((\sqrt{N_sN_s^*}+\lambda\sqrt{N_s})(\boldsymbol{x}^{[N_s^*]}-\hat{\mathbb{E}}(\boldsymbol{x}))\geq\lambda N_s^*\hat{\mathbb{S}}(\boldsymbol{x})^*\right) && (5.10e)\\
&=\mathbb{P}\left((\boldsymbol{x}^{[N_s^*]}-\hat{\mathbb{E}}(\boldsymbol{x}))\geq\frac{\lambda N_s^*}{\sqrt{N_sN_s^*}+\lambda\sqrt{N_s}}\hat{\mathbb{S}}(\boldsymbol{x})^*\right) && (5.10f)\\
&=\mathbb{P}\left(\frac{N_s}{N_s^*}(\boldsymbol{x}^{[N_s^*]}-\hat{\mathbb{E}}(\boldsymbol{x}))\geq\frac{\lambda\sqrt{N_s}}{\sqrt{N_s^*}+\lambda}\hat{\mathbb{S}}(\boldsymbol{x})^*\right) && (5.10g)\\
&=\mathbb{P}\left(\boldsymbol{x}^{[N_s^*]}-\hat{\mathbb{E}}(\boldsymbol{x})^*\geq\frac{\lambda\sqrt{N_s}}{\sqrt{N_s^*}+\lambda}\hat{\mathbb{S}}(\boldsymbol{x})^*\right) && (5.10h)\\
&=\mathbb{P}\left(\boldsymbol{x}^{[N_s^*]}-\hat{\mathbb{E}}(\boldsymbol{x})^*\geq\kappa\hat{\mathbb{S}}(\boldsymbol{x})^*\right) && (5.10i)
\end{aligned}
$$

Where κ is a simple substitution. Here, $\lambda > 0$ implies $\kappa > 0$. So, by Lemma 5.1,

$$
\begin{aligned}
\mathbb{P}\left(\boldsymbol{x}^{[N_s^*]}-\hat{\mathbb{E}}(\boldsymbol{x})^*\geq\kappa\hat{\mathbb{S}}(\boldsymbol{x})^*\right) &\leq\frac{1}{\kappa^2+1} && (5.10j)\\
&=\frac{1}{\left(\frac{\lambda\sqrt{N_s}}{\sqrt{N_s^*+\lambda}}\right)^2+1} && (5.10k)
\end{aligned}
$$

Simplifying (5.10k) leads to (5.2). □

Theorem 5.1 provides a bound for deviations of a random variable $\boldsymbol{x}$ from the sample mean. For the purpose of generating open loop controllers in an optimization framework, this will allow us to bound chance constraints based on sample statistics of sample disturbance data.

To address the need for Assumption 5.2, I observe that

$$\lim_{\lambda\to\infty} f(\lambda)=\frac{1}{N_s^*} \tag{5.11}$$

For any probabilistic violation threshold smaller than this value, Theorem 5.1 will not

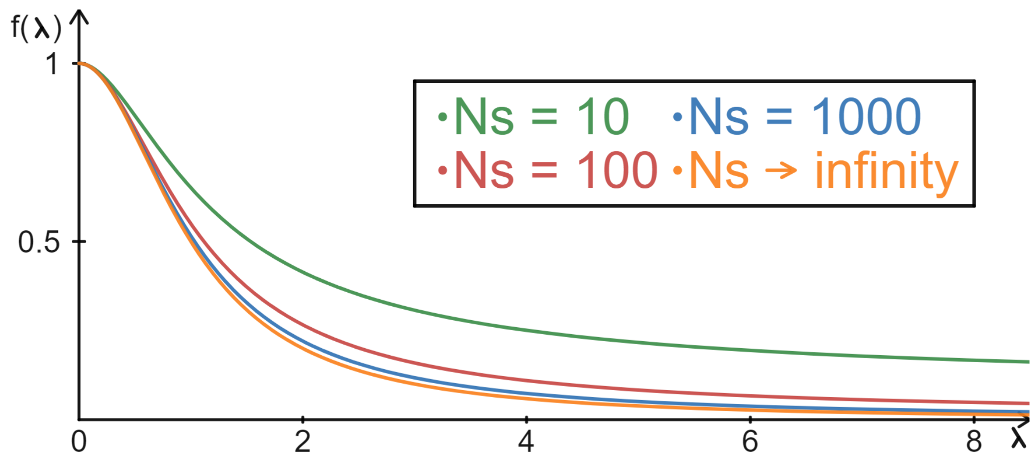

Figure 5.1: Graph of (5.11) for values of $N_s \in \{10, 100, 1000\}$ and as $N_s \to \infty$.

be sufficiently tight to bound the constraint. Figure 5.1 graphs (5.3) for N_s taking the values 10, 100, and 1000, and as $N_s \to \infty$.

Note that I did not use Bessel's correction [61] in the sample variance formula to simplify the probabilistic bound. Accordingly, the sample variance statistic I used is biased in relation to the variance of the distribution. An analogous result can be derived with Bessel's correction, however, the bound becomes more complex.

I can easily find the lower tail bound with Theorem 5.1 by substituting $\boldsymbol{x}$ with $-\boldsymbol{x}$ as

$$\mathbb{P}\Big(\boldsymbol{x} - \hat{\mathbb{E}}(\boldsymbol{x}) \leq -\lambda \hat{\mathbb{S}}(\boldsymbol{x})\Big) \leq f(\lambda) \tag{5.12}$$

This observation will be useful in the reformulation of the collision avoidance constraints.

5.3.2 Polytopic Target Set Constraint

First, consider the reformulation of (2.13a). Without loss of generality, I presume $N_v = 1$ and $N = 1$ for brevity. From (2.14), I can write

$$\mathbb{P}(\vec{\boldsymbol{x}}_i(k) \in \mathcal{T}_i(k)) = \mathbb{P}\left(\bigcap_{j=1}^{N_{ik}} \vec{G}_{ika} \vec{\boldsymbol{x}}_i(k) \leq h_{ika}\right) \tag{5.13}$$

where $\vec{G}_{ika} \in \mathbb{R}^n$ and $h_{ika} \in \mathbb{R}$. I take the complement and employ Boole's inequality to separate the combined chance constraints into a series of individual chance constraints,

$$\mathbb{P}(\boldsymbol{x}_i(k) \notin \mathcal{T}_i(k)) = \mathbb{P}\left(\bigcup_{j=1}^{N_{ik}} \vec{G}_{ika}\vec{\boldsymbol{x}}_i(k) \geq h_{ika}\right) \tag{5.14a}$$

$$\leq \sum_{j=1}^{N_{ik}} \mathbb{P}\Big(\vec{G}_{ika}\vec{\boldsymbol{x}}_i(k) \geq h_{ika}\Big) \tag{5.14b}$$

Using the approach in [25], I introduce ω_{ika} to allocate risk for each individual chance constraint,

$$\mathbb{P}\Big(\vec{G}_{ika}\vec{\boldsymbol{x}}_i(k) \geq h_{ika}\Big) \leq \omega_{ika} \tag{5.15a}$$

$$\sum_{j=1}^{N_{ik}} \omega_{ika} \leq \alpha \tag{5.15b}$$

$$\omega_{ika} \geq 0 \tag{5.15c}$$

To find a solution to (5.15), I need to find an appropriate value for ω_{ika}. To that end, I add the additional constraints

$$\hat{\mathbb{E}}\Big(\vec{G}_{ika}\vec{\boldsymbol{x}}_i(k)\Big) + \lambda_{ika}\hat{\mathbb{S}}\Big(\vec{G}_{ika}\vec{\boldsymbol{x}}_i(k)\Big) \leq h_{ika} \tag{5.16a}$$

$$\lambda_{ika} > 0 \tag{5.16b}$$

with $\lambda_{ika} > 0$ where $\hat{\mathbb{E}}[\vec{G}_{ika}\vec{\boldsymbol{x}}_i(k)]$ and $\hat{\mathrm{Std}}(\vec{G}_{ika}\vec{\boldsymbol{x}}_i(k))$ are the sample mean and sample standard deviation, respectively. For brevity, I denote

$$\hat{\mathbb{F}}(\vec{\boldsymbol{x}}_i(k), \lambda_{ika}) = \hat{\mathbb{E}}\Big(\vec{G}_{ika}\vec{\boldsymbol{x}}_i(k)\Big) + \lambda_{ika}\hat{\mathbb{S}}\Big(\vec{G}_{ika}\vec{\boldsymbol{x}}_i(k)\Big) \tag{5.17}$$

Enforcement of (5.16) guarantees that

$$\mathbb{P}\Big(\vec{G}_{ika}\vec{\boldsymbol{x}}_i(k) \geq h_{ika}\Big) \leq \mathbb{P}\Big(\vec{G}_{ika}\vec{\boldsymbol{x}}_i(k) \geq \hat{\mathbb{F}}(\vec{\boldsymbol{x}}_i(k), \lambda_{ika})\Big) \tag{5.18}$$

allowing us to write (5.15) as

$$\mathbb{P}\Big(\vec{G}_{ika}\vec{\boldsymbol{x}}_i(k) \geq \hat{\mathbb{F}}(\vec{\boldsymbol{x}}_i(k), \lambda_{ika})\Big) \leq \omega_{ika} \tag{5.19a}$$

$$\hat{\mathbb{F}}(\vec{\boldsymbol{x}}_i(k), \lambda_{ika}) \geq h_{ika} \tag{5.19b}$$

$$\sum_{j=1}^{N_{ik}} \omega_{ika} \leq \alpha \tag{5.19c}$$

$$\omega_{ika} \geq 0 \tag{5.19d}$$

$$\lambda_{ika} > 0 \tag{5.19e}$$

Then, by Assumptions 5.1-5.3 and Theorem 5.1, I can substitute

$$\omega_{ika} = f(\lambda_{ika}) \tag{5.20}$$

via (5.2). Then (5.19) becomes

$$\mathbb{P}\Big(\vec{G}_{ika}\vec{\boldsymbol{x}}_i(k) \geq \hat{\mathbb{F}}(\vec{\boldsymbol{x}}_i(k), \lambda_{ika})\Big) \leq f(\lambda_{ika}) \tag{5.21a}$$

$$\hat{\mathbb{F}}(\vec{\boldsymbol{x}}_i(k), \lambda_{ika}) \geq h_{ika} \tag{5.21b}$$

$$\sum_{j=1}^{N_{ik}} f(\lambda_{ika}) \leq \alpha \tag{5.21c}$$

$$f(\lambda_{ika}) \geq 0 \tag{5.21d}$$

$$\lambda_{ika} > 0 \tag{5.21e}$$

To use Theorem 5.1, I must impose the restriction $N_s \geq 2$. This restriction will be in addition to Assumption 5.2.

I can simplify (5.15b) as (5.21b)-(5.21c) enforce (5.21a) and (5.21e) enforces (5.21d). Hence, (5.15b) becomes

$$\hat{\mathbb{F}}(\vec{\boldsymbol{x}}_i(k), \lambda_{ika}) \geq h_{ika} \tag{5.22a}$$

$$\sum_{j=1}^{N_{ik}} f(\lambda_{ika}) \leq \alpha \tag{5.22b}$$

$$\lambda_{ika} > 0 \tag{5.22c}$$

with (5.22a) and (5.22c) iterated over the index $j \in \mathbb{N}_{[1,N_{ik}]}$.

Next, I show that $\hat{\mathbb{F}}(\vec{\boldsymbol{x}}_i(k), \lambda_{ika})$ has a closed and convex form. Observe that the sample mean vector and sample variance-covariance matrix of $\vec{\boldsymbol{W}}$ are

$$\hat{\mathbb{E}}\left(\vec{\boldsymbol{W}}_i\right) = \frac{1}{N_s} \sum_{[i]=1}^{N_s} \vec{\boldsymbol{W}}_i^{[i]} \tag{5.23a}$$

$$\hat{\mathbb{V}}\left(\vec{\boldsymbol{W}}_i\right) = \frac{1}{N_s} \sum_{[i]=1}^{N_s} \left(\vec{\boldsymbol{W}}_i^{[i]} - \hat{\mathbb{E}}\left(\vec{\boldsymbol{W}}_i\right)\right) \left(\vec{\boldsymbol{W}}_i^{[i]} - \hat{\mathbb{E}}\left(\vec{\boldsymbol{W}}_i\right)\right)^\top \tag{5.23b}$$

Then, the sample mean and standard deviation for the each half-space constraint is

$$\hat{\mathbb{E}}\left(\vec{G}_{ika}\vec{\boldsymbol{x}}_i(k)\right) = \vec{G}_{ika} \left(A^k \vec{x}_i(0) + \mathcal{C}(k)\vec{U}_i + \mathcal{D}(k)\hat{\mathbb{E}}\left(\vec{\boldsymbol{W}}_i\right)\right) \tag{5.24a}$$

$$\hat{\mathbb{S}}\left(\vec{G}_{ika}\vec{\boldsymbol{x}}_i(k)\right) = \sqrt{\vec{G}_{ika}\mathcal{D}(k)\hat{\mathbb{V}}\left(\vec{\boldsymbol{W}}_i\right) \mathcal{D}^\top(k)\vec{G}_{ijk}^\top} \tag{5.24b}$$

So,

$$\begin{aligned} &\hat{\mathbb{F}}(\vec{\boldsymbol{x}}_i(k), \lambda_{ika}) \\ &= \vec{G}_{ika} \left(A^k \vec{x}_i(0) + \mathcal{C}(k)\vec{U}_i + \mathcal{D}(k)\hat{\mathbb{E}}\left(\vec{\boldsymbol{W}}_i\right)\right) + \lambda_{ika}\sqrt{\vec{G}_{ika}\mathcal{D}(k)\hat{\mathbb{V}}\left(\vec{\boldsymbol{W}}_i\right) \mathcal{D}^\top(k)\vec{G}^\top} \end{aligned} \tag{5.25}$$

which is affine, and hence convex, in the control input.

Finally, I note that (5.22b) is not convex over the set $\lambda_{ika} > 0$. Here, I must find the values of λ_{ika} that make the constraint (5.22b) convex. Observe the second partial derivative of $f(\lambda)$ with respect to λ is

$$\frac{\partial^2}{\partial\lambda^2} f(\lambda) = \frac{2N_s\left(\lambda^3(N_s^*)^{3/2} + 3\lambda^2(N_s^*)^2 - (N_s^*)^2\right)}{\left(N_s\lambda^2 + \left(\lambda + \sqrt{N_s^*}\right)^2\right)^3} \tag{5.26}$$

Then $f(\lambda)$ has inflection points where

$$\frac{2}{\sqrt{N_s^*}}\lambda^3 + 3\lambda^2 - 1 = 0 \tag{5.27}$$

The function (5.27) has three real roots with the only positive root being [99]

$$\lambda = \underbrace{\sqrt{N_s^*}\left[\cos\left(\frac{1}{3}\arccos\left(-\frac{N_s - 1}{N_s^*}\right)\right) - \frac{1}{2}\right]}_{\Theta(N_s)} \tag{5.28}$$

Further, for $\Theta(N_s)$ defined in (5.28), observe that $\lambda > \Theta(N_s) \Leftrightarrow f''(\lambda) > 0$ implying that $f(\lambda)$ is convex. Hence, the inequalities (5.22) become

$$\hat{\mathbb{F}}(\vec{\boldsymbol{x}}_i(k), \lambda_{ika}) \leq h_{ika} \tag{5.29a}$$

$$\sum_{j=1}^{N_{ik}} f(\lambda_{ika}) \leq \alpha \tag{5.29b}$$

$$\lambda_{ika} \geq \Theta(N_s) \tag{5.29c}$$

with (5.29a) and (5.29c) iterated over the index $j \in \mathbb{N}_{[1,N_{ik}]}$.

In practice, it may be simpler to substitute $\Theta(N_s)$ with $3^{-1/2}$ as $3^{-1/2} \geq \Theta(N_s)$ for all values of N_s. Here, $\lambda \leq 3^{-1/2} \Leftrightarrow f(\lambda) \geq 0.75$. In most cases, probabilistic violation thresholds will not take values this large, and outcomes will not be affected as a result.

Formally, the final reformulation is written as

$$\vec{G}_{ika}\left(A^k\vec{x}_i(0)+\mathcal{C}(k)\vec{U}_i+\mathcal{D}(k)\hat{\mathbb{E}}\left(\vec{\boldsymbol{W}}_i\right)\right)+\lambda_{ika}\sqrt{\vec{G}_{ika}\mathcal{D}(k)\hat{\mathbb{V}}\left(\vec{\boldsymbol{W}}_i\right)\mathcal{D}^\top(k)\vec{G}_{ika}^\top}\leq h_{ika} \tag{5.30a}$$

$$\sum_{j=1}^{N_{ik}}\frac{(\sqrt{N_s^*}+\lambda_{ika})^2}{\lambda_{ika}^2N_s+(\sqrt{N_s^*}+\lambda_{ika})^2}\leq\alpha \tag{5.30b}$$

$$\sqrt{N_s^*}\left[\cos\left(\frac{1}{3}\arccos\left(-\frac{N_s-1}{N_s^*}\right)\right)-\frac{1}{2}\right]\leq\lambda_{ika} \tag{5.30c}$$

Lemma 5.2. *The constraint reformulation (5.30) will always be convex in $\vec{U}_i$ and λ_{ika}.*

Proof. Here, (5.30a) is affine and hence convex, in both $\vec{U}_i$ and λ_{ika}. Further, $f(\lambda)$ is convex by the restriction (5.30c). Since, (5.30b) is the sum of convex functions, it too is convex. Finally, the control authority $\mathcal{U}$ is a closed and convex set. Therefore, the chance constraint reformulation (5.30) will always be convex. □

Lemma 5.3. *For the controllers $\vec{U}_1,\dots,\vec{U}_{N_v}$, if there exists risk allocation variables λ_{ika} satisfying (5.30) for constraints in the form of (2.13a), then $\vec{U}_1,\dots,\vec{U}_{N_v}$ satisfies (2.15d) almost surely.*

Proof. Satisfaction of (5.30a) implies (5.18) holds. Theorem 5.1 upper bounds (5.18). Boole's inequality and De Morgan's law guarantee that if (5.22b) holds then (2.15d) is satisfied. □

I take a moment to discuss Assumption 5.2. From (5.11), I see that (5.30b) is lower bounded by

$$\frac{N_{ik}}{N_s^*}\leq\textstyle\sum_{k=1}^{N}\sum_{i=1}^{N_{ik}}f(\lambda_{ika}) \tag{5.31}$$

In theory, this means the number of samples need to be

$$N_s \geq \frac{\sum_{k=1}^{N} N_{ik}}{\alpha} - 1 \tag{5.32}$$

such that there may exist a solution that satisfies (5.30b). However, since (5.11) is an asymptotic bound, more samples will be required to allow for finite values of λ_{ika}. In practice, the minimum number of samples needed will be dependent on α, the volume of the polytopic region, number of hyperplane constraints, and the magnitude of the variance term.

5.3.3 2-Norm Based Collision Avoidance Constraints

Next, consider the reformulations of the 2-norm constraints (2.13b)-(2.13c). Here, I will derive the reformulation of (2.13c), but the reformulation of (2.13b) is nearly identical. Without loss of generality define

$$\vec{z} = S\left(A^k\left(\vec{x}_i(0) - \vec{x}_j(0)\right) + \mathcal{C}(k)\left(\vec{U}_i - \vec{U}_j\right)\right) \tag{5.33a}$$

$$\vec{\boldsymbol{z}}^{[i]} = S\mathcal{D}(k)\left(\vec{\boldsymbol{W}}_i^{[i]} - \vec{\boldsymbol{W}}_j^{[i]}\right) \tag{5.33b}$$

to be the non-stochastic and stochastic element of $S(\vec{\boldsymbol{x}}_i^{[i]}(k) - \vec{\boldsymbol{x}}_j^{[i]}(k))$, respectively. Then, I can write the norm as,

$$\|S(\vec{\boldsymbol{x}}_i(k) - \vec{\boldsymbol{x}}_j(k))\| = \|\vec{z} + \vec{\boldsymbol{z}}\| \tag{5.34}$$

I start by observing

$$\mathbb{P}\left(\bigcap_{i=1}^{N_v-1}\bigcap_{j=i+1}^{N_v}\bigcap_{k=1}^{N}\|\vec{z} + \vec{\boldsymbol{z}}\| \geq r\right) = \mathbb{P}\left(\bigcap_{i=1}^{N_v-1}\bigcap_{j=i+1}^{N_v}\bigcap_{k=1}^{N}\|\vec{z} + \vec{\boldsymbol{z}}\|^2 \geq r^2\right) \tag{5.35}$$

as the norm is non-negative. Thus, I can write the 2-norm constraint as

$$\mathbb{P}\left(\bigcap_{i=1}^{N_v-1} \bigcap_{j=i+1}^{N_v} \bigcap_{k=1}^{N} \|\vec{z} + \vec{\boldsymbol{z}}\|^2 \geq r^2\right) \geq 1 - \gamma \tag{5.36}$$

By taking the complement and applying Boole's inequality,

$$\mathbb{P}\left(\bigcup_{i=1}^{N_v-1} \bigcup_{j=i+1}^{N_v} \bigcup_{k=1}^{N} \|\vec{z} + \vec{\boldsymbol{z}}\|^2 \leq r^2\right) \leq \sum_{i=1}^{N_v-1} \sum_{j=i+1}^{N_v} \sum_{k=1}^{N} \mathbb{P}\big(\|\vec{z} + \vec{\boldsymbol{z}}\|^2 \leq r^2\big) \tag{5.37}$$

Using the approach in [25], I introduce risk variables ω_{ika} to allocate risk to each of the individual probabilities

$$\mathbb{P}\big(\|\vec{z} + \vec{\boldsymbol{z}}\|^2 \leq r^2\big) \leq \omega_{ijk} \tag{5.38a}$$

$$\sum_{i=1}^{N_v-1} \sum_{j=i+1}^{N_v} \sum_{k=1}^{N} \omega_{ijk} \leq \gamma \tag{5.38b}$$

$$\omega_{ijk} \geq 0 \tag{5.38c}$$

In a similar fashion to Section 5.3.2, I add an additional constraint based on the sample mean and sample tandard deviation of $\|\vec{z} + \vec{\boldsymbol{z}}\|^2$ to (5.38) such that the constraint becomes

$$\mathbb{P}\big(\|\vec{z} + \vec{\boldsymbol{z}}\|^2 \leq r^2\big) \leq \omega_{ijk} \tag{5.39a}$$

$$\hat{\mathbb{E}}\big(\|\vec{z} + \vec{\boldsymbol{z}}\|^2\big) - \lambda_{ijk}\hat{\mathbb{S}}\big(\|\vec{z} + \vec{\boldsymbol{z}}\|^2\big) \geq r^2 \tag{5.39b}$$

$$\sum_{i=1}^{N_v-1} \sum_{j=i+1}^{N_v} \sum_{k=1}^{N} \omega_{ijk} \leq \gamma \tag{5.39c}$$

$$\omega_{ijk} \geq 0 \tag{5.39d}$$

$$\lambda_{ijk} \geq 0 \tag{5.39e}$$

For brevity, I denote

$$\hat{\mathbb{G}}(\vec{\boldsymbol{x}}_i(k), \vec{\boldsymbol{x}}_j(k), \lambda_{ijk}) = \hat{\mathbb{E}}\big(\|\vec{z} + \vec{\boldsymbol{z}}\|^2\big) - \lambda_{ijk}\hat{\mathbb{S}}\big(\|\vec{z} + \vec{\boldsymbol{z}}\|^2\big) \tag{5.40}$$

Enforcement of (5.39b) guarantees that

$$\mathbb{P}\big(\|\vec{z} + \vec{\boldsymbol{z}}\|^2 \leq r^2\big) \leq \mathbb{P}\Big(\|\vec{z} + \vec{\boldsymbol{z}}\|^2 \leq \hat{\mathbb{G}}(\vec{\boldsymbol{x}}_i(k), \vec{\boldsymbol{x}}_j(k), \lambda_{ijk})\Big) \tag{5.41}$$

Then, by Assumptions 5.1-5.3 and Theorem 5.1, I can substitute

$$\omega_{ijk} = f(\lambda_{ijk}) \tag{5.42}$$

and determine the value for λ_{ijk} in terms of ω_{ijk},

$$\lambda_{ijk} = \frac{\sqrt{N_s^* \left(1 - \omega_{ijk}\right)}}{\sqrt{N_s \omega_{ijk}} - \sqrt{1 - \omega_{ijk}}} \tag{5.43}$$

so long as $\lambda \geq 0$. Here, $\omega_{ijk} > 0 \Leftrightarrow \lambda_{ijk} > 0$. Then, I can write (5.39) as

$$\mathbb{P}\big(\|\vec{z} + \vec{\boldsymbol{z}}\|^2 \leq r^2\big) \leq \omega_{ijk} \tag{5.44a}$$

$$\hat{\mathbb{G}}\left(\vec{\boldsymbol{x}}_i(k), \vec{\boldsymbol{x}}_j(k), \frac{\sqrt{N_s^*(1 - \omega_{ijk})}}{\sqrt{N_s \omega_{ijk}} - \sqrt{1 - \omega_{ijk}}}\right) \geq r^2 \tag{5.44b}$$

$$\sum_{i=1}^{N_v - 1} \sum_{j=i+1}^{N_v} \sum_{k=1}^{N} \omega_{ijk} \leq \gamma \tag{5.44c}$$

$$\omega_{ijk} \geq 0 \tag{5.44d}$$

Since Theorem 5.1 guarantees that satisfaction of (5.44b) also satisfies (5.44a) for any value $\omega_{ijk} > 0$, (5.44a) is redundant and can be removed. The constraint is then

$$\hat{\mathbb{G}}\left(\vec{\boldsymbol{x}}_i(k), \vec{\boldsymbol{x}}_j(k), \frac{\sqrt{N_s^*(1-\omega_{ijk})}}{\sqrt{N_s\omega_{ijk}} - \sqrt{1-\omega_{ijk}}}\right) \geq r^2 \tag{5.45a}$$

$$\sum_{i=1}^{N_v-1} \sum_{j=i+1}^{N_v} \sum_{k=1}^{N} \omega_{ijk} \leq \gamma \tag{5.45b}$$

$$\omega_{ijk} \geq 0 \tag{5.45c}$$

Next, I show that $\hat{\mathbb{G}}(\vec{\boldsymbol{x}}_i(k), \vec{\boldsymbol{x}}_j(k), \lambda_{ijk})$ has a difference of convex and closed form in $\vec{U}_i - \vec{U}_j$. Observe that the sample mean vector and sample variance-covariance matrix of $\vec{\boldsymbol{z}}$ are

$$\hat{\mathbb{E}}(\vec{\boldsymbol{z}}) = \frac{1}{N_s} \sum_{[i]=1}^{N_s} \vec{\boldsymbol{z}}^{[i]} \tag{5.46a}$$

$$\hat{\mathbb{V}}(\vec{\boldsymbol{z}}) = \frac{1}{N_s} \sum_{[i]=1}^{N_s} \left(\vec{\boldsymbol{z}}^{[i]} - \hat{\mathbb{E}}(\vec{\boldsymbol{z}})\right)\left(\vec{\boldsymbol{z}}^{[i]} - \hat{\mathbb{E}}(\vec{\boldsymbol{z}})\right)^\top \tag{5.46b}$$

$$\tag{5.46c}$$

the sample mean and sample variance of $\vec{\boldsymbol{z}}^\top \vec{\boldsymbol{z}}$ are

$$\hat{\mathbb{E}}\left(\vec{\boldsymbol{z}}^\top \vec{\boldsymbol{z}}\right) = \frac{1}{N_s} \sum_{[i]=1}^{N_s} \vec{\boldsymbol{z}}^{[i]\top} \vec{\boldsymbol{z}}^{[i]} \tag{5.46d}$$

$$\hat{\mathbb{V}}\left(\vec{\boldsymbol{z}}^\top \vec{\boldsymbol{z}}\right) = \frac{1}{N_s} \sum_{[i]=1}^{N_s} \left(\vec{\boldsymbol{z}}^{[i]\top} \vec{\boldsymbol{z}}^{[i]} - \hat{\mathbb{E}}\left(\vec{\boldsymbol{z}}^\top \vec{\boldsymbol{z}}\right)\right)^2 \tag{5.46e}$$

and the sample covariance vector between $\vec{\boldsymbol{z}}$ and $\vec{\boldsymbol{z}}^\top \vec{\boldsymbol{z}}$ is

$$\hat{\mathbb{C}}\left(\vec{\boldsymbol{z}}, \vec{\boldsymbol{z}}^\top \vec{\boldsymbol{z}}\right) = \frac{1}{N_s} \sum_{[i]=1}^{N_s} \left(\vec{\boldsymbol{z}}^{[i]} - \hat{\mathbb{E}}(\vec{\boldsymbol{z}})\right)\left(\vec{\boldsymbol{z}}^{[i]\top} \vec{\boldsymbol{z}}^{[i]} - \hat{\mathbb{E}}\left(\vec{\boldsymbol{z}}^\top \vec{\boldsymbol{z}}\right)\right) \tag{5.46f}$$

Then the sample mean for the 2-norm constraint is

$$\hat{\mathbb{E}}\left(\|\vec{z}+\vec{\boldsymbol{z}}\|^2\right) = \frac{1}{N_s}\sum_{[i]=1}^{N_s} \|\vec{z}+\vec{\boldsymbol{z}}^{[i]}\|^2 \tag{5.47a}$$

$$= \left\| \begin{bmatrix} I_q & \hat{\mathbb{E}}(\vec{\boldsymbol{z}}) \\ \hat{\mathbb{E}}(\vec{\boldsymbol{z}})^\top & \hat{\mathbb{E}}\left(\vec{\boldsymbol{z}}^\top\vec{\boldsymbol{z}}\right) \end{bmatrix}^{\frac{1}{2}} \begin{bmatrix} \vec{z} \\ 1 \end{bmatrix} \right\|^2 \tag{5.47b}$$

and the sample standard deviation for the 2-norm constraint is

$$\hat{\mathbb{S}}\left(\|\vec{z}+\vec{\boldsymbol{z}}\|^2\right) = \sqrt{\frac{1}{N_s}\sum_{[i]=1}^{N_s}\left(\|\vec{z}+\vec{\boldsymbol{z}}^{[i]}\|^2 - \hat{\mathbb{E}}\left(\|\vec{z}+\vec{\boldsymbol{z}}\|^2\right)\right)^2} \tag{5.48a}$$

$$= \left\| \begin{bmatrix} 4\hat{\mathbb{V}}(\vec{\boldsymbol{z}}) & 2\hat{\mathbb{C}}\left(\vec{\boldsymbol{z}},\vec{\boldsymbol{z}}^\top\vec{\boldsymbol{z}}\right) \\ 2\hat{\mathbb{C}}\left(\vec{\boldsymbol{z}},\vec{\boldsymbol{z}}^\top\vec{\boldsymbol{z}}\right)^\top & \hat{\mathbb{V}}\left(\vec{\boldsymbol{z}}^\top\vec{\boldsymbol{z}}\right) \end{bmatrix}^{\frac{1}{2}} \begin{bmatrix} \vec{z} \\ 1 \end{bmatrix} \right\| \tag{5.48b}$$

Finally, I can write $\hat{\mathbb{G}}\left(\vec{\boldsymbol{x}}_i(k),\vec{\boldsymbol{x}}_j(k),\frac{\sqrt{N_s^*(1-\omega_{ijk})}}{\sqrt{N_s\omega_{ijk}}-\sqrt{1-\omega_{ijk}}}\right)$ as

$$\begin{aligned} &\hat{\mathbb{G}}\left(\vec{\boldsymbol{x}}_i(k),\vec{\boldsymbol{x}}_j(k),\frac{\sqrt{N_s^*(1-\omega_{ijk})}}{\sqrt{N_s\omega_{ijk}}-\sqrt{1-\omega_{ijk}}}\right) \\ &= \underbrace{\left\| \begin{bmatrix} I_q & \hat{\mathbb{E}}(\vec{\boldsymbol{z}}) \\ \hat{\mathbb{E}}(\vec{\boldsymbol{z}})^\top & \hat{\mathbb{E}}\left(\vec{\boldsymbol{z}}^\top\vec{\boldsymbol{z}}\right) \end{bmatrix}^{\frac{1}{2}} \begin{bmatrix} \vec{z} \\ 1 \end{bmatrix} \right\|^2}_{\hat{\mathbb{E}}(\|\vec{z}+\vec{\boldsymbol{z}}\|^2)} \\ &\quad - \underbrace{\frac{\sqrt{N_s^*(1-\omega_{ijk})}}{\sqrt{N_s\omega_{ijk}}-\sqrt{1-\omega_{ijk}}}}_{\lambda_{ijk}} \underbrace{\left\| \begin{bmatrix} 4\hat{\mathbb{V}}(\vec{\boldsymbol{z}}) & 2\hat{\mathbb{C}}\left(\vec{\boldsymbol{z}},\vec{\boldsymbol{z}}^\top\vec{\boldsymbol{z}}\right) \\ 2\hat{\mathbb{C}}\left(\vec{\boldsymbol{z}},\vec{\boldsymbol{z}}^\top\vec{\boldsymbol{z}}\right)^\top & \hat{\mathbb{V}}\left(\vec{\boldsymbol{z}}^\top\vec{\boldsymbol{z}}\right) \end{bmatrix}^{\frac{1}{2}} \begin{bmatrix} \vec{z} \\ 1 \end{bmatrix} \right\|}_{\hat{\mathbb{S}}(\|\vec{z}+\vec{\boldsymbol{z}}\|^2)} \end{aligned} \tag{5.49}$$

Both $\hat{\mathbb{E}}(\|\vec{z}+\vec{\boldsymbol{z}}\|^2)$ and $\hat{\mathbb{S}}(\|\vec{z}+\vec{\boldsymbol{z}}\|^2)$ are convex terms containing the controller $\vec{U}_i - \vec{U}_j$. Hence, (5.49) is a difference of convex function per Definition 2.1.

Note that (5.49) is biconvex [91] from the interaction of ω_{ijk} and $\vec{U}_i - \vec{U}_j$ in

$\lambda_{ijk}\hat{\mathbb{S}}(\|\vec{z}+\vec{\boldsymbol{z}}\|^2)$. For known risk allocation values $\tilde{\omega}_{ijk}$, the constraint (5.49) becomes,

$$\hat{\mathbb{G}}\left(\vec{\boldsymbol{x}}_i(k), \vec{\boldsymbol{x}}_j(k), \frac{\sqrt{N_s^*(1-\tilde{\omega}_{ijk})}}{\sqrt{N_s\tilde{\omega}_{ijk}} - \sqrt{1-\tilde{\omega}_{ijk}}}\right) \geq r^2 \tag{5.50}$$

Lemma 5.4. *The constraint (5.50) is always a difference-of-convex function constraint in $\vec{U}_i$ for constraints in the form (2.13b) and in $\vec{U}_i - \vec{U}_j$ for constraints in the form (2.13c).*

Proof. Observe that $\vec{z}$ is affine in the control input. Then both (5.47b) and (5.48b) are quadratic functions about a positive semi-definite matrix. Hence, both terms are convex. Then (5.49) is a difference of convex function per Definition 2.1. As $\tilde{\omega}_{ijk} > 0$ and is fixed, it follows that (5.50) is always a difference-of-convex functions constraint. □

Lemma 5.5. *If the controller $\vec{U}_1, \ldots, \vec{U}_{N_v}$, satisfies (5.50) for constraints in the form of (2.13b)-(2.13c), then $\vec{U}_1, \ldots, \vec{U}_{N_v}$ satisfy (2.15d) almost surely.*

Proof. Satisfaction of (5.50) implies (5.41) is satisfied for

$$\lambda_{ijk} = \frac{\sqrt{N_s^*(1-\omega_{ijk})}}{\sqrt{N_s\omega_{ijk}} - \sqrt{1-\omega_{ijk}}} \tag{5.51}$$

Assumption 5.2 guarantees λ_{ijk} is sufficiently tight. Then Theorem 5.1 guarantees satisfaction of (2.15d) almost surely. □

5.3.4 Difference of Convex Programming

Combining the results from Sections 5.3.2 and 5.3.3, I obtain a new optimization problem.

$$
\begin{aligned}
\underset{\substack{\vec{U}_1,\ldots,\vec{U}_{N_v} \\ \lambda_{ika}}}{\text{minimize}} \quad & J\left(\vec{\boldsymbol{X}}_1,\ldots,\vec{\boldsymbol{X}}_{N_v},\vec{U}_1,\ldots,\vec{U}_{N_v}\right) && \text{(5.52a)} \\
\text{subject to} \quad & \vec{U}_1,\ldots,\vec{U}_{N_v} \in \mathcal{U}^N, && \text{(5.52b)} \\
& \text{Sample mean and standard deviation} && \text{(5.52c)} \\
& \text{terms defined by (5.24) and (5.47)} - \text{(5.48)} && \\
& \text{Constraints (5.30) and (5.50)} && \text{(5.52d)}
\end{aligned}
$$

Reformulation 5.1. *Under Assumptions 5.1-5.2, solve the stochastic optimization problem (5.52) with probabilistic violation thresholds α, β, and γ for open loop controllers $\vec{U}_1,\ldots,\vec{U}_{N_v} \in \mathcal{U}^N$ and optimization variables λ_{ika}.*

Lemma 5.6. *Solutions to Reformulation 5.1 are conservative solutions to Problem 1.3.*

Proof. Lemmas 5.3 and 5.5 guarantee the probabilistic constraints (2.13) are satisfied almost surely. Chance constraint bounds provided by Theorem 5.1 are asymptotically convergent (in N_s) to Cantelli's inequality. As Cantelli's inequality is conservative, so is Theorem 5.1. The sample mean and standard deviation terms in Reformulation 5.1 encompass and replace the dynamics used in Problem 1.3. The cost and input constraints remain unchanged. □

Note that (5.52) is a difference-of-convex functions optimization problem. As in previous chapters, I employ the convex-concave procedure [64] to solve (5.52). Here, the first order approximation transforms the difference of convex function constraint (5.50) into the convex constraint

$$\frac{\sqrt{N_s^*(1-\omega_{ijk})}}{\sqrt{N_s\omega_{ijk}}-\sqrt{1-\omega_{ijk}}}\left\|\begin{bmatrix} 4\hat{\mathbb{V}}(\vec{\boldsymbol{z}}) & 2\hat{\mathbb{C}}\left(\vec{\boldsymbol{z}},\vec{\boldsymbol{z}}^\top\vec{\boldsymbol{z}}\right) \\ 2\hat{\mathbb{C}}\left(\vec{\boldsymbol{z}},\vec{\boldsymbol{z}}^\top\vec{\boldsymbol{z}}\right)^\top & \hat{\mathbb{V}}\left(\vec{\boldsymbol{z}}^\top\vec{\boldsymbol{z}}\right)\end{bmatrix}^{\frac{1}{2}}\begin{bmatrix}\vec{z}\\ 1\end{bmatrix}\right\|$$
$$-\underbrace{\left(\left\|\begin{bmatrix} I_q & \hat{\mathbb{E}}(\vec{\boldsymbol{z}}) \\ \hat{\mathbb{E}}(\vec{\boldsymbol{z}})^\top & \hat{\mathbb{E}}\left(\vec{\boldsymbol{z}}^\top\vec{\boldsymbol{z}}\right)\end{bmatrix}^{\frac{1}{2}}\begin{bmatrix}\vec{z}^p\\ 1\end{bmatrix}\right\|^2 + 2\left(\vec{z}^p+\hat{\mathbb{E}}(\vec{\boldsymbol{z}})\right)S\mathcal{C}(k)\left((\vec{U}_i-\vec{U}_j)-(\vec{U}_i^p+\vec{U}_j^p)\right)\right)}_{\text{First order approximation of } \hat{\mathbb{E}}(\|\vec{z}+\vec{\boldsymbol{z}}\|^2) \text{ based on previous iteration's solution.}}$$
$$\leq -r^2 \tag{5.53}$$

where the superscript p indicated the value from the previous iteration's solution. When using a difference of convex functions optimization problem, Lemma 5.5 guarantees a feasible but locally optimal solution.

5.4 Results

I demonstrate my method on a multi-satellite rendezvous problem with two different simulated disturbances that impact the relative satellite dynamics. All computations were done on a 1.80GHz i7 processor with 16GB of RAM, using MATLAB, CVX [78] and Gurobi [79]. Polytopic construction and plotting was done with MPT3 [80]. All code is available at `https://github.com/unm-hscl/shawnpriore-sample-bound-mpc`.

Consider a scenario in which N_v satellites, called the deputies, are stationed in geostationary Earth orbit, and tasked to rendezvous with a refueling spacecraft, called the chief. The satellites are tasked with reaching a new configuration represented by polytopic target sets. Each deputy must avoid other deputies while navigating to their respective target sets as shown in Figure 1.1. The relative planar dynamics of each deputy, with respect to the position of the chief are described by the equations (2.12) with sampling time Δt= 60s.

5.4.1 Gaussian Disturbance

I compare my method against the method in [1], the asymptotic and analytic counterpart of the method proposed in this work based on Cantelli's inequality (see Theorem 4.2). This approach is effective for and has been demonstrated on systems which have target constraints and can be solved via convex optimization. I extend this method to accommodate 2-norm based collision constraints (as in Section 5.3.3) for the purpose of comparison with my own approach.

As mentioned in the proof of Lemma 5.6, Theorem 5.1 is asymptotically convergent in N_s to the Cantelli's inequality [35] inequality per the central limit theorem [61]. In this demonstration, I show that Theorem 5.1 does not add significant conservatism in comparison to Cantelli's inequality despite using sample statistics over analytic expressions of moments. This can be particularly useful as computing sample statistics requires little computational overhead and no knowledge of the underlying disturbance.

Experimental Setup

I presume there are three deputies with the initial conditions are given by Table 5.1, the admissible control set is $\mathcal{U}_i = [-4, 4]^3 N \cdot \Delta\mathrm{t}^{-1}$, and time horizon $N = 5$, corresponding to 5 minutes of operation. The performance objective is based on fuel consumption.

$$J(\vec{U}_1, \dots, \vec{U}_3) = \sum_{i=1}^{3} \vec{U}_i^\top \vec{U}_i \tag{5.54}$$

I presume the disturbance is a zero-mean Gaussian distribution,

$$\boldsymbol{W}_i \sim \mathcal{N}(\vec{0}, I_5 \otimes \mathrm{blkdiag}(10^{-5} \cdot I_3, 10^{-8} \cdot I_3)) \tag{5.55}$$

Here, I have selected the sample size for the proposed method to be $N_s = 5,000$. For comparison, I use the expectation and covariance matrix parameters(5.55) to compute a solution with the method of [1].

The terminal sets $\mathcal{T}_i(N)$ are $5 \times 5 \times 5$m boxes centered around desired terminal locations in x, y coordinates approximately 11m away from the origin, with velocity bounded in all directions by $[-0.25, 0.25]$m/s. For collision avoidance, I presume that the deputies must remain at least $r = 10$m away from each other and the chief, hence $S = \begin{bmatrix} I_3 & 0_3 \end{bmatrix}$ to extract the positions. Violation thresholds for terminal sets and collision avoidance are $\alpha = \beta = \gamma = 0.05$, respectively. The chance constraints are defined as

$$\mathbb{P}\left(\bigcap_{i=1}^{3} \vec{\boldsymbol{x}}_i(N) \in \mathcal{T}_i(N)\right) \geq 1 - \alpha \tag{5.56}$$

$$\mathbb{P}\left(\bigcap_{k=1}^{5} \bigcap_{i=1}^{3} \|S\vec{\boldsymbol{x}}_i(k)\| \geq r\right) \geq 1 - \beta \tag{5.57}$$

$$\mathbb{P}\left(\bigcap_{k=1}^{5} \bigcap_{i,j=1}^{3} \|S\left(\vec{\boldsymbol{x}}_i(k) - \vec{\boldsymbol{x}}_j(k)\right)\| \geq r\right) \geq 1 - \gamma \tag{5.58}$$

Here $S = \begin{bmatrix} I_3 & 0_3 \end{bmatrix}$.

As has been established [25, 91], biconvexity associated with having both risk allocation and control variables can be addressed in an iterative fashion, by alternately solving for the risk allocation variables, then for the control. However, for my demonstration, to isolate the impact of Theorem 5.1, I presume a fixed risk allocation. I uniformly allocate risk such that

$$\mathbb{P}(\|S\boldsymbol{x}_i(k)\| \geq r) \geq 1 - \hat{\beta} \qquad \forall\, i, k \tag{5.59}$$

$$\mathbb{P}(\|S\left(\boldsymbol{x}_i(k) - \boldsymbol{x}_j(k)\right)\| \geq r) \geq 1 - \hat{\gamma} \qquad \forall\, i, j, k \tag{5.60}$$

where $\hat{\gamma} = \frac{\gamma}{15 \text{ constraints}} = \frac{.05}{15} = 0.00\overline{3}$ and similarly $\hat{\beta} = 0.00\overline{3}$. These values remain constant throughout the iterative solution finding process.

I define the solution convergence thresholds for the convex-concave procedure as both

	Chief	Dep 1	Dep 2	Dep 3
Radius (km)	42164.14	0.080	0.085	0.087
Eccentricity	0	0	0	0
Inclination (°)	10	-2×10^{-5}	0	10^-5
RAAN (°)	0	0	0	0
Arg. of perigee (°)	0	0	0	0
True anomaly (°)	90	1.8×10^{-5}	-9×10^{-6}	9×10^{-6}

Table 5.1: Orbital Elements Describing The Initial Orbits Of Each Satellite. Values For The Deputies Are Relative To The Chief's Position.

the difference of sequential performance objectives as less than 10^{-6} and the sum of slack variables as less than 10^{-8}. Difference of convex programs were limited to 100 iterations. The first order approximations of the reverse convex constraints were instantiated with no system input.

Experimental Results

Figure 5.2 shows the resulting trajectories of the two methods and Table 5.2 compares the time to compute a solution, solution cost, and empirical chance constraint satisfaction with 10^4 additional samples disturbances. The two methods preformed near identically. The only notable difference is that the proposed method resulted in an approximate 2% increase in solution cost. This is a small increase if I consider the proposed method does not require full knowledge of the underlying distribution. Here, I have shown that the proposed method results in only a small deviation for a finite sample size in comparison to that of its asymptotic and analytic counterpart as in [1].

5.4.2 Disturbance from Gravitational Effects

The CWH equations (2.8) are the result of a Taylor series expansion of the relative dynamics modeled via the 2-body problem [67]. While the 2-body problem models the predominant force in satellite motion, it ignores all the lesser forces that effect satellite motion. Forces such as the J_2 effect, solar and lunar third body gravity, and drag can

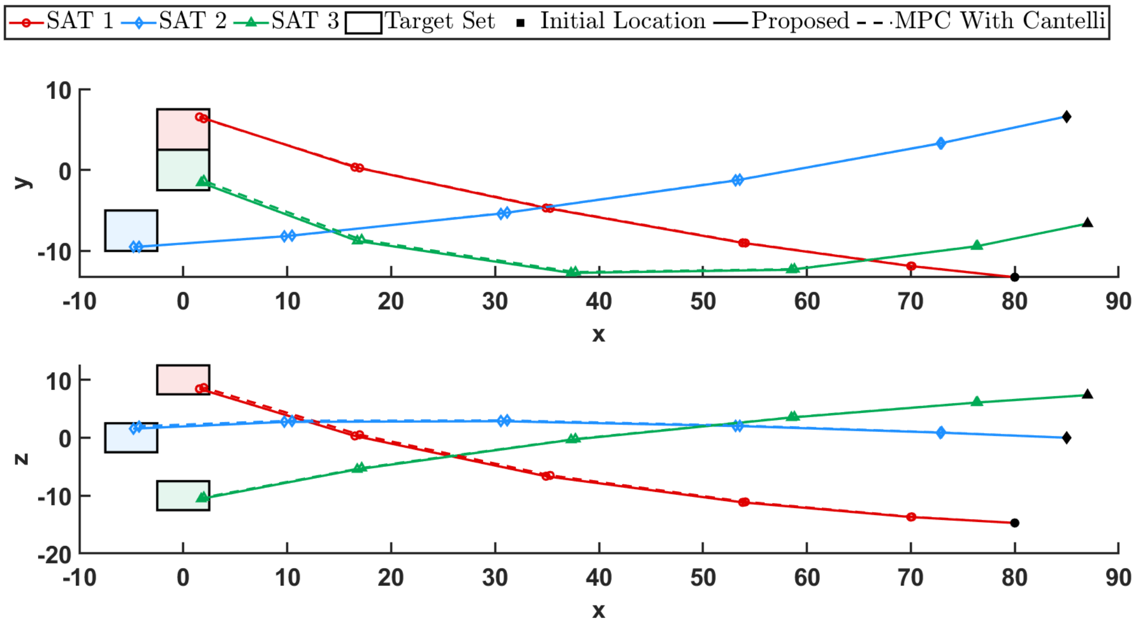

Figure 5.2: Comparison of mean trajectories between proposed method (solid line) and MPC approach using Cantelli's inequality [1] (dashed line) for CWH dynamics with Gaussian disturbance. Notice the trajectories are nearly identical.

Metric	Proposed	MPC with Cantelli's Ineq. [1]
Solve Time (sec)	6.9472	6.9833
Iterations	8	8
Solution Cost (N^2)	0.2020	0.1971
Terminal Set (5.56)	1.0000	1.0000
Avoid the Chief (5.57)	1.0000	1.0000
Avoid Each Other (5.58)	1.0000	1.0000

Table 5.2: Solution Cost, Computation Time, and Empirical Constraint Satisfaction for CWH Dynamics with Gaussian Disturbance and probabilistic violation thresholds $\alpha = \beta = \gamma = 0.05$. Constraint Satisfaction is Measured as a Ratio of 10^4 Monte Carlo Disturbance Samples that Satisfy the Constraint.

	Chief	Dep 1
Radius (km)	42164.14	0.012
Eccentricity	0	0
Inclination (°)	10	9×10^{-6}
RAAN (°)	0	0
Arg. of perigee (°)	0	0
True anomaly (°)	90	-8.1×10^{-6}

Table 5.3: Orbital Elements Describing The Initial Orbits Of The Deputy in Section 5.4.2. Values of The Deputy are Relative To The Chief's Position.

greatly affect the trajectory of the satellite over a long enough time horizon. In the 2-body model, these forces must be considered as disturbances despite lacking a standard distribution form [11, 10]. It is disturbances like these that motivate my approach.

In this demonstration, I use the disturbance term to capture the three largest disturbances to satellites at altitudes equivalent to geostationary orbit, the J_2 effect, and solar and lunar third body gravity. I compare the proposed method with the scenario approach in [4, 5], and the particle control approach in [6]. These methods are commonly used to address chance constraints with sample data. Note that neither the scenario approach or the particle control approach can accommodate the 2-norm collision avoidance constraint without embedding an *arbitrarily chosen* polytopic approximation of the collision avoidance region. To facilitate a fair comparison, I only consider the convex target set chance constraint so that I need not choose a particular polytopic approximation that may bias the results.

Experimental Setup

I presume there is one deputy with an initial condition given in Table 5.3, the admissible control set is $\mathcal{U}_i = [-0.04, 0.04]^3 N \cdot \Delta\mathrm{t}^{-1}$, and time horizon $N = 5$, corresponding to 5 minutes of operation. The performance objective is based on fuel consumption.

$$J(\vec{U}_1) = \vec{U}_1^\top \vec{U}_1 \tag{5.61}$$

I choose target sets $\mathcal{T}_1(k)$ that represent a line-of-sight cone for time steps 1 to $N-1$ and a docking position for the terminal time step. The line-of-sight cone for time steps 1 to $N-1$ is defined by

$$G_k = \begin{bmatrix} -1 & 0 & 1 & 0 & 0 & 0 \\ -1 & 1 & 0 & 0 & 0 & 0 \\ -1 & 0 & -1 & 0 & 0 & 0 \\ -1 & -1 & 0 & 0 & 0 & 0 \\ 1 & 0 & 0 & 0 & 0 & 0 \end{bmatrix} \quad \vec{h}_k = \begin{bmatrix} 0 \\ 0 \\ 0 \\ 0 \\ 10 \end{bmatrix} \tag{5.62}$$

The terminal set is defined by

$$G_N = I_6 \otimes \begin{bmatrix} 1 \\ -1 \end{bmatrix} \quad \vec{h}_N = \begin{bmatrix} 2 \\ 0 \\ \vec{1}_4 \\ 0.5 \cdot \vec{1}_6 \end{bmatrix} \tag{5.63}$$

This scenario was previously represented in Figure 4.3. The chance constraint is defined as

$$\mathbb{P}\left(\bigcap_{k=1}^{5} \boldsymbol{\vec{x}}_1(k) \in \mathcal{T}_1(k) \right) \geq 1 - \alpha \tag{5.64}$$

The violation threshold is chosen to be $\alpha = 0.05$.

I compare all three methods with the same sample set. Because the scenario approach has the largest sample size requirement, I will use its sample size for all three methods. To determine the number of samples needed for the scenario approach, I use the formula

$$N_s \geq \frac{2}{\alpha} \left(\ln \frac{1}{\beta} + N_o \right) \tag{5.65}$$

where $\beta \in (0, 1)$ is the confidence bound and N_o is the number of optimization variables [38]. I set $\beta = 10^{-16}$ and observe that $N_o = 15$, hence, I use $N_s = 2,073$ samples.

To generate my disturbance data, I propagate the chief and the deputy in one time step increments via both the 2-body equations and the force model:

$$\ddot{\vec{x}} = \frac{1}{m}\left(F_{GM} + F_{J2} + F_{Sun} + F_{Moon}\right) \tag{5.66}$$

where F_{GM} is the 2-body force, F_{J2} is the force created by the J_2 gravitational harmonic, and F_{Sun} and F_{Moon} are the third body gravity forces from the Sun and Moon, respectively. For the equations of motion, and the position calculations for the Sun and Moon, I follow Sections 3.2 and 3.3 of [100]. I do not include them here for brevity. I then convert the propagated trajectories into the chief's body fixed local frame and take the difference as the disturbance. This process was completed for $N_s = 2,073$ sample disturbances with sun and moon positions calculated with a random and uniformly distributed time between midnight on November 13$^{\text{th}}$, 2022 and January 12$^{\text{th}}$, 2023. Figure 5.3 plots a histogram for each element of the Deputy's disturbance vector at time step 0, $\vec{\boldsymbol{w}}_1^{[i]}(0)$. As I can see, each of the histograms display very different and non-Gaussian disturbances. Each of these distributions would be challenging to characterize with standard distributions, leading to poor results from modeling-based approaches.

Experimental Results

Figure 5.4 shows the resulting trajectories of the three methods. I see that while the trajectories of the scenario approach and particle control are similar, the proposed method resulted in a trajectory that is less smooth. The lack of smoothness is an embodiment of the conservatism present in my approach. Solution statistics and empirical chance constraint satisfaction can be found in Table 5.4. I see the solution cost was larger for the proposed method, as expected. To assess constraint satisfaction, I generated 10^4 additional disturbances and empirically tested whether the target set constraint was satisfied. I expect the proposed method to always empirically satisfy the chance constraint given

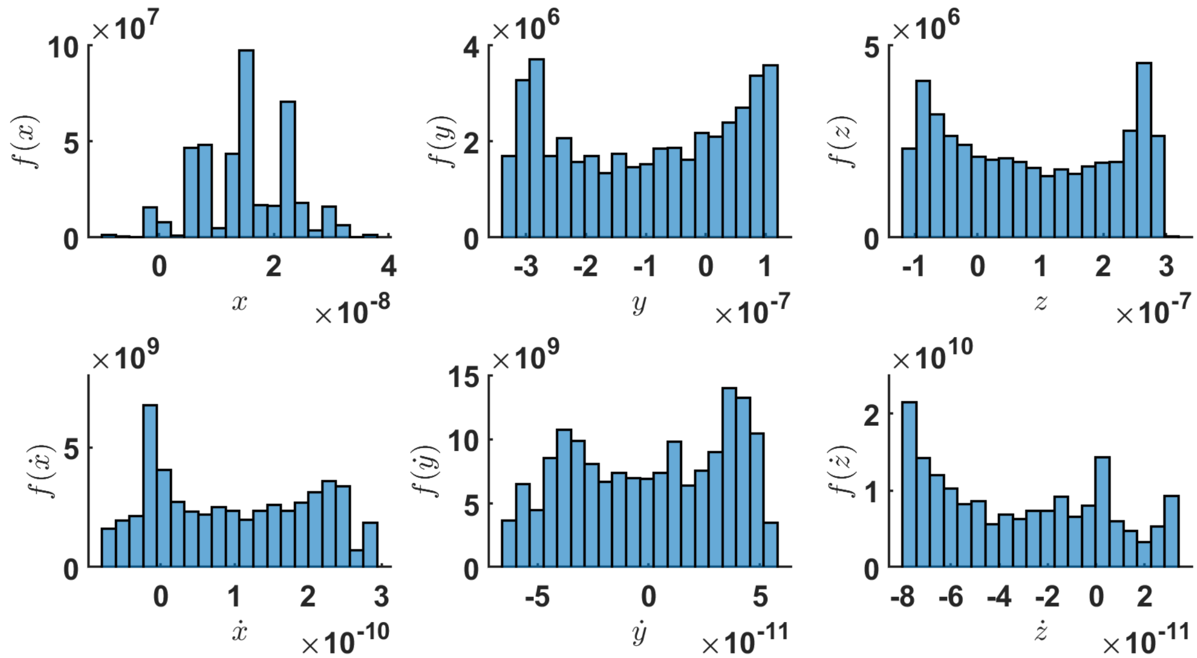

Figure 5.3: Histograms of $N_s = 2,073$ sampled disturbances for each element of the Deputy's disturbance vector at time step 0, $\vec{\boldsymbol{w}}_1^{[i]}(0)$. Disturbance samples were collected as the difference of positions between a model propagated with the 2-body model and a model propagated with (5.66). Notice they all have highly irregular shapes.

Lemma 5.3. However, this guarantee cannot be made for either the scenario approach or the particle control approach. While in this instance, the scenario approach did satisfy the chance constraint empirically, the particle control approach did not.

I point out in Table 5.4 the large difference in computation time between the three methods. The time to solve the solution with the proposed method is *two orders of magnitude faster than both the scenario approach and the particle control approach.* Here, the computational benefits and almost surely guarantees of chance constraint satisfaction present a strong case to use this method in instances where chance constraint satisfaction and speed are important.

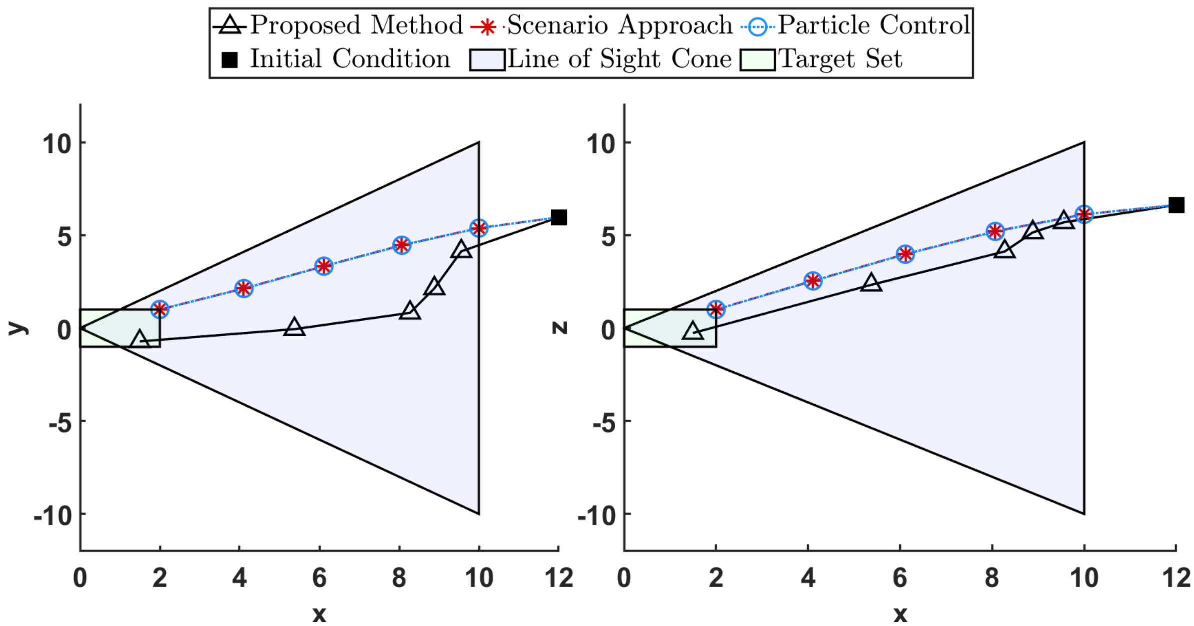

Figure 5.4: Comparison of mean trajectories between proposed method (solid line) and robust control approach (dashed line) for CWH dynamics. Disturbances were sampled from the difference in the CWH frame between 2-body dynamics and dynamics with 2-body acceleration, J_2 gravitational acceleration, and solar and lunar acceleration.

Metric	Proposed	Scenario Approach [4, 5]	Particle Control [6]
Solve Time (sec)	0.3472	15.7706	64.8701
Solution Cost ($10^{-3}N^2$)	6.1954	1.5832	1.5824
Terminal Set (5.64)	1.0000	1.0000	0.2061

Table 5.4: Solution Cost, Computation Time, and Empirical Constraint Satisfaction for CWH Dynamics with Simulated J_2, Sun, and Moon Acceleration Disturbance and probabilistic violation threshold $\alpha = 0.05$. Constraint Satisfaction is the Ratio of 10^4 Additional Simulated Disturbance Samples that Satisfied the Constraint.

5.5 Summary

I proposed a method based on sample statistics to solve chance constrained stochastic optimal control problems with almost surely guarantees of chance constraint satisfaction. This work focuses on probabilistic requirements for polytopic target sets and 2-norm based collision avoidance constraints in disturbed LTI systems. I derived a concentration inequality that allow us to bound tail probabilities of a random variable being a set number of sample standard deviations away from the sample mean. My approach relies on a derived theorem to reformulate joint chance constraints into a series of inequalities that can be readily solved as a difference of convex functions optimization problem. I demonstrated my method on two multi-satellite rendezvous scenarios. The first scenario was modeled with disturbance data generated from the J_2 gravitational harmonic, and third body gravity from the Sun and Moon, and compared against the scenario approach and particle control. The second scenario was modeled with a zero-mean Gaussian disturbance and compared against a model predictive control approach using Cantelli's inequality, the analytic analogue of Theorem 5.1. In the two examples, I showed that this approach is amenable to probabilistic guarantees, is efficient to compute, and may be a effective alternative to moment based model predictive control methods.

Chapter 6

Conclusion

This dissertation proposes novel theory to solve chance constrained stochastic optimal control problems with arbitrary disturbances in a computationally efficient manner through exploitation of statistical theory. I developed three frameworks that are amenable to arbitrary disturbances and solve chance constraints for both target set acquisition and collision avoidance. Each of the proposed methods allows for either almost surely guarantees or asymptotic guarantees of chance constraint satisfaction. Further, each method results in a difference of convex reformulation to handle the 2-norm collision avoidance chance constraint. This allows for us to show the methods proposed are conservative, but solutions satisfy Problem 1. Each method was demonstrated on multiple satellite rendezvous problems.

6.1 Summary of Contributions

I first developed an extension of the quantile-based approaches to accommodate collision avoidance constraints. I then present a approximation of the quantile function via a Taylor series expansion. The Taylor series approximation is built on the fact that derivatives of the quantile are functions of the probability density function and its derivatives via the inverse function theorem. The Taylor series approximation implies chance constraint satisfaction can only be guaranteed asymptotically. This method was experimentally validated through three multi-satellite rendezvous problems involving Gaussian, Cauchy, and multivariate-t disturbances. These experiments show that the proposed method is not only computationally efficient but also adaptable to many scenarios.

Second, I develop an extension of existing moment-based methods to accommodate 2-norm collision avoidance constraints. I show that for constrains that are represented by unimodal random variable and have well defined moments, I can employ the one-sided Vysochanskij-Petunin inequality to bound the chance constraints probability. The one-sided Vysochanskij-Petunin inequality reduced the conservatism by at least a factor of 5/9 over existing methods. As this method relies on the one-sided Vysochanskij-Petunin inequality, chance constraint satisfaction is guaranteed almost surely. This method is experimentally validated with a multi-satellite rendezvous problem involving an exponential disturbance and a planning scenario with a single satellite with a Gaussian disturbance. These experiments show that the proposed method is less conservative than existing moment-based approaches and is computationally efficient in comparison to existing and commonly used methods.

Finally, I present a sample-based method that uses sample statistics to reformulate chance constraints. In this work, I develop a concentration inequality based on the deviation of a random variable from the sample mean. The derived theorem allows for almost surely guarantees of chance constraint satisfaction despite not needing any information about the underlying disturbance process. This method is experimentally validated with two multi-satellite rendezvous problems involving an disturbance generated from J_2, and solar and lunar third body gravity, and a Gaussian disturbance. These experiments show that the proposed method is both computationally efficient and can handle odd disturbances that can arise in real world applications.

6.2 Future Work

This dissertation presents several new methods that analyze chance constrained stochastic optimal control with arbitrary disturbances. I describe a few of the exciting directions that may be explored next.

- *Arbitrary chance constraints*: The methods developed in this work are focused on reformulations for two common chance constraints that arise in multi-vehicle planning problems a) convex target sets and b) collision avoidance. In practice, a target set may not be convex, connected, or polytopic. Each of these scenarios would be a challenge for the methods developed. Extensions of this work to arbitrary chance constraints would provide a powerful tool for the stochastic optimal control community.

- *Non-linear systems*: The methods developed in this work required systems to be linear such that we can develop closed form reformulations of the chance constraints. Each method presented in this work could, in theory, be extended to non-linear systems. There are non-linear systems, particularly systems with polynomial dynamics, that could allow for easy extensions of the methods presented in this work.

- *Better concentration inequalities*: The methods presented in Chapters 4-5 are based on either existing or derived concentration inequalities. For certain classes of distribution, such as log-concave or infinitely divisible distributions, there is potential for new and less conservative concentration inequalities to be developed. This could allow for moment-based approaches that provide tighter bounds and reduce the conservatism commonly associated with these methods.

- *Methods to bypass Boole's inequality*: Each of the methods presented in this work use Boole's inequality to separate joint chance constraints into a series of individual chance constraints. Boole's inequality is conservative by nature and this conservatism propagates into solutions. Methods that can compute bounds or values for joint probabilities can significantly reduce the conservatism of the methods presented in this work.

References

[1] J. Paulson, E. Buehler, R. Braatz, and A. Mesbah, "Stochastic model predictive control with joint chance constraints," *Int'l J. Ctrl.*, pp. 1–14, 2017.

[2] L. Blackmore, M. Ono, and B. Williams, "Chance-constrained optimal path planning with obstacles," *IEEE Trans. Robot.*, vol. 27, no. 6, pp. 1080–1094, 2011.

[3] S. Priore, A. Vinod, V. Sivaramakrishnan, C. Petersen, and M. Oishi, "Stochastic multi-satellite maneuvering with constraints in an elliptical orbit," in *2021 American Control Conference (ACC)*, pp. 4261–4268, 2021.

[4] G. Calafiore and M. Campi, "The scenario approach to robust control design," *IEEE Trans. Autom. Control*, vol. 51, no. 5, pp. 742–753, 2006.

[5] M. C. Campi, S. Garatti, and F. A. Ramponi, "A general scenario theory for non-convex optimization and decision making," *IEEE Trans. Autom. Control*, vol. 63, no. 12, pp. 4067–4078, 2018.

[6] L. Blackmore, M. Ono, A. Bektassov, and B. C. Williams, "A probabilistic particle-control approximation of chance-constrained stochastic predictive control," *IEEE Trans. on Robotics*, vol. 26, pp. 502–517, June 2010.

[7] P. Letier, T. Siedel, M. Deremetz, E. Pavlovskis, B. Lietaer, K. Nottensteiner, M. A. Roa Garzon, J. Sánchez Garcia, J. L. Corella, and J. Gancet, "Hotdock: Design and

validation of a new generation of standard robotic interface for on-orbit servicing," in *71st International Astronautical Congress, IAC 2020*, IAF, 2020.

[8] V. Dubanchet, J. B. Romero, K. N. Gregertsen, H. Austad, J. Gancet, K. Natusiewicz, J. Vinals, G. Guerra, G. Rekleitis, I. Paraskevas, *et al.*, "Eross project–european autonomous robotic vehicle for on-orbit servicing," in *International Symposium on Artificial Intelligence, Robotics and Automation in Space,(i-SAIRAS'20). USA: Pasadena, California*, 2020.

[9] W.-J. Li, D.-Y. Cheng, X.-G. Liu, Y.-B. Wang, W.-H. Shi, Z.-X. Tang, F. Gao, F.-M. Zeng, H.-Y. Chai, W.-B. Luo, *et al.*, "On-orbit service (oos) of spacecraft: A review of engineering developments," *Progress in Aerospace Sciences*, vol. 108, pp. 32–120, 2019.

[10] Y. Chihabi and S. Ulrich, "Spacecraft formation guidance law using a state transition matrix with gravitational, drag and third-body perturbations," in *Proceedings of the AIAA Scitech 2020 Forum*, AIAA, 2020.

[11] A. F. B. de Almeida Prado, "Third-body perturbation in orbits around natural satellites," *Journal of Guidance, Control, and Dynamics*, vol. 26, no. 1, pp. 33–40, 2003.

[12] V. Pisarenko and M. Rodkin, *Heavy-Tailed Distributions in Disaster Analysis.* Advances in Natural and Technological Hazards Research, Springer Dordrecht, 2010.

[13] E. Popescu and N. Popescu, "Modeling fluctuations of solar wind parameters with heavy-tailed distributions," *Romanian Astronomical Journal*, 01 2010.

[14] Z. Bouabbache, E. Busvelle, and M. Aidene, "Some results on optimal control of stochastic systems with state chance constraints," in *2017 6th International Conference on Systems and Control (ICSC)*, pp. 303–307, 2017.

[15] M. Farina, L. Giulioni, and R. Scattolini, "Stochastic linear model predictive control with chance constraints–a review," *J. Process Ctrl.*, vol. 44, pp. 53–67, 2016.

[16] J. Yong, "Stochastic optimal control – a concise introduction," *Mathematical Control and Related Fields*, vol. 12, no. 4, pp. 1039–1136, 2022.

[17] L. Blackmore and M. Ono, "Convex chance constrained predictive control without sampling," in *AIAA Guidance, Navigation and Control Conference*, 2009.

[18] R. Chai, A. Savvaris, A. Tsourdos, S. Chai, and Y. Xia, "Stochastic spacecraft trajectory optimization with the consideration of chance constraints," *IEEE Trans. on Control Systems Technology*, vol. 28, no. 4, pp. 1550–1559, 2020.

[19] R. Bellman, "The mathematical theory of optimal processes," 1965.

[20] L. S. Pontryagin, "The mathematical theory of optimal processes and differential games," *Trudy Mat. Inst. Steklov*, vol. 169, pp. 119–158, 1985.

[21] L. D. Berkovitz, *Optimal control theory*, vol. 12. Springer Science & Business Media, 2013.

[22] L. Blackmore, "A probabilistic particle control approach to optimal, robust predictive control," in *Proceedings of the AIAA Guidance, Navigation, and Control Conference and Exhibit*, AIAA, 2006.

[23] B. Gravell and T. Summers, "Stochastic stability via robustness of linear systems," in *2021 60th IEEE Conference on Decision and Control (CDC)*, pp. 5918–5923, 2021.

[24] G. Favero and W. Runggaldier, "A robustness result for stochastic control," in *Proceedings of the 39th IEEE Conference on Decision and Control (Cat. No.00CH37187)*, vol. 4, pp. 3349–3350 vol.4, 2000.

[25] M. Ono and B. Williams, "Iterative risk allocation: A new approach to robust model predictive control with a joint chance constraint," in *IEEE Conf. Dec. & Control*, pp. 3427–3432, 2008.

[26] F. A. Cuzzola, J. C. Geromel, and M. Morari, "An improved approach for constrained robust model predictive control," *Automatica*, vol. 38, no. 7, pp. 1183–1189, 2002.

[27] E. C. Kerrigan, *Robust constraint satisfaction: Invariant sets and predictive control*. PhD thesis, University of Cambridge, 2001.

[28] A. Ben-Tal, L. El Ghaoui, and A. Nemirovski, *Robust Optimization*. Princeton Series in Applied Mathematics, Princeton University Press, October 2009.

[29] A. P. Vinod, V. Sivaramakrishnan, and M. Oishi, "Piecewise-affine approximation-based stochastic optimal control with gaussian joint chance constraints," in *Proc. Amer. Ctrl. Conf.*, pp. 2942–2949, 2019.

[30] A. P. Vinod, V. Sivaramakrishnan, and M. M. K. Oishi, "Sampling-free enforcement of non-gaussian chance constraints via fourier transforms," in *Proceedings of the Fifth International Workshop on Symbolic-Numeric Methods for Reasoning about CPS and IoT*, Snr '19, (New York, NY, USA), p. 9–11, Association for Computing Machinery, 2019.

[31] S. Samuelson and I. Yang, "Safety-aware optimal control of stochastic systems using conditional value-at-risk," in *2018 Annual American Control Conference (ACC)*, pp. 6285–6290, 2018.

[32] M. Idan and J. L. Speyer, "Characteristic function approach to smoothing of linear scalar systems with additive cauchy noises," in *2019 27th Mediterranean Conference on Control and Automation (MED)*, pp. 238–243, 2019.

[33] V. Sivaramakrishnan, A. P. Vinod, and M. Oishi, "Convexified open-loop stochastic optimal control for linear non-gaussian systems," *arXiv:2010.02101*, 2021.

[34] A. Vinod, B. HomChaudhuri, and M. Oishi, "Forward stochastic reachability analysis for uncontrolled linear systems using Fourier transforms," in *Proceedings of the Conference on Hybrid Systems: Computation and Control*, (Pittsburgh, PA, USA), pp. 35–44, 2017.

[35] S. Boucheron, G. Lugosi, and P. Massart, *Concentration Inequalities: A Nonasymptotic Theory of Independence*. Oxford University Press, 02 2013.

[36] J. Darlington, C. Pantelides, B. Rustem, and B. Tanyi, "Decreasing the sensitivity of open-loop optimal solutions in decision making under uncertainty," *European Journal of Operational Research*, vol. 121, no. 2, pp. 343–362, 2000.

[37] M. B. Saltık, L. Özkan, and S. Weiland, "Moment based model predictive control for linear systems: Additive perturbations case," *International Journal of Robust and Nonlinear Control*, vol. 32, no. 15, pp. 8252–8279, 2022.

[38] M. C. Campi, S. Garatti, and M. Prandini, "The scenario approach for systems and control design," *IFAC Proceedings Volumes*, vol. 41, no. 2, pp. 381–389, 2008. 17th IFAC World Congress.

[39] N. Kariotoglou, K. Margellos, and J. Lygeros, "On the computational complexity and generalization properties of multi-stage and stage-wise coupled scenario programs," *Systems & Control Letters*, vol. 94, pp. 63–69, 2016.

[40] Y. Yang and C. Sutanto, "Chance-constrained optimization for nonconvex programs using scenario-based methods," *ISA Trans.*, vol. 90, pp. 157–168, 2019.

[41] H. Sartipizadeh, A. P. Vinod, B. Açikmeşe, and M. Oishi, "Voronoi partition-based scenario reduction for fast sampling-based stochastic reachability computation of linear systems," in *2019 American Control Conference (ACC)*, pp. 37–44, 2019.

[42] D. Stahl and J. Hauth, "Pf-mpc: Particle filter-model predictive control," *Systems & Control Letters*, vol. 60, no. 8, pp. 632–643, 2011.

[43] G. Manganini, M. Pirotta, M. Restelli, L. Piroddi, and M. Prandini, "Policy search for the optimal control of Markov Decision Processes: A novel particle-based iterative scheme," *IEEE Trans. on Cybernetics*, pp. 1–13, 2015.

[44] M. Campi and S. Garatti, "A sampling-and-discarding approach to chance-constrained optimization: Feasibility and optimality," *J. Optim Theory Appl.*, vol. 148, no. 2, pp. 257–280, 2011.

[45] A. Carè, S. Garatti, and M. C. Campi, "Fast–fast algorithm for the scenario technique," *Ops. Res.*, vol. 62, no. 3, pp. 662–671, 2014.

[46] U. Eren, A. Prach, B. B. Koçer, S. V. Raković, E. Kayacan, and B. Açıkmeşe, "Model predictive control in aerospace systems: Current state and opportunities," *Journal of Guidance, Control, and Dynamics*, vol. 40, no. 7, pp. 1541–1566, 2017.

[47] A. P. Vinod and M. M. Oishi, "Optimal trade-off analysis for efficiency and safety in the spacecraft rendezvous and docking problem," *IFAC-PapersOnLine*, vol. 51, no. 12, pp. 136–141, 2018. IFAC Workshop on Networked & Autonomous Air & Space Systems NAASS 2018.

[48] K. Jin, D. K. Geller, and J. Luo, "Robust trajectory design for rendezvous and proximity operations with uncertainties," *Journal of Guidance, Control, and Dynamics*, vol. 43, no. 4, pp. 741–753, 2020.

[49] D. Repperger and A. Koivo, "Optimal terminal rendezvous as a stochastic differential game problem," *IEEE Trans. on Aerospace and Electronic Systems*, vol. AES-8, no. 3, pp. 319–326, 1972.

[50] S. Priore, C. Petersen, and M. Oishi, "Approximate quantiles for stochastic optimal control of lti systems with arbitrary disturbances," in *2022 American Control Conference (ACC)*, pp. 1814–1821, 2022.

[51] S. Priore and M. Oishi, "Chance constrained stochastic optimal control for linear systems with a time varying random control matrix," 2023.

[52] D. Malyuta, T. Reynolds, M. Szmuk, B. Acikmese, and M. Mesbahi, "Fast trajectory optimization via successive convexification for spacecraft rendezvous with integer constraints," in *AIAA Scitech 2020 Forum*, p. 0616, 2020.

[53] R. Bonalli, T. Lew, and M. Pavone, "Sequential convex programming for nonlinear stochastic optimal control," *ESAIM: Control, Optimisation and Calculus of Variations*, vol. 28, p. 64, 2022.

[54] D. Malyuta, T. P. Reynolds, M. Szmuk, T. Lew, R. Bonalli, M. Pavone, and B. Açıkmeşe, "Convex optimization for trajectory generation: A tutorial on generating dynamically feasible trajectories reliably and efficiently," *IEEE Control Systems Magazine*, vol. 42, no. 5, pp. 40–113, 2022.

[55] Z. Zhao, H. Shang, and B. Wei, "Tackling nonconvex collision avoidance constraints for optimal trajectory planning using saturation functions," *Journal of Guidance, Control, and Dynamics*, vol. 45, no. 6, pp. 1002–1016, 2022.

[56] C. D. Enriquez and R. García-Pelayo, "Short-term collision probability algorithm for parallelepiped-shaped satellites," *Journal of Guidance, Control, and Dynamics*, vol. 45, no. 6, pp. 1093–1107, 2022.

[57] J. DiMatteo, D. Florakis, A. Weichbrod, and M. Milam, "Proximity operations testing with a rotating and translating resident space object," in *AIAA Guidance, Navigation, and Control Conference*, American Institute of Aeronautics and Astronautics, 2012.

[58] M. Maestrini and P. Di Lizia, "Guidance strategy for autonomous inspection of unknown non-cooperative resident space objects," *Journal of Guidance, Control, and Dynamics*, vol. 45, no. 6, pp. 1126–1136, 2022.

[59] Y. Ulybyshev, "Trajectory optimization for spacecraft proximity operations with constraints," in *AIAA Guidance, Navigation, and Control Conference*, 2011.

[60] M. Mercadier and F. Strobel, "A one-sided vysochanskii-petunin inequality with financial applications," *European Journal of Operational Research*, vol. 295, no. 1, pp. 374–377, 2021.

[61] G. Casella and R. Berger, *Statistical Inference*. Duxbury advanced series in statistics and decision sciences, Cengage Learning, 2002.

[62] S. Boyd and L. Vandenberghe, *Convex Optimization*. Cambridge University Press, 2004.

[63] P. Hartman, "On functions representable as a difference of convex functions.," *Pacific Journal of Mathematics*, vol. 9, no. 3, pp. 707 – 713, 1959.

[64] T. Lipp and S. Boyd, "Variations and extension of the convex–concave procedure," *Optimization and Eng.*, vol. 17, pp. 263–287, 2016.

[65] R. Horst, P. M. Pardalos, and N. V. Thoai, *Introduction to global optimization*. Springer Science & Business Media, 2000.

[66] W. H. Clohessy and R. S. Wiltshire, "Terminal guidance system for satellite rendezvous," *Journal of the Aerospace Sciences*, vol. 27, no. 9, pp. 653–658, 1960.

[67] W. Wiesel, *Spaceflight Dynamics*. New York: McGraw–Hill, 1989.

[68] A. Mesbah, "Stochastic model predictive control: An overview and perspectives for future research," *IEEE Ctrl. Syst. Mag.*, vol. 36, no. 6, pp. 30–44, 2016.

[69] A. Nemirovski and A. Shapiro, "Convex approximations of chance constrained programs," *J. Optimization*, vol. 17, pp. 969–996, 2006.

[70] G. Calafiore and L. Ghaoui, "On distributionally robust chance-constrained linear programs," *J. Optim Theory Appl.*, vol. 130, no. 1, pp. 1–22, 2006.

[71] F. Oldewurtel, C. Jones, A. Parisio, and M. Morari, "Stochastic model predictive control for building climate control," *IEEE Trans. Control Syst. Technol.*, vol. 22, no. 3, pp. 1198–1205, 2014.

[72] M. P. Vitus and C. J. Tomlin, "On feedback design and risk allocation in chance constrained control," in *2011 50th IEEE Conference on Decision and Control and European Control Conference*, pp. 734–739, 2011.

[73] M. Abramowitz and I. A. Stegun, *Handbook of mathematical functions with formulas, graphs, and mathematical tables*, vol. 55. US Government printing office, 1964.

[74] K. Kafadar and J. W. Tukey, "A bidec t table," *Journal of the American Statistical Association*, vol. 83, no. 402, pp. 532–539, 1988.

[75] M. J. Wichura, "Algorithm as 241: The percentage points of the normal distribution," *Journal of the Royal Statistical Society. Series C (Applied Statistics)*, vol. 37, no. 3, pp. 477–484, 1988.

[76] C. Yu and D. Zelterman, "A general approximation to quantiles," *Communications in Statistics - Theory and Methods*, vol. 46, no. 19, pp. 9834–9841, 2017.

[77] P. Baxandall and H. Liebeck, *Vector Calculus*, ch. The Inverse Function Theorem, pp. 214–225. New York: Oxford University Press, 1986.

[78] M. Grant and S. Boyd, "CVX: Matlab software for disciplined convex programming, version 2.1." http://cvxr.com/cvx, Mar. 2014.

[79] L. Gurobi Optimization, "Gurobi optimizer reference manual," 2020.

[80] M. Herceg, M. Kvasnica, C. Jones, and M. Morari, "Multi-Parametric Toolbox 3.0," in *Proc. Euro. Ctrl. Conf.*, (Zürich, Switzerland), pp. 502–510, July 17–19 2013.

[81] S. Kotz and S. Nadarajah, *Introduction*, ch. 1, pp. 1–35. Cambridge University Press, 2004.

[82] B. C. Sutradhar, "On the characteristic function of multivariate student t-distribution," *The Canadian Journal of Statistics / La Revue Canadienne de Statistique*, vol. 14, no. 4, pp. 329–337, 1986.

[83] N. Johnson, S. Kotz, and N. Balakrishnan, *Continuous Univariate Distributions, Volume 2*. Wiley Series in Probability and Statistics, Wiley, 1995.

[84] F. W. Steutel and K. v. Harn, *Infinite divisibility of probability distributions on the real line*. CRC Press, 1 ed., 2003.

[85] R. F. Lyon, "On closed-form tight bounds and approximations for the median of a gamma distribution," *PLoS One*, vol. 16, p. e0251626, May 2021.

[86] Z. Zhou and R. Cogill, "Reliable approximations of probability-constrained stochastic linear-quadratic control," *Automatica*, vol. 49, no. 8, pp. 2435–2439, 2013.

[87] J. Xu, T. van den Boom, and B. De Schutter, "Model predictive control for stochastic max-plus linear systems with chance constraints," *IEEE Trans. Autom. Control*, vol. 64, no. 1, pp. 337–342, 2019.

[88] M. Farina, L. Giulioni, L. Magni, and R. Scattolini, "An approach to output-feedback mpc of stochastic linear discrete-time systems," *Automatica*, vol. 55, pp. 140–149, 2015.

[89] E. M. J. Bertin, I. Cuculescu, and R. Theodorescu, *Strong unimodality*, pp. 183–200. Dordrecht: Springer Netherlands, 1997.

[90] I. A. Ibragimov, "On the composition of unimodal distributions," *Theory of Probability & Its Applications*, vol. 1, no. 2, pp. 255–260, 1956.

[91] J. Gorski, F. Pfeuffer, and K. Klamroth, "Biconvex sets and optimization with biconvex functions: a survey and extensions," *Mathematical Methods of Operations Research*, vol. 66, pp. 373–407, Dec 2007.

[92] F. Yilmaz and M.-S. Alouini, "Sum of weibull variates and performance of diversity systems," in *Proceedings of the 2009 International Conference on Wireless Communications and Mobile Computing: Connecting the World Wirelessly*, Iwcmc '09, (New York, NY, USA), p. 247–252, Association for Computing Machinery, 2009.

[93] F. D. A. Garcia, F. R. A. Parente, G. Fraidenraich, and J. C. S. S. Filho, "Light exact expressions for the sum of weibull random variables," *IEEE Wireless Communications Letters*, vol. 10, no. 11, pp. 2445–2449, 2021.

[94] S. Saha, E. Özkan, F. Gustafsson, and V. Šmídl, "Marginalized particle filters for bayesian estimation of gaussian noise parameters," in *2010 13th International Conference on Information Fusion*, pp. 1–8, 2010.

[95] R. Madankan, P. Singla, and T. Singh, "A robust data assimilation approach in the absence of sensor statistical properties," in *2015 American Control Conference (ACC)*, pp. 5206–5211, 2015.

[96] M. R. Rajamani and J. B. Rawlings, "Estimation of the disturbance structure from data using semidefinite programming and optimal weighting," *Automatica*, vol. 45, no. 1, pp. 142–148, 2009.

[97] C.-P. Lam, A. Y. Yang, and S. S. Sastry, "An efficient algorithm for discrete-time hidden mode stochastic hybrid systems," in *2015 European Control Conference (ECC)*, pp. 1212–1218, 2015.

[98] R. Verma and D. Del Vecchio, "Control of hybrid automata with hidden modes: Translation to a perfect state information problem," in *49th IEEE Conf. Dec. & Control*, pp. 5768–5774, 2010.

[99] I. J. Zucker, "92.34 the cubic equation - a new look at the irreducible case," *The Mathematical Gazette*, vol. 92, no. 524, p. 264–268, 2008.

[100] O. Montenbruck and E. Gill, *Satellite Orbits: Models, Methods and Applications*, pp. 53–116. Berlin, Heidelberg: Springer Berlin Heidelberg, 2000.